DISSERTATION

TRPM4 IN CEREBRAL ARTERY SMOOTH MUSCLE CELLS

Submitted by

Albert Louis Gonzales

Department of Biomedical Sciences

In partial fulfillment of the requirements

For the Degree of Doctor of Philosophy

Colorado State University

Fort Collins, Colorado

Fall 2012

Doctoral Committee:

Advisor: Scott Earley

Gregory C. Amberg
Frank A. Dinenno
John E. Rash
Michael M. Tamkun

ABSTRACT

TRPM4 IN CEREBRAL ARTERY SMOOTH MUSCLE CELLS

Cerebral arterial tone is dependent on the depolarizing and hyperpolarizing currents regulating membrane potential and governing the influx of Ca^{2+} needed for smooth muscle contraction. Several ion channels have been proposed to contribute to membrane depolarization, but the underlying molecular mechanisms are not fully understood. In this review, we will discuss the historical and physiological significance of the Ca^{2+}-activated cation channel, TRPM4, in regulating membrane potential of cerebral artery smooth muscle cells. As a member of the recently described transient receptor potential super family of ion channels, TRPM4 possesses the biophysical properties and upstream cellular signaling and regulatory pathways that establish it as a major physiological player in smooth muscle membrane depolarization.

TABLE OF CONTENTS

ABSTRACT ii

CHAPTER 1

Introduction 1

SMOOTH MUSCLE MEMBRANE POTENTIAL 2
TRPM4 7

CHAPTER 2

Ca^{2+} Release from the Sarcoplasmic Reticulum is Required for Sustained TRPM4 Activity in Cerebral Artery Smooth Muscle Cells 14

INTRODUCTION 14
MATERIAL AND METHODS 16
Animals. *16*
Isolated cerebral artery smooth muscle cell preparation. *16*
RNAi and Reverse Permeabilization. *17*
Real-Time RT-PCR. *18*
Immunocytochemistry. *18*
Electrophysiological Recordings. *19*
Calculations and Statistics. *21*
RESULTS 21
Sustained Transient Cation Channel Activity in Freshly Isolated Smooth Muscle Cells. *21*
TRPM4 siRNA Selectively Silences TRPM4 Expression. *24*
TRPM4 Expression is Required for TICC Activity. *25*
TICCs are Activated by IP_3R-dependent SR Ca^{2+} Release. *26*
DISCUSSION 27

CHAPTER 3

Endogenous Cytosolic Ca^{2+} Buffering is Necessary for TRPM4 Activity in Cerebral Artery Smooth Muscle Cells 41

INTRODUCTION 41
MATERIAL AND METHODS 44
Animals *44*

A7r5 Cell Culture and Transient DNA Transfection *44*
Isolation of Cerebral Artery Smooth Muscle Cells *45*
RNAi and Reversible Permeabilization *45*
Immunocytochemistry and Membrane Staining. *46*
General Electrophysiological Recordings *47*
Electrophysiological Recording Solutions *48*
Electrophysiological Recordings from TRPM4-Expressing A7r5 Cells *49*
Electrophysiological Recordings from Isolated Smooth Muscle Cells *49*
Calculations and Statistics *50*
RESULTS 50
Disruption of the Intracellular Environment Leads to Ca^{2+}-Dependent TRPM4 Inactivation. *50*
EGTA Emulates Endogenous Cytosolic Ca^{2+} Buffering. *52*
Sustained TRPM4 Currents Under Conventional Whole Cell Patch Clamp Conditions. *53*
Whole-Cell TICCs are Activated by IP_3R-dependent SR Ca^{2+} Release. *56*
Whole-Cell TICC Activity is Modulated by the Cytosolic Buffering with BAPTA. *57*
TRPM4 and IP_3R are Proximate. *59*
DISCUSSION 60

CHAPTER 4

Pharmacological Inhibition of TRPM4 Hyperpolarizes Vascular Smooth Muscle 81

INTRODUCTION 81
MATERIALS AND METHODS 83
Animals *83*
Cerebral Artery Smooth Muscle Cell Preparation *83*
Human Embryonic Kidney (HEK) Cell Culture *84*
General Patch Clamp Electrophysiology *84*
TRPC3 and TRPC6 Currents in HEK Cells *84*
Large conductance Ca^{2+}-activated K^+ (BK_{Ca}) and TRPM4 Currents in Smooth Muscle Cells *86*
Voltage-Dependent K^+ (K_V) Currents in Smooth Muscle Cells *87*
Inwardly-Rectifying (K_{IR}) Currents in Smooth Muscle Cells *88*
Isolated Vessel Experiments *89*
Smooth Muscle Cell Membrane Potential *90*
Calculations and Statistics *90*
RESULTS 91
9-Phenanthrol Selectively Blocks Sustained TRPM4 Currents *91*

9-Phenanthrol Does not Block BK_{Ca}, Kv, or K_{IR} Channels in Smooth Muscle Cells *92*
Voltage-Dependent Ca^{2+} Channels are not Blocked by 9-Phenanthrol *93*
9-Phenanthrol Hyperpolarizes Vascular Smooth Muscle Cells *93*
9-Phenanthrol Dilates Pressurized Cerebral Arteries *94*
DISCUSSION 96

CHAPTER 5

Summary and Perspective 108

TRPM4 IN CEREBRAL ARTERY SMOOTH MUSCLE CELLS 108
REGULATION OF TRPM4 IN CEREBRAL ARTERY SMOOTH MUSCLE CELLS 111
TRPM4 IN HYPERTENSION 119

CHAPTER 1

Introduction

The degree of arterial tone controlling blood flow within the microcirculation is dependent on the contractile state of smooth muscle cells encircling the vessel wall. Movement of ions across the plasma membrane determines resting membrane potential and myocyte contraction. The ions channels responsible for these responses are still being characterized. Depolarization of the plasma membrane triggers smooth muscle contraction by increasing Ca^{2+} influx through dihydropyridine-sensitive voltage-dependent (L-type) Ca^{2+} channels. The subsequent rise in intracellular [Ca^{2+}] initiates calmodulin-dependent cross-bridge cycling, leading to myocyte shortening and arterial constriction. Due to the steep voltage sensitivity of L-type Ca^{2+} channels (85), small variations in membrane potential can elicit significant changes in smooth muscle intracellular Ca^{2+} and vessel diameter (7.5 nM mV^{-1} and 7.5 µm mV^{-1} respectively, for cerebral arteries) (85). Therefore, ion channels influencing resting membrane potential and governing the opening of L-type Ca^{2+} channels play an essential role in regulating the contractile state of vascular smooth muscle cells. Efflux of K^+ has been established as the major mechanism leading to membrane hyperpolarization and myocyte relaxation (79, 86, 148, 174), but less is known of the ion channels physiologically responsible for membrane depolarization in vascular smooth muscle cells. In the present review, we will summarize the contribution of Ca^{2+}-activated cation channels in establishing the resting membrane potential of cerebral artery myocytes and discuss the

upstream mechanisms of channel regulation that are essential for smooth muscle cell contraction.

SMOOTH MUSCLE MEMBRANE POTENTIAL

K^+ channels regulate arterial smooth muscle function through modulations of membrane excitability. Increases in K^+ conductance through channels present in the plasma membrane lead to membrane hyperpolarization, Four types of K^+ channels have been identified in arterial smooth muscle: 1) Ca^{2+}-activated K^+ (K_{Ca},) channels, 2) voltage-dependent K^+ (K_V) channels, 3) inward rectifier K^+ (K_{IR}) channels, and 4) ATP-sensitive K^+ (K_{ATP}) channels. Each type serves a unique role in regulating resting membrane potential (121). K_{Ca} channels are activated by intracellular Ca^{2+} and play a fundamental role in establishing intrinsic tone of resistance arteries (17, 117). In particular, large-conductance Ca^{2+}-activated K^+ (BK_{Ca}) channels are activated by highly localized intracellular Ca^{2+} release events from ryanodine receptors on the sarcoplasmic reticulum (78, 118). These events cause local Ca^{2+} concentrations to be elevated for a short period of time, inducing a coordinated efflux of K^+ through multiple BK_{Ca} channels and give rise to spontaneous transient outward currents (STOCs) (78, 121). K_V channels are sensitive to changes in membrane potential within the physiological range (-40 to -60 mV) (67) and activate following membrane depolarization, suggesting they may play a role in limiting the extent of depolarization within smooth muscle cells (69, 155, 188). K_{IR} channels are activated by extracellular K^+ [(44)] and mediate external K^+-induced hyperpolarization and can link the metabolic demand of surrounding cells to changes myocyte contractility. Strong evidence for the role of K_{ir} channels is observed

in functional hyperemia, or coupling of neuronal activity to localized cerebral blood flow. Extracellular K^+ released from astrocytic endfeet encompassing paremchymal arteries activates K_{ir} channels localized smooth muscle cells, and causes a rapid and profound hyperpolarization and vessel dilation (49). Additionally, K_{ir} channels are present at the junctions between endothelial and smooth muscle cells and contribute to the endothelial-dependent vasodilatation of cerebral and mesenteric arteries (96). K_{ATP} channel activity is stimulated by an increasing ratio of intracellular ATP to ADP (6), and plays a role in sensing reductions in cytosolic ATP (123). Hypoxia-mediated vasodilation is attenuated by the K_{ATP}-specific blocker glibenclamide, suggesting a role of K_{ATP} channels in linking intracellular metabolic demand to changes in myocyte contractility (174). Muscle relaxation is clearly mediated by several different K^+ channels, all having distinct biophysical properties and clear functional niches in contributing to membrane hyperpolatization.

Under normal physiological ionic gradients, the K^+ equilibrium potential is approximately -80 mV, yet resting membrane potential is consistently reported in pressurized cerebral arteries to be more depolarized at around -45 mV (121). Therefore, K^+ channel activity cannot completely determine membrane excitability. Channels permeable to cations (Ca^{2+} and Na^+ influx) or anions (Cl^- efflux) are present in smooth muscle cells, but the ions triggering membrane depolarization in smooth muscle cells are still unclear. The predominant divalent cation current in smooth muscle cells are from voltage-dependent L-type Ca^{2+} channels, but these channels do not contribute to membrane excitability. Even though the inhibition of L-type Ca^{2+} channels and blocking Ca^{2+} influx by dihydropyridine compounds causes myocyte relaxation, it does not alter

the resting membrane potential (86). Dihydropyridine-insensitive (T-type) Ca^{2+} channels have been reported in some, but not all, types of arterial smooth muscle cells (1, 10, 12, 122, 161, 176); however, due to their kinetic properties, including rapid inactivation and low active voltage range (-65 mV to -45 mV) (10), these channels are thought to have a more transient or specialized role. Thus, Ca^{2+} ions entering through L-type Ca^{2+} channels do not have a major role in regulation of membrane excitability preceding contraction.

Cl^- currents can be recorded from vascular smooth muscle cells (4, 19, 93, 137), but, because the molecular identities of these channels was only recently discovered and due to the lack of specific pharmacology the significance of these currents has been difficult to determine. Some Cl^- channel blockers, like DIDS (4,4'-diisothiocyanatostilbene-2,2'disulphonic acid), SITS 4,acetamino-4'isothiocyanatostilbene-2,2'-disulphonic acid), and IAA-94 are effective in inhibiting pressure-induced vasoconstriction (4), but others, including 9-AC (9-anthracene chloride) and niflumic acid, have no effect (119). It was later shown that many of the Cl^- channel blockers reported to reduce myogenic response also inhibited nonselective cation channels (195) and L-type Ca^{2+} channels (33). The strongest evidence for the involvement of Cl^- channels in smooth muscle cell regulation comes from recent reports examining the role of transmembrane protein 16A (TMEM16A), a Ca^{2+} activated Cl^- channel (19, 26). Hyposmotic solution-induced cell swelling activated Cl^- currents in arterial smooth muscle cells and were diminished following inhibition of TMEM16A channels through siRNA-mediated downregulation and channel specific blocking antibodies (19). Ca^{2+} activated Cl^- currents contribute to membrane depolarization and

pressure-dependent vasoconstriction of cerebral arteries (19). Additionally, the small molecular blocker of TMEM16A, $T16A_{inh}$-A01, reduced Ca^{2+}-activated Cl^- currents in isolated myocytes and relaxed pre-constricted mouse thoracic arteries (26). These experiments clearly show that Cl^- conductance can contribute to membrane excitability, but additional experiments are needed to further and more acutely elucidate the physiological contributions of these channels in cerebral arteries.

The Cl^- equilibrium potential (-30 mV) is slightly depolarized compared to resting membrane potential (-40 mV) of arterial myocytes, and due to the relatively small driving force the Cl^- conductance may yield only a small depolarization. In contrast, the ionic gradient for Na+ is relatively large (E_{Na} = +60 mV), and replacement of Na^+ with the non-permeable cation N-Methyl-D-glucamine (NMDG) causes myocyte hyperpolarization in rabbit posterior cerebral arteries (66). In addition, swelling- or pressure-induced depolarization of rat cerebral artery myocytes are reported to arise from activation of cation channels (27, 195). These findings strongly suggest that cation influx, in particular, Na^+ ions, is a major contributor to membrane depolarization, but molecular identity of the ion channels responsible was not determined. The presence of conventional voltage-gated Na^+ channels in arterial smooth muscle cells has been a point of controversy. Tetrodotoxin-sensitive Na^+ currents are present in various types of cultured arterial myocytes (22, 103, 143, 149) and portal vein smooth muscle cells (162), but were not detected from cerebral arteries (63) and freshly isolated smooth muscle cells (103, 149). The isolation protocol used to liberate smooth muscle cells from arteries may influence detection of Na^+ channels (14). In one study, when the serine protease elastase was used to enzymattically dissociated cells from mesenteric

arteries, Na^+ channel activity was detected, but when the cysteine protease papain was used Na^+ currents were absent (14). Additional experiments examining the effects of cell culturing and enzymes digestion on voltage-gated Na^+ channels are required to determine the presence or contributions of this family of ion channels in the resting membrane potential of arterial smooth muscle cells.

Ca^{2+}-activated non-selective cation channels (NSC_{Ca}) have been observed in numerous cell types (183) , and until recent years the molecular identity and physiological significance of these channels were unknown. Since their first discovery by Hamill et al (1981), NSC_{Ca} currents have been recorded from numerous cell types, including; fibroblasts, mast cells, sensory neurons, cochlear outer hair cells, renal tubules, cardiac myocytes, and capillary endothelium (for review see (183)). The biophysical properties of NSC_{Ca} channels distinguish them from other channels (Figure 1.1). NSC_{Ca} channels have a unitary conductance ranging from 18-34 pS, are selective for monovalent cations with a low or undetectable Ca^{2+} permeability (P_{Ca}/P_{Na} = 0-0.14), and are activated by intracellular Ca^{2+} (183). Channels within this group exhibit a diverse range of Ca^{2+} sensitivities (100 nM to 100 mM) (183). In pancreatic acini, NSC_{Ca} channels required 100 nM intracellular Ca^{2+} for activation, but following exposure to Ca^{2+} currents rapidly inactivate (100). Sturgess et al. (1986) showed that NSC_{Ca} channels are also inhibited by intracellular ATP (177). NSC_{Ca} channels until recently have rarely been associated with a clear physiological function in any of the aforementioned cell types (183). In excitable cells, NSC_{Ca} channels were proposed to be a major contributor to long lasting membrane depolarization (139), but due to lack of

pharmacology and molecular tools at the time of this study the channel's molecular nature was not resolved.

TRPM4

The discovery of the mammalian Transient Receptor Potential (TRP) superfamily of cation channels in 1995 provided novel insight into the molecular identity of NSC_{Ca} channels and the ion channels responsible for smooth muscle membrane depolarization. The TRP superfamily consists of 28 gene products forming cation channels that respond to extracellular stimuli and mediate responses to chemical compounds and changes in temperature, osmolarity, light, and pressure (108). TRP channels are subdivided into six subfamilies: TRPA (ankyrin, 1), TRPC (canonical, 1-7), TRPM (melastatin, 1-8), TRPML (mucolipin, 1-3), TRPP (polycystin, 1-3), and TRPV (vanilloid, 1-6). Several Ca^{2+}-permeable members of the TRPC, TRPV, TRPM, TRPP channels are involved in smooth muscle cell intracellular Ca^{2+} homeostasis and dynamics, including receptor-activated and mechanosensitive calcium entry (for review see (35, 36)). Non-selective cation-conducting TRP channels, including TRPC3 and TRPC6, can conduct Na^{+} as well as Ca^{2+} and have important roles in smooth muscle membrane excitability in cerebral arteries (151, 194). TRPC3 channels are involved in receptor-mediated membrane depolarization and constriction of arterial smooth muscle (152), whereas TRPC6 channels are intrinsically mechanosensitive (173) and contribute to pressure-dependent membrane depolarization of cerebral arteries (194). However, due to little, or no, ion selectivity of these channels, the downstream contribution of either Na^{+} or Ca^{2+} ions is still debated. Additional work is needed to determine whether

Na^+ influx via TRPC3 or TRPC6 initiates membrane depolarization, or if Ca^{2+} influx through these channels activate a downstream Ca^{2+} sensitive mechanism influencing membrane depolarization. One member of the TRPM subfamily of TRP channels, TRPM4, is present in cerebral arteries and due to its ion selectivity it has become a prime candidate for the regulation of membrane depolarization and smooth muscle contraction.

TRPM4 and its closest relative TRPM5 have biophysical properties that differ from other members of the TRP channel superfamily, and are reminiscent of NSC_{Ca} channels (Figure 1.1). TRPM4 and TRPM5 channels do not conduct Ca^{2+} but are highly selective for monovalent cations (95). As determined by ion substitution experiments in HEK 293 expression systems, TRPM4 is equally permeable for Na^+ and K^+, and to a lesser extent, Cs^+ and Li^+ ($Na^+ \approx K^+ > Cs^+ > Li^+$) (128). Additionally, replacement of extracellular Na^+ with the non-permeable cation $NMDG^+$ has little effect on outward currents at depolarizing potentials, but completely abolished inward currents at hyperpolarizing potentials, suggesting that Na^+ is the major ion conducted at physiological membrane potentials (128). The current-voltage (IV) relationship from single-channel recordings of inside-out patches in symmetrical cation solutions exhibits a non-rectifying conductance of ~25 pS (95). Conventional whole-cell macroscopic currents recorded from TRPM4-expressing HEK 293 cells exhibit a large outward and smaller inward rectification (95, 128). TRPM4 is not considered to be classically voltage-dependent. Although shifts in the resting membrane potential can increase or decrease the total open probability of the channel, changes in voltage do not gate it, with channel activation being primarily dependent on intracellular Ca^{2+} concentrations.

TRPM4 has an unusual relationship with Ca^{2+}, as Ca^{2+} is required to stimulate the channel but also leads to channel inactivation. TRPM4 channel activity is dependent upon a rise in intracellular Ca^{2+} above global resting levels. Under whole-cell conditions, channels are more sensitive to Ca^{2+} (EC_{50} = 400 nM) (95) compared with recordings from the inside-out configuration (EC_{50} = 200 μM) (43, 128). This difference in Ca^{2+} sensitivity suggests the presence of a Ca^{2+}-sensitive intracellular channel modulator under whole cell conditions that is lost when membrane patches are excised. In addition to requiring Ca^{2+} for activation, TRPM4 exhibits a rapid Ca^{2+}-dependent inactivation, leading to loss of current within two minutes following exposure to high global Ca^{2+} (40, 41, 43, 95, 125, 131). The channel's Ca^{2+} sensitivity may provide insight to regulatory mechanisms, where high Ca^{2+} is required for activation, but prolonged exposure or improper removal of Ca^{2+} leads to loss of channel activity.

Ca^{2+} sensitivity of TRPM4 is regulated by several intracellular pathways. The channel contains a putative phosphatidylinositol 4, 5-bisphosphate (PIP_2) binding site, five calmodulin binding sites, several Protein Kinase C (PKC) phosphorylation sites, and six possible ATP-binding sites (125, 130, 131). PIP_2 modulates channel activity by shifting the IV relationship resulting in an increase in TRPM4 current magnitude at negative holding potentials (125). Blocking of phospholipase C (PLC) activity (125) or including PIP_2 in the recording pipette solution (125, 202) can prevent Ca^{2+}-dependent inactivation. Maintaining channel activity by supplementing the cells with a phospholipid source or inhibiting phosphoinositide 3-kinase activity suggests the involvement of Ca^{2+}-dependent PLC isoforms in regulating channel activity. With five possible binding sites, two on the N-terminus and three on the C-terminus, the Ca^{2+} binding protein calmodulin

can directly influences the Ca^{2+} sensitivity of TRPM4 (131). Overexpression of a truncated C-terminus mutant for TRPM4 or expression with dominant negative calmodulin mutants drastically decreases the amplitude of Ca^{2+}-activated TRPM4 currents (131). TRPM4 also contains multiple possible interaction sites for PKC, suggesting phosphorylation-dependent modulation of the channel. The PKC activating compound phorbol 12-myristate 13- acetate (PMA) increased the incidence of occurrence and current density of TRPM4 channels by enhancing the Ca^{2+} sensitivity of the channel (131). Intracellular ATP inhibits TRPM4 currents with a half maximal inhibitory concentration (IC_{50}) around 2-19 μM (130). TRPM4 is also modulated by adenine nucleotides with the highest sensitivity to ADP and least to adenosine (ADP > ATP > AMP >> adenosine) (133). The nucleotide triphosphates GTP, UTP, and CTP have no effect at concentrations lower than 1 mM (133). In addition to the inhibition of TRPM4 by free ATP, higher concentrations (in the millimolar range) can prevent Ca^{2+}-dependent inactivation of the channel (131). Mutations of putative ATP binding sites on TRPM4 abolish this effect, indicating that prevention of Ca^{2+}-dependent inactivation is associated with direct binding of ATP to the channel (131). In a similar manner, heat shifts the voltage-dependent activation curve for TRPM4 (Q_{10} = -5.6 ± 0.5 mV °C^{-1}) (181), a phenomenon also observed in other thermosensitive TRP channels (29, 38). Modulation of the monovalent cation conductance through TRPM4 by voltage, adenine nucleotides, phospholipids, and heat and dependence on intracellular Ca^{2+} for activation are consistent with NSC_{Ca} channels previously described in many cell types, suggesting the identity of these channels as TRPM4.

The pharmacology for TRPM4 is limited. The most commonly used TRPM4 blockers include flufenamic acid, spermine, Gd^{3+}, and sulfonylurea glibenclamide (28, 128, 133, 186) are poorly selective. Recently, a hydroxytricyclic derivative, 9-phenanthrol, has been shown to inhibit TRPM4 current with no effect on its closest relative TRPM5 (60). Additionally, at a concentration that nearly abolished TRPM4 channel activity (60), 9-phenanthrol did not alter TRPC3, TRPC6, voltage-gated K^+ Channels (K_v), large-conductance Ca^{2+}-activated K^+ channels (BK_{Ca}), inwardly rectifying K^+ channels (K_{IR}), or L-type Ca^{2+} channel currents (58). These data suggest that 9-phenanthrol may be a specific inhibitor of TRPM4. Pharmacological activators for TRPM4 include decavanadate (130) and the pyrazole derivative BTP2 (N-[4-3, 5-bis(trifluromethyl)pyrazol-1-yl]-4-methyl-1,2,3-thiadiazole-5-carboxamide) (180), however, these agents also lack specificity. Decavanadate interferes with ATP-dependent inhibition of TRPM4 channel activity but can also interact with other ion channels, including IP_3R and purinoreceptors (P2X) (104). BTP2 increases TRPM4 channel activity and reduces Ca^{2+}-dependent inactivation, but can also inhibit TRPC3 and TRPC5 channels (64). 9-phenanthrol is currently the most useful pharmacological tool for unmasking the functional significance of TRPM4.

With the advancements of molecular techniques, previous observations of NSC_{Ca} currents now can be identified as TRPM4 channels. Similar to the broad distribution reported for NSC_{Ca} channels, TRPM4 channels have been detected at high levels in the heart, pancreas, placenta, and prostate (for review see (62)), and with lower levels of TRPM4 detected in kidney, skeletal muscle, liver, intestines, thymus, and spleen (62). The functional significance and expression of TRPM4 have been extensively

characterized in four cell types. TRPM4 regulates cytokine secretion in lymphocytes and insulin secretion in pancreatic β-cells (for review see (168)). TRPM4 plays a role in controlling respiratory rhythmogenesis in neurons of the pre-Bötzinger complex (for review see (61)). Gain of function mutations within the TRPM4 gene in Purkinje fibers suggests it plays a role in isolated cardiac conduction disease in human heart (for review see (61)). Lastly, and as the focus of the current dissertation, TRPM4 is essential for smooth muscle membrane depolarization and vasoconstriction in cerebral arteries.

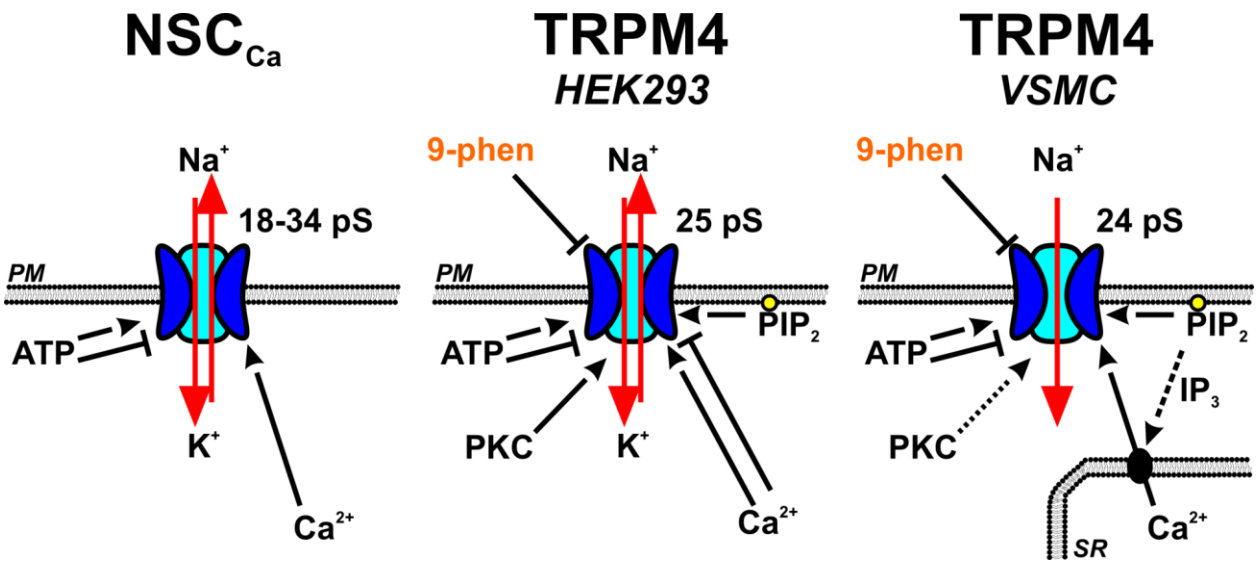

Figure 1.1. Comparison of Nonselective Ca^{2+}-activated cation channels (NSC_{Ca}), recombinant human TRPM4 channels expressed in HEK 293 cells, and native TRPM4 channels in vascular smooth muscle cells (VSMC). ATP, adenosine triphosphate; PM, plasma membrane; SR, sarcoplasmic reticulum; 9-phen, 9-phenanthrol; PKC, Protein Kinase C; and PIP_2, phosphatidylinositol 4, 5-bisphosphate.

CHAPTER 2

Ca^{2+} Release from the Sarcoplasmic Reticulum is Required for Sustained TRPM4 Activity in Cerebral Artery Smooth Muscle Cells

INTRODUCTION

The melastatin (M) Transient Receptor Potential (TRP) channel TRPM4 is a crucial mediator of pressure-induced vascular smooth muscle membrane depolarization and vasoconstriction (43), but regulation of the channel is poorly understood. Single-channel (43, 95, 127) and whole-cell patch clamp recordings (40) of TRPM4 activity in HEK cell expression systems and cerebral artery myocytes show that the level of intracellular Ca^{2+} required for channel activation (1-10 μM) is greater than that reported for average cytosolic or "global" [Ca^{2+}] in arterial myocytes (100-300 nM) (86). However, TRPM4 also undergoes a fast desensitization, leading to decreased activity within two minutes following exposure to high global Ca^{2+} (40, 43, 94, 126, 132). We propose that desensitization under these conditions is an artifact of prolonged exposure to high levels of intracellular Ca^{2} rather than an inherent property of the channel itself. To overcome this limitation and to limit disruption of native Ca^{2+} signaling pathways, we used the amphotericin B perforated patch clamp configuration to study TRPM4 activity in freshly isolated cerebral arterial myocytes.

Intracellular Ca^{2+} in smooth muscle cells is not uniformly distributed. Localized, transient elevations in intracellular Ca^{2+} arise from Ca^{2+} influx via persistent activity of L-type Ca^{2+} channels (Ca^{2+} sparklets) (115, 165) and Ca^{2+} release from sarcoplasmic reticulum (SR) (Ca^{2+} sparks, puffs, and waves) (15, 77, 107, 118, 201). Temporal and

spatial separation of SR Ca^{2+} release events result from the proximity of the SR and the plasma membrane (144) and strong intrinsic cytosolic Ca^{2+} buffering mechanisms (99). This architecture allows for Ca^{2+}-sensitive ion channels located at the plasma membrane to be activated by intracellular Ca^{2+} release events (77, 118). For example, Ca^{2+} sparks result from Ca^{2+} release events from ryanodine receptors on the SR located close to the plasma membrane (118). These events cause local [Ca^{2+}] to be elevated for a short period of time and open multiple large-conductance Ca^{2+}-activated K^+ (BK_{Ca}) channels, giving rise to spontaneous transient outward currents (STOCs) (78, 118). We hypothesize that TRPM4 channels may also be activated by intracellular Ca^{2+} signaling in smooth muscle cells.

Using the amphotericin B perforated patch clamp configuration we recorded and characterized persistent, rapidly opening and closing cation currents from native vascular smooth muscle cells. We call these events “Transient Inward Cation Currents” (TICCs). TICC activity was diminished in cells isolated from cerebral arteries treated with siRNA against TRPM4, suggesting that TICCs are formed by TRPM4 channels. TICC activity is reduced by inhibition of the sarco(endo)plasmic reticulum Ca^{2+} ATPase (SERCA) and blockade of inositol 1,4,5-trisphosphate receptor (IP_3R)-mediated Ca^{2+} release from the sarcoplasmic reticulum (SR). Our findings indicate that in cerebral artery myocytes, TRPM4 channels are regulated by SR Ca^{2+} release from IP_3R.

MATERIAL AND METHODS

Animals.

Male Sprague-Dawley rats (250–350 g; Harlan) were used for these studies. Animals were deeply anesthetized with pentobarbital sodium (50 mg ip) and euthanized by exsanguination according to a protocol approved by the Institutional Animal Care and Use Committees (IACUC) of Colorado State University. Brains were isolated in cold 3-(N-morpholino) propanesulfonic acid (MOPS)-buffered saline (in mM): 3 MOPS (pH 7.4), 145 NaCl, 5 KCl, 1 $MgSO_4$, 2.5 $CaCl_2$, 1 KH_2PO_4, 0.02 EDTA, 2 pyruvate, and 5 glucose and 1% bovine serum albumin. Cerebral and cerebellar arteries were dissected from the brain, cleaned of connective tissue, and stored in MOPS-buffered saline prior to further manipulation.

Isolated cerebral artery smooth muscle cell preparation.

Vessels were placed in the following cell isolation solution (in mM): 60 NaCl, 80 Na-glutamate, 5 KCl, 2 $MgCl_2$, 10 glucose, and 10 HEPES (pH 7.2). Arterial segments were initially incubated in 1.2 mg/ml papain (Worthington) and 2.0 mg/ml dithioerythritol for 17 min at 37°C, followed by 15 min incubation at 37°C in 1.0 mg/ml type II collagenase (Worthington). The digested segments were then washed three times in ice-cold cell isolation solution and incubated on ice for 30 min. Following this incubation period, vessels were triturated to liberate smooth muscle cells and stored in ice-cold cell isolation solution for use. Smooth muscle cells were studied within 6 hours following isolation.

RNAi and Reverse Permeabilization.

Small interfering RNAs (siRNA) against TRPM4 were used to down-regulate expression of the channel in isolated cerebral arteries. siRNA molecules purchased from Qiagen (1027280 [AllStars Negative Control], SI02868292 [Rn_Trpm4_1], and SI02868313 [Rn_Trpm4_4]) were dissolved as instructed at a concentration of 20 μM in siRNA Suspension Buffer. Control siRNA or TRPM4 siRNA molecules were introduced into intact cerebral arteries using a reversible permeabilization procedure. To permeabilize the arteries, segments were first incubated for 20 minutes at 4^{o}C in the following solution (in mM): 120 KCl, 2 $MgCl_{2,}$ 10 EGTA, 5 Na_2ATP, and 20 TES; (pH 6.8). Arteries were then placed in a similar solution containing siRNA (40 nM) for 3 hours at 4^{o}C and then transferred to a third siRNA-containing solution with elevated $MgCl_2$ (10 mM) for 30 minutes at 4°C. Permeabilization was reversed by placing arteries in a MOPS-buffered physiological siRNA-containing solution consisting of (in mM): 140 NaCl, 5 KCl, 10 $MgCl_{2,}$ 5 glucose, and 2 MOPS; (pH 7.1, 22^{o}C) for 30 minutes at room temperature. Ca^{2+} was gradually increased in the latter solution from nominally Ca^{2+}-free to 0.01, 0.1, and 1.8 mM over a 45 minute period. Following the reversible permeabilization procedures, arteries were organ cultured for two to three days in D-MEM/F-12 culture media supplemented with L-glutamine (2 mM) (Gibco), and 0.5% penicillin-streptomycin (Gibco). Arteries were then used for smooth muscle cell isolation or real time-RT PCR.

Real-Time RT-PCR.

Arteries containing siRNA were enzymatically dissociated as described above, and RNA was immediately isolated and purified using an RNeasy® Protect Mini Kit (Qiagen). mRNA was synthesized into cDNA with the aid of an Omniscript® Reverse Transcriptase Kit (Qiagen) using 100ng RNA/reaction. Down-regulation of TRPM4 was detected using a real-time SYBR Green detection assay (Bio-Rad), QuantiTect primers spanning intron/exon boundaries of TRPM4 (Qiagen), and an iQ5 Multicolor Real-Time PCR Detection System (Bio-Rad). Samples were normalized to β-Actin, and cycling parameters were selected based on the protocol for QuantiTect primer assays (Qiagen). β-Actin primers were designed based on a published sequence (NM_031144), and were purchased from Integrated DNA Technologies, Inc. Sequences were as follows: 5'-TTGCTGACAGGATGCAGAAGGAGA-3' (forward) and 5'-ACTCCTGCTTGCTGATCCACATCT-3' (reverse). Down-regulation of TRPM4 mRNA was calculated according to the Pfaffl Method (142).

Immunocytochemistry.

Cells were enzymatically dissociated from siRNA-treated vessels as described above, and allowed to adhere to glass slides for 20 minutes at 4°C. Cells were fixed with 4% formaldehyde for 10 minutes, permeabilized with cold methanol (-80°C), blocked with 2% bovine serum albumin, and incubated with primary antibodies overnight at 4°C. The following primary antibodies were used; rabbit anti-TRPM4 at 1:250, (Abcam, ab63080), sheep anti-TRPC3 at 1:250, (Abcam, ab63012); and goat anti-TRPC6 at 1:100, (Santa Cruz, sc-19197). Cells were subsequently washed and

incubated with appropriate fluorescent secondary antibody for 2 hours at room temperature. The following secondary antibodies were used at 1:1000; anti-rabbit conjugated to Texas Red, (Santa Cruz, sc-2780), anti-sheep conjugated to FITC, (Santa Cruz, sc-2704), and anti-goat conjugated to Texas Red, (Santa Cruz, sc-2783). Immunofluorescence images were obtained using a Fluoview 1000 laser scanning confocal microscope (Olympus) and a 60x, 1.4 numerical aperture oil immersion objective, with the pinhole diameter set for 1 Airy Unit. Excitation of Texas Red was by illumination with the 543-nm line set at 74% transmission, and emission collected using a variable bandpass filter set to 555-655 nm. Excitation for FITC was accomplished by illumination with the 488-nm line set at 1.4% transmission, and emission collected using a variable bandpass filter set at 500-543 nm. All images were acquired at 1024x1024 pixels at 4.0 µs/pixel and were analyzed in ImageJ version 1.42q (NIH). Membrane Fluorescence (FM) was determined using the mean fluorescence of a region of interest (ROI) isolating the membrane, and Total Fluorescence was determined using the mean fluorescence of the ROI for the cytosol of the total cell.

Electrophysiological Recordings.

Isolated smooth muscle cells were placed into a recording chamber (Warner Instruments) and allowed to adhere to glass coverslips for 20 min at room temperature. Whole-cell currents were recorded using an AxoPatch 200B amplifier equipped with an Axon CV 203BU headstage (Molecular Devices). Recording electrodes (1-3 MΩ) were pulled, polished, and coated with wax to reduce capacitance. GΩ seals were obtained in a magnesium based physiological saline solution (Mg-PSS) containing (in mM) 5 KCl,

140 NaCl, 2 $MgCl_2$, 10 HEPES, and 10 glucose. Amphotericin B (40 µM) was included in the pipette solution to perforate the membrane. Perforation was deemed acceptable if series resistance was less than 50 MΩ. STOC and TICC activity were recorded in normal external bathing solution containing (in mM) 134 NaCl, 6 KCl, 1 $MgCl_2$ 2 $CaCl_2$, 10 HEPES, and 10 glucose at pH 7.4 (NaOH). The pipette solution contained (in mM) 110 K-aspartate, 1 $MgCl_2$, 30 KCl, 10 NaCl, 10 HEPES, and 5 µM EGTA at pH 7.2 (NaOH). Additional external solutions include, Na^+-free external solution containing (in mM) 134 N-methyl-D-glucamine (NMDG), 1 $MgCl_2$, 2 $CaCl_2$, 6 KCl, 10 HEPES, 10 glucose at pH 7.4 (KOH); and Ca^{2+} free external solution containing 134 NaCl, 6 KCl, 1 $MgCl_2$ 0.73 $CaCl_2$, 1 EGTA, 10 HEPES, and 10 glucose at pH 7.4 (NaOH). Currents were filtered at 1 kHz, digitized at 40 kHz, and stored for subsequent analysis. Clampex and Clampfit versions 10.2 (Molecular Devices) were used for data acquisition and analysis, respectively. For most experiments, isolated smooth muscle cells were held at a membrane potential (E_m) of +20 mV or -70 mV, and all recordings are performed at room temperature (22°C). In our recording solutions, the calculated reversal potential for total monovalent cations is -1.8 mV and -30.6 mV for monovalent anions (Cl^-). STOCs were defined as transient events greater than 10 pA (more than one BK_{Ca} channel), and the frequency was calculated by dividing the number of events by the time between the first and last event. TICC activity at -70 mV was calculated as the sum of the open channel probability (NP_o) of multiple open states of 1.75 pA. This value was based on the reported unitary conductance of TRPM4 (25 pS). Channel open probability (NP_o) was calculated using the following equation:

$$NP_o = \sum_{j=1}^{N} \frac{(t_j \cdot j)}{T}$$

Where:

t_j = time spent in seconds with j = 1,2,….N channels open

N = max number of channels observed

T = duration of measurement.

Calculations and Statistics.

All data are means ± SE. Values of *n* refer to the number of cells for immnocytochemistry and patch clamp experiments. Data were compared using paired t-tests. A level of $P \leq 0.05$ was accepted as statistically significant for all experiments. All histograms were constructed in Origin 8.1 (OriginLab Corp.).

RESULTS

Sustained Transient Cation Channel Activity in Freshly Isolated Smooth Muscle Cells.

The amphotericin B perforated patch clamp configuration, which allows for membrane voltage control with minimal disruption of intracellular Ca^{2+} dynamics (71) was used to record TRPM4 currents in native cerebral artery myocytes. Following seal formation and perforation, cells were voltage clamped at +20 mV and STOCs were recorded to demonstrate cell viability (Figure 2.1A). STOC frequency was 2.8 ± 0.7 Hz with an average amplitude of 22.7 ± 2.4 pA (Figure 2.1A). Cells were then voltage clamped at -70 mV to record inward currents. Under these conditions, we observed rapidly opening and closing, or “flickery”, currents (TICCs) with an average amplitude of

-8.6 ± 1.6 pA (n = 8) and a frequency of 19.5 ± 2.9 Hz (n = 5) (Figure 2.1B). When physiological intracellular Ca^{2+} signaling activity is maintained, we are able to resolve single-channel TRPM4 currents using this method. The high TICC frequency suggests that on average, and under these conditions, at least one TRPM4 channel is open. TICCs could be recorded for as long as seal viability could be maintained, up to 30 minutes for some cells. The total open probability (NP_o) for TICCs recorded under control conditions have mean value for 0.75 ± 0.08 and passed the Shapiro-Wilk test for normality (p = 0.184). A peak amplitude histogram was constructed (Figure 2.1C) using the measured amplitude of channel(s). Seven peaks (solid lines) were identified and are consistent with calculated current amplitude for multiple (1, 2, 3, etc) channels opening. The apparent unitary TICC current amplitude at a holding potential of -70 mV was -1.7 ± 0.1 pA (n=5), and is consistent with the reported unitary conductance for TRPM4 channels (25 pS) (39, 95) (Figure 2.1C). Additionally, we observe two peaks (dashed lines) that did not coincide with any predicted TRPM4 current amplitude peak. These peaks occur at -2.7 and -4.2 pA at -70 mV, and are suggestive of the presence of ~38 pS and ~60 pS channels. The reported unitary conductance for TRPC6 and TRPC3 are 35 pS (70) and 66 pS (204), respectively, and could account for these peaks. These currents account for a minor portion of TICC activity (~16%). TICCs were eliminated when Na^+ in the bathing solution was replaced with the non-permeable cation N-methyl-D-glucamine (NMDG) (Figure 2.1D). To rule out the influence of BK_{Ca} channels, recording were made in the presence of the selective BK_{Ca} channel blocker paxilline (5 μM). Paxilline abolished STOCs, but TICC activity was not changed (n = 3) demonstrating that these currents are independent of BK_{Ca} channel activity.

The mean peak amplitude (pA) of TICC activity was recorded in the presence of paxilline at different holding potentials between -80 and +80 mV to examine the current-voltage (I-V) relationship. TICCs displayed modest inward rectification, and consistent with cation current activity, reversed at ~0 mV (Figure 2.2). The calculated ionic reversal potentials for the solutions used for this study (symmetrical for total cations) is -1.8 mV vs. -30.6 mV for Cl^-. When Na^+ is replaced by the non-permeable cation, NMDG, and in the presence of paxilline, TICCs are abolished. This lack of channel activity at different holding potentials suggests that we have isolated a Na^+-dependent current. These findings demonstrate that perforated patch clamp configurations can be used to record sustained cation currents in freshly isolated cerebral smooth muscle cells.

TICC activity was recorded in the presence of reported pharmacological inhibitors of TRPM4. Fluflenamic acid has been previously reported to inhibit TRPM4 (EC_{50} = 2.8 µM) and TRPM5 (EC_{50} = 24.5 µM) currents (186). TICC activity was absent following the administration fluflenamic acid (10 µM) (n=5, Figure 2.3A). The hydroxytricyclic derivative, 9-phenanthrol, has also been shown to specifically inhibit TRPM4 and not the closely related channel TRPM5 (60). TICC activity was diminished following the administration of 9-phenanthrol (n=3, 100 µM) (Figure 2.3B). These findings demonstrate that TICC activity is suppressed by compounds known to block TRPM4, suggesting that in smooth muscle cells, TICCs are whole-cell TRPM4 currents under near-physiological conditions.

TRPM4 siRNA Selectively Silences TRPM4 Expression.

To test the hypothesis that TRPM4 expression is required for TICC activity, we suppressed expression of the channel using RNA interference (RNAi) technology. TRPM4 specific or control siRNA molecules were introduced into isolated cerebral arteries using a reversable permeabilization technique (194). Arteries were cultured for two to three days after siRNA treatment to allow for down-regulation before smooth muscle cells were enzymatically dispersed from the vessels. In some experiments Alexa-555 tagged control siRNA was introduced into permeabilized arteries. Using fluorescence confocal microscopy, we found that approximately 70-80% of the isolated smooth muscle cells contained tagged siRNA (Figure 2.4A), consistent with the findings of a prior study (21). Quantitative real time RT-PCR was used to evaluate the effects of TRPM4 siRNA on TRPM4 mRNA levels. We found that TRPM4 mRNA levels in arteries treated with siRNA against TRPM4 were 60-70% less compared to negative siRNA treated vessels (Figure 2.4B).

A quantitative immunocytochemical approach was used to characterize the effects of TRPM4 siRNA on TRPM4 protein expression (Figure 2.4C). Cell fluorescence was normalized as a ratio of membrane fluorescence (F_M) to total cytosolic fluorescence (F_T), where a (F_M/F_T) value significantly greater than 1.0 indicates increased labeling near the plasma membrane. Control cells not exposed to primary antibodies have a F_M/F_T value of 1.1 (n=10). Cells isolated from vessels treated with control siRNA and incubated with the appropriate TRPM4 primary antibody, have a F_M/F_T value of 4.1 (n=30), comparable to that of cells from freshly isolated cerebral arteries (F_M/F_T=5.4, n=15). In TRPM4 siRNA treated vessels there are two distinct

populations of fluorescently labeled isolated cells. Most (23 of 29 cells, 79.3%) of the cells from this group exhibit only background fluorescence levels (F_M/F_T=1.2) (Figure 2.4C), suggesting that down regulation of TRPM4 expression is nearly complete in cells that take up the siRNA. A second, smaller population of cells (6 of 29 cells, 20.7%), exhibit fluorescence similar to that of cells isolated from vessels treated with control siRNA (F_M/F_T=4.2) (Figure 2.4C). These findings suggest that silencing of TRPM4 expression is nearly complete in the ~70-80% of cells that take up siRNA.

To test whether TRPM4 siRNA alters the relative protein expression levels of other TRP channels, we used the same quantitative immunocytochemical approach. TRPC3 and TRPC6 channels are present in cerebral artery smooth muscle cells and influence membrane potential and vascular tone (152, 173, 194). Cells were isolated from vessels treated with TRPM4 or control siRNA and fluorescently labeled for TRPC3 or TRPC6. Treatment with TRPM4 siRNA had no effect on total TRPC3 or TRPC6 cell fluorescence compared with cells isolated from control siRNA treated vessels (Figure 2.4D). These findings demonstrate that our siRNA procedures diminishes TRPM4 mRNA and protein levels and do not alter expression of other TRP channels involved in smooth muscle cell function.

TRPM4 Expression is Required for TICC Activity.

To further examine the hypothesis that TRPM4 expression is required for TICC activity, we studied the effects of TRPM4 siRNA on STOCs and TICCs. Smooth muscle cells enzymatically isolated from siRNA treated cerebral arteries were patch clamped in the perforated-patch configuration, and STOC and TICC activity were

recorded in the same cells at +20 mV and -70 mV, respectively (Figure 2.5A and B). The frequency and average amplitude of STOCs did not differ between cells isolated from cerebral arteries treated with TRPM4- versus control-siRNA (Figure 2.5C). These findings show that the siRNA treatment does not disrupt BK_{Ca} channel activity or intracellular Ca^{2+} release events that generate STOCs. In contrast, TRPM4 siRNA nearly abolished TICC activity (Figure 2.5A, B, and D). Although some channel activity was observed in cells isolated from TRPM4 siRNA treated arteries, these events were less frequent and smaller in amplitude compared with TICC recordings from control siRNA treated vessels (Figure 2.5A and B, right). The total open probability (NP_o) for TICC activity in smooth muscle cells dispersed from cerebral arteries treated with TRPM4 siRNA was significantly less than from cells from vessels treated with control siRNA (Figure 2.5D). These findings support the hypothesis that the molecular identity of the channel responsible for TICCs recorded from cerebral artery myocytes under perforated patch clamp conditions is TRPM4.

TICCs are Activated by IP_3R-dependent SR Ca^{2+} Release.

Previous work has shown that TRPM4 activation requires intracellular Ca^{2+} concentrations greater than resting cytosolic levels reported for native smooth muscle cells (95, 127, 129). We propose that under physiological conditions, TRPM4 channels are activated by locally elevated levels of intracellular Ca^{2+} that result from influx of Ca^{2+} from the extracellular space or from release of Ca^{2+} from intracellular stores. To determine if Ca^{2+} influx activates TRPM4, we recorded TICC activity during removal of extracellular Ca^{2+}. Lack of extracellular Ca^{2+} did not acutely (within two minutes) disrupt

TICC activity, but prolonged exposure (greater than 5 minutes) to a Ca^{2+}-free bathing solution eventually resulted in decreased TICC activity (Figure 2.6A). These findings suggest TICC activity is not dependent on Ca^{2+} influx *per se*, but Ca^{2+} influx may be important in maintaining SR Ca^{2+} stores at levels sufficient to support channel activity. To examine this idea, we recorded TICC activity following disruption of SR Ca^{2+} stores, and found that inhibition of the SERCA pump with cyclopizonic acid (CPA, 10µM) attenuated TICC activity (Figure 2.6B).

To further examine the role of SR Ca^{2+} stores in the activation of TRPM4 in smooth muscle cells, we used ryanodine to disrupt ryanodine receptor (RyR) function, and the selective IP_3R blocker, Xestospongin C, to inhibit SR Ca^{2+} release events. Ryanodine (50 µM) eliminated STOCs (n=4), but had no effect on the TICC activity over the same time course (Figure 2.7A). In contrast, administration of Xestospongin C (1 µM) did not alter STOC frequency or amplitude (n=5), but TICC activity was greatly diminished (Figure 2.7B). These findings suggest that in native cerebral artery myocytes, TRPM4 is activated by Ca^{2+} released from the SR through IP_3R (Figure 2.8).

DISCUSSION

The current study demonstrates a new method for recording sustained TRPM4 channel activity in freshly isolated smooth muscle cells. An important feature of this technique is the ability to record cation currents with minimal disruption of intracellular Ca^{2+} signaling dynamics. This patch clamp method was used to examine the mechanism of Ca^{2+}-dependent regulation of the channel in native smooth muscle cells. Our major findings are: (1) Sustained Transient Inward Cation Currents (TICCs) can be

recorded from cerebral artery myocytes using the perforated patch clamp configuration; (2) RNAi-mediated down regulation of TRPM4 expression attenuates TICC activity; and (3) TRPM4-dependent TICC activity is independent of Ca^{2+} influx *per se* but is attenuated by blockade of SERCA pump activity and IP_3R-mediated SR Ca^{2+} release. These findings provide the first sustained whole-cell recordings of TRPM4 activity in native smooth muscle cells with intact intracellular Ca^{2+} signaling and are the first demonstration of regulation of TRPM4 activity by IP_3R-mediated SR Ca^{2+} release.

TRPM4 channels are necessary for pressure- and PKC-induced smooth muscle depolarization and vasoconstriction (40, 43), and the autoregulation of cerebral blood flow *in vivo* (151). Efforts to understand regulation of TRPM4 have been hampered by rapid (~2 min) desensitization under conventional patch clamp conditions when nonphysiological levels of Ca^{2+} (~10-100 μM) are present in the intracellular solution. Inhibition of phospholipase C (PLC) prolongs TRPM4 activity under these conditions, suggesting that a Ca^{2+}-activated PLC isoform is responsible for TRPM4 rundown (126, 202). PLC-dependent desensitization of TRPM4 may result from localized depletion of phosphatidylinositol 4,5-bisphosphate (125, 202). We propose that rapid desensitization of TRPM4 activity is an artifact of recording conditions rather than an inherent property of the channel. To test this possibility, we sought a method that would allow whole-cell TRPM4 currents to be recorded under native conditions. The amphotericin B perforated patch clamp configuration allows whole cell currents to be recorded with minimal disruption of subcellular Ca^{2+} signaling pathways (71). This technique has been successfully used to record BK_{Ca} channel activation in smooth muscle cells in response to Ca^{2+} sparks (120), and we reasoned that this technique

could also be used to record whole-cell TRPM4 currents activated by transient Ca^{2+} events. We find that sustained currents (TICCs) recorded from native cerebral artery myocytes under these conditions. TICCs have a high frequency of occurrence (19.5 ± 2.9 Hz), but this is not unexpected. Our previous work shows that TRPM4 activity can be recorded from ~50% of inside-out membrane patches pulled from freshly isolated smooth muscle cells, suggesting that TRPM4 channels are abundant in these cells (43). Additionally, TICCs have biophysical properties that are consistent with those of TRPM4. For example, TICCs have and an apparent single channel conductance of ~25 pS, in agreement with the reported unitary conductance of TRPM4 (134, 138, 199). TICCs reversed at ~0 mV in the symmetrical cationic solutions used for this study (E_{Cl} = -30.6 mV) and substitution of the impermeant cation NMDG for Na^+ in the bathing solution completely blocked TICC activity. These findings are consistent with the selectivity of TRPM4 for monovalent cations (95, 127). Furthermore, TICCs were suppressed by the TRPM4 blockers fluflenamic acid and 9-phenanthrol, supporting the hypothesis that TRPM4 is the major channel responsible for this activity. We further probed the relationship between TICCs and TRPM4 using siRNA-mediated downregulation of TRPM4 expression. The efficacy and specificity of our TRPM4 siRNA treatment was confirmed using immunocytochemistry. Our data suggest that ~80% of smooth muscle cells take up the TRPM4 siRNA and exhibit nearly complete knockdown of TRPM4 protein expression. Additionally, cells isolated from TRPM4 siRNA vessels did not show a change in expression of TRPC3 or TRPC6 protein. TICC activity is decreased in smooth muscle cells isolated from arteries treated with TRPM4-specific siRNA compared to cells isolated from vessels treated with negative control

siRNA. Thus, we conclude that TICCs represent TRPM4 activity in native cerebral artery myocytes. The virtually total inhibition of TICCs following treatment with TRPM4 siRNA suggest that most of the cells used for these experiments come from the population of cells that received siRNA and have nearly complete knockdown of TRPM4 expression. The perforated patch technique described here provides a novel method for recoding sustained TRPM4 currents under near-physiological conditions and should be useful for further characterization of the channel in smooth muscle cells.

We unexpectedly found that whole-cell single-channel TICC activity exhibits modest inward rectification. In previous work, single channel recordings from inside-out patches exhibited a linear current-voltage relationship (43), whereas whole-cell TRPM4 currents exhibited both inwardly and outwardly rectification (40, 127). Dual rectification reported for conventional whole-cell TRPM4 currents may be an artifact of recording conditions. Under conventional whole-cell patch clamp conditions, the cytosolic environment is disrupted when the cell is dialyzed with the pipette solution, whereas the perforated-patch clamp configuration allows the intracellular environment to remain largely intact. TRPM4 currents are blocked by the polyamine spermine (126, 132), which could be dialyzed from the cell under conventional whole-cell conditions. Polyamine block is responsible for inward rectification of inwardly-rectifying K^+ (K_{IR}) channels in vascular smooth muscle cells (135, 175). We propose that this mechanism is also responsible for inward rectification of TICCs and that this mechanism contributes to the voltage dependency of TRPM4 channels under physiological conditions in vascular smooth muscle cells. Interestingly, the current-voltage relationship we report for TICC activity would result in increased depolarizing current in response to

membrane hyperpolarization and could be important for maintaining stable membrane potential in arterial myocytes.

The level of intracellular Ca^{2+} required to activate TRPM4 channels in whole-cell and inside-out patch clamp experiments is far greater than the average cytosolic [Ca^{2+}] of arterial myocytes (100-300 nM) (85). However, downregulation of TRPM4 expression impairs pressure-induced myocyte depolarization, vasoconstriction, and autoregulation of cerebral blow flow (43, 151), demonstrating that the channel is active under physiological conditions. Subcellular regions of elevated Ca^{2+} can result from Ca^{2+} influx from the extracellular space (115, 165) and from Ca^{2+} released from intracellular stores (15, 77, 78, 107, 201), and these dynamic Ca^{2+} events can further regulate the activity of Ca^{2+}-sensitive ion channels (120). We tested the hypothesis that increases in intracellular Ca^{2+} activate TRPM4 in native smooth muscle cells. We found that removal of extracellular Ca^{2+} did not initially change TICC activity, but prolonged exposure to Ca^{2+}-free bathing solution eventually decreased these events, possibly due to diminished refilling of SR stores. Blockade of the SERCA pump also diminished TICC activity, consistent with a role for SR Ca^{2+} release in TRPM4 regulation. RyRs inhibition did not alter TICC activity, but these currents were decreased by the IP_3R receptor blocker xestospongin C. These findings indicate that Ca^{2+} released from IP_3Rs receptors activate TRPM4 channels in cerebral artery smooth muscle cells (Figure 2.8).

Ca^{2+} release from IP_3R is associated with the generation of "Ca^{2+} puffs" which have been described in Xenopus oocytes (201) and isolated smooth muscle cells (8, 15). Our data suggests that some basal level of PLC-dependent generation of IP_3 and IP_3R-mediated Ca^{2+} release is present in freshly isolated cerebral artery smooth muscle

cells and supports sustained TICC activity. IP_3R-mediated Ca^{2+} release is also associated with spontaneous synchronous and asynchronous Ca^{2+} waves in smooth muscle cells in intact arteries (15, 77). The physiological function of these Ca^{2+} signaling events is not fully understood. Our findings show that TRPM4 activity in native cerebral artery myocytes requires IP_3R-mediated SR Ca^{2+} release, and we propose that TRPM4-mediated membrane depolarization in response to these Ca^{2+} signals may be central to vascular tone regulation. Consistent with this hypothesis, it has been proposed that synchronous Ca^{2+} waves in intact vessels may coordinate the membrane potential of smooth muscle cells along a segment of the vascular wall to effect uniform arterial contraction (106). Our findings suggest that TRPM4 activity could translate changes in synchronized Ca^{2+} waves into changes in smooth muscle cell membrane potential (140). Alternatively, asynchronous Ca^{2+} wave frequency reportedly increases in the presence of contractile agonists (15, 77), and this response may be important for smooth muscle contraction (77). It is possible that during agonist-stimulated increases in asynchronous Ca^{2+} wave activity, low, non-contractile amounts of Ca^{2+} are released from IP_3Rs activate TRPM4 to depolarize the membrane and initiate Ca^{2+} influx via VDCCs.

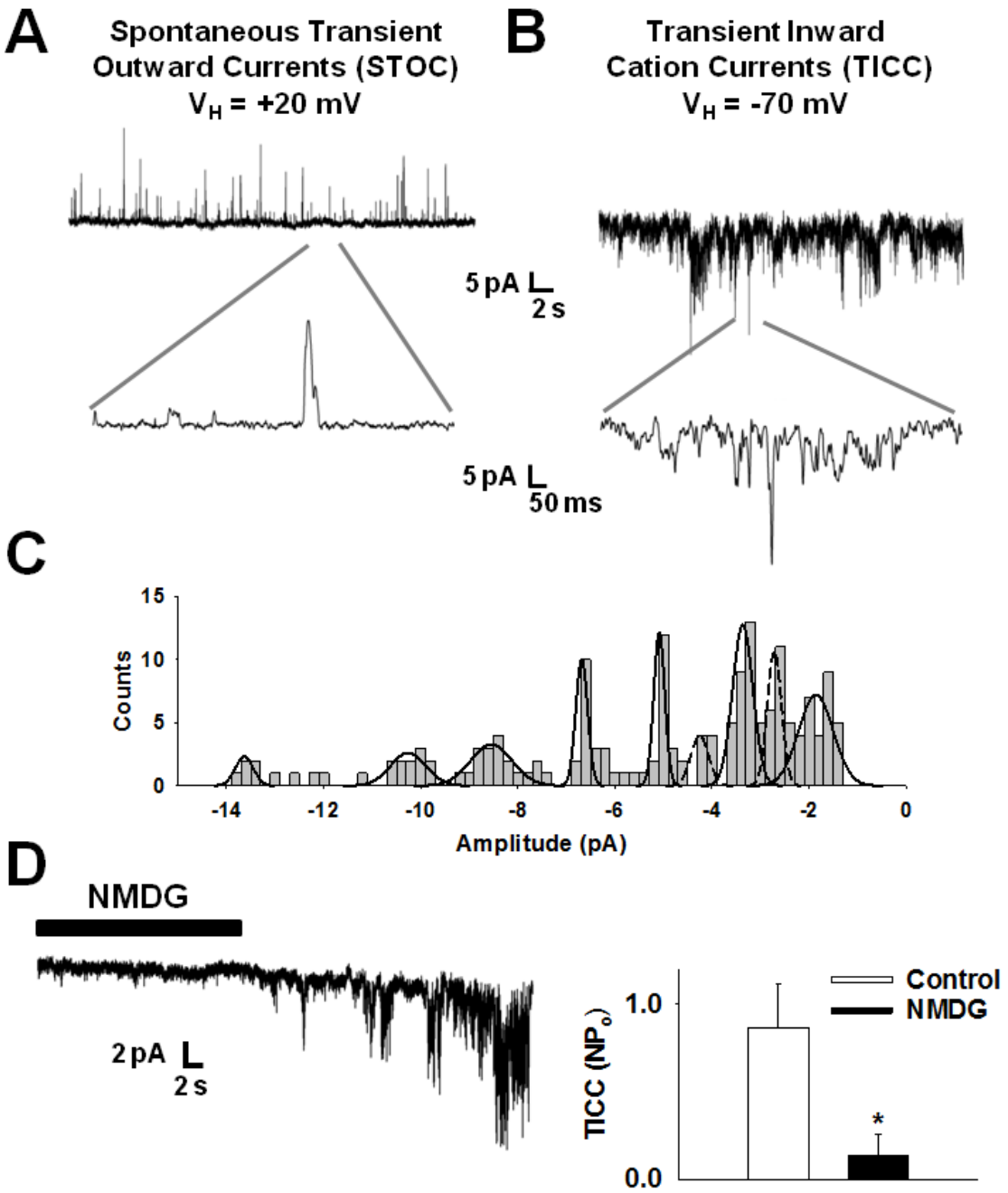

Figure 2.1: Sustained Transient Cation Channel Activity in Freshly Isolated Smooth Muscle Cells. A and B: Representative perforated-patch clamp recordings of Spontaneous Transient Outward Currents (STOC) and Transient Inward Cation Currents (TICC) in the same cell. Representative of ~30 cells. Insert shows expanded time scale. C: Peak amplitude histogram of TICC activity recorded from freshly isolated smooth muscle (0.2 pA bins). Data are fitted with multiple Gaussian functions. The solid-line peaks match calculated current amplitude for TRPM4 channel openings. The dash-line peaks do not match with calculated current amplitude for TRPM4 channel openings. D: Representative trace and summary data of TICC activity with Na^+ replaced with the non-permeabale cation N-methyl-D-glucamine (NMDG), n=3, *P≤0.05 vs. Control.

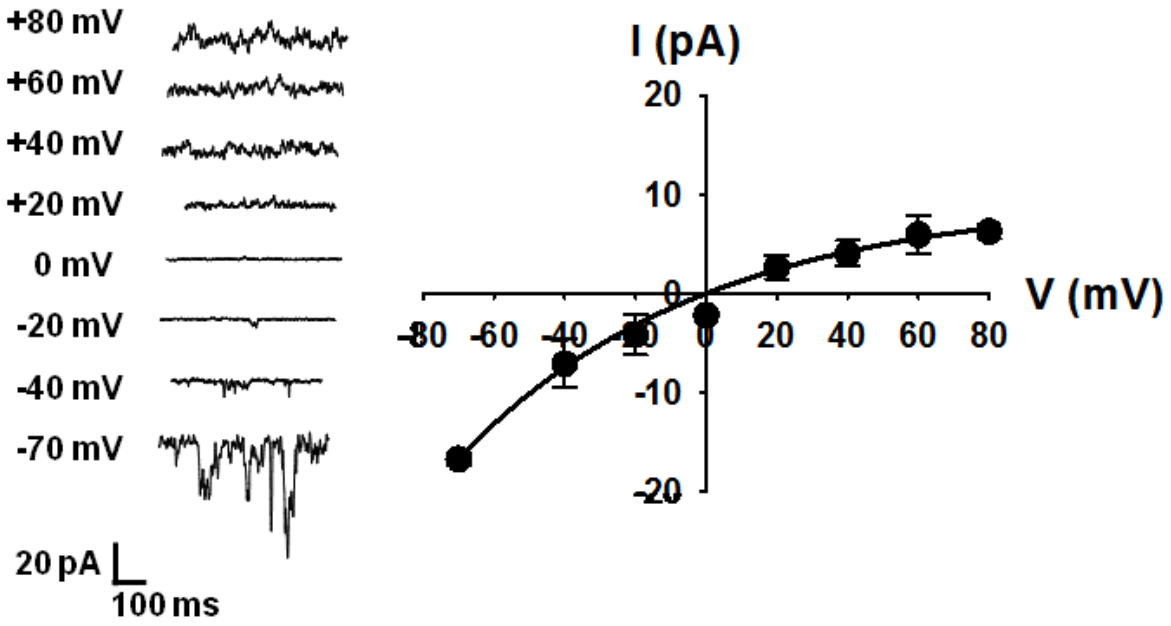

Figure 2.2: Current-Voltage Relationship for TICC Activity in Freshly Isolated Smooth Muscle Cells. Sample traces of TICC recordings obtained at holding potentials (V_H) from +80 to -70 mV. Average current amplitude to voltage relationship (I/V) for cells (n=3) with symmetrical total cations solutions under perforated-patch clamp conditions.

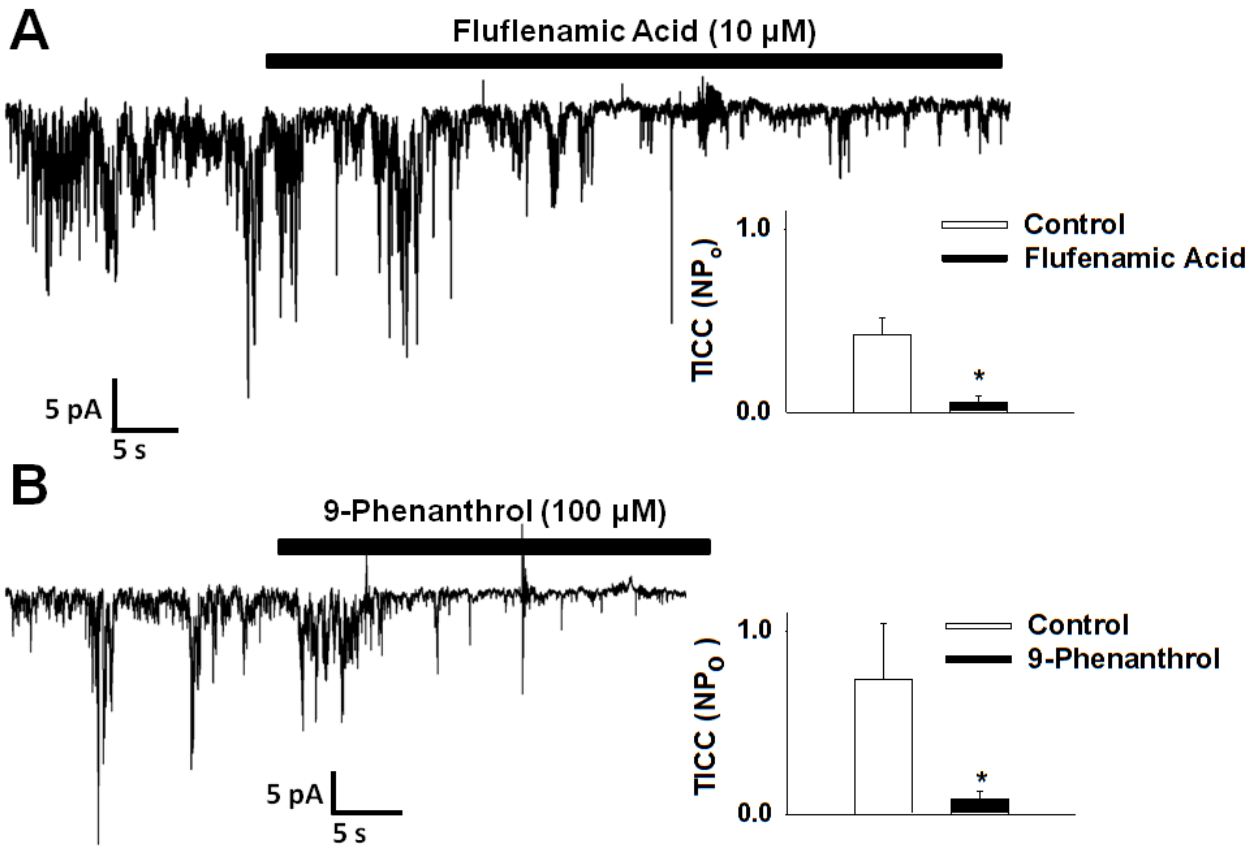

Figure 2.3: TICC Activity is Blocked by TRPM4 inhibitors. A: Representative trace and summary data of TICC activity in the presence of the fluflenamic acid (10 µM, n=5). B: Representative traces of TICC activity in the presence of 9-phenanthrol (100 µM, n=3).

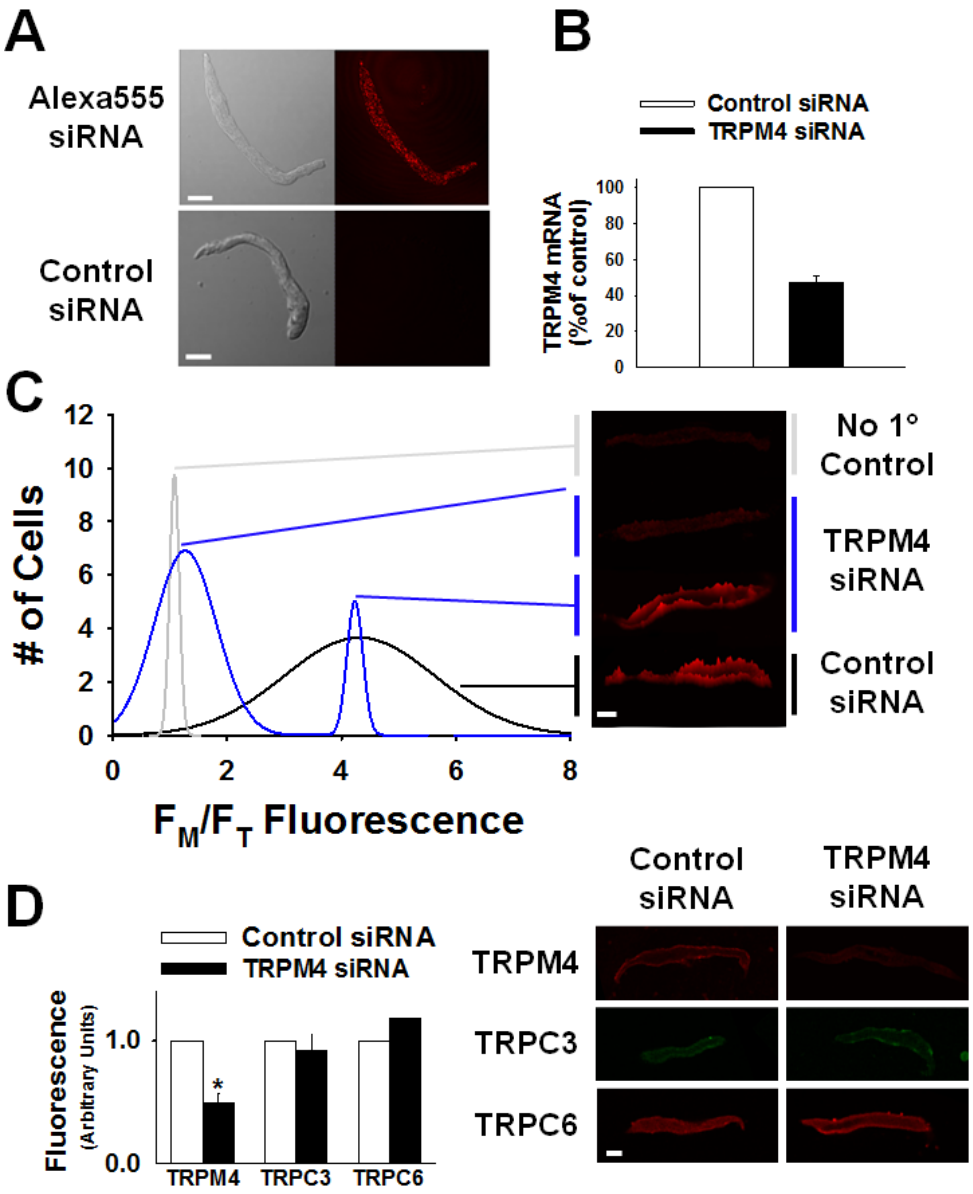

Figure 2.4: siRNA-Mediated Knockdown of TRPM4 Expression in Freshly Isolated Smooth Muscle Cells. A: Freshly isolated rat cerebral artery smooth muscle cells from arteries treated with control siRNA tagged with Alexa 555 (*top*) or untagged siRNA (*bottom*). Scale Bar = 11 µm. B: Summary data for siRNA-mediated down-regulation of TRPM4 mRNA levels in cerebral arteries as determined through real time, quantitative RT-PCR (n=3). C. Frequency histogram of the normalized membrane fluorescence (F_M/F_T) from cells: with no 1° antibody (n=10, grey); isolated from TRPM4-siRNA treated vessels (n=30, blue); and control siRNA treated vessels (n=30, black). Surface plot representatives of images obtained for each treatment (right). Scale Bar = 10 µm. D. Summary data of TRPM4-siRNA vs. control siRNA treatment on the total cell fluorescence labelling for TRPM4 (n=40), TRPC3 (n=30), and TRPC6 (n=20). *P≤0.05 vs. control siRNA. Representative images of total fluorescence for TRPM4, TRPC3, and TRPC6 (right). Scale Bar = 10 µm.

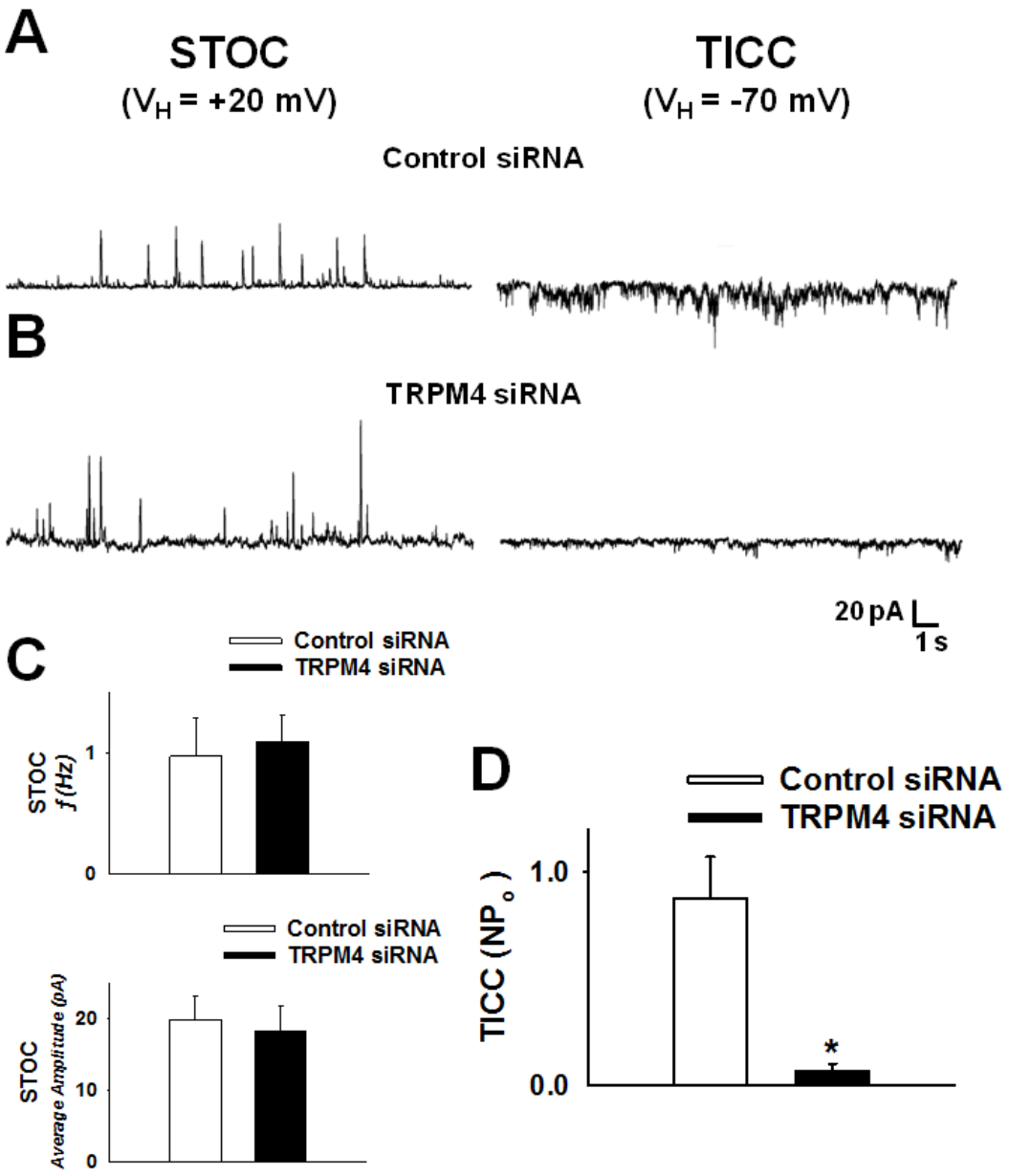

Figure 2.5: TRPM4 Expression is Required for TICC Activity. A: Representative recordings of STOC and TICC activity from the same cell isolated from arteries treated with control siRNA. B: Representative recordings of STOC and TICC activity from the same cell isolated from arteries treated with TRPM4 siRNA. C: Summary data of STOC frequency (*f, top*) and average STOC amplitude (*bottom*). D: TICC NP_o for vessels treated with control siRNA (n=4) or TRPM4 siRNA (n=5). *P≤0.05 vs. control siRNA.

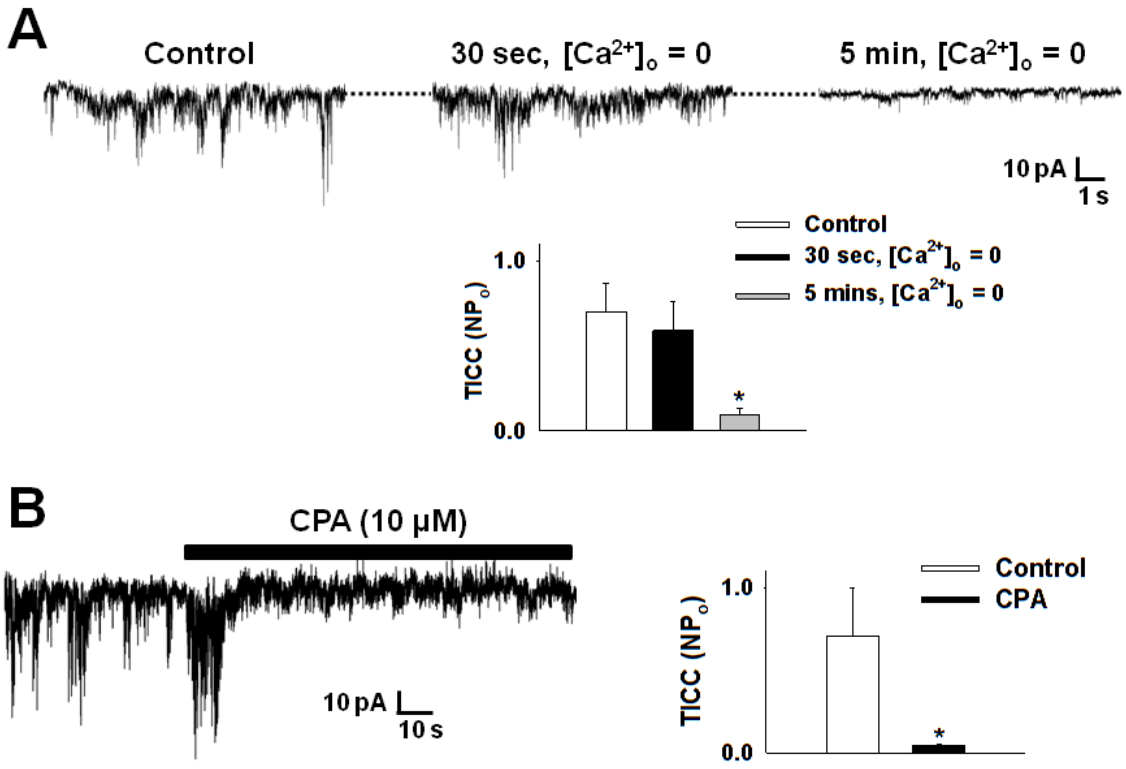

Figure 2.6: TICC are Activated by SR Ca^{2+} Release. A. Representative trace and summary data of TICC activity in the presence of extracellular Ca^{2+} (n=6) and at 30 sec [1] (n=6) and ~5 minutes [2] (n=6) after extracellular Ca^{2+} is removed. B: Representative trace and summary data of TICC activity in the presence of the SERCA pump blocker Cyclopiazonic acid (CPA, 10 µM, n=5).

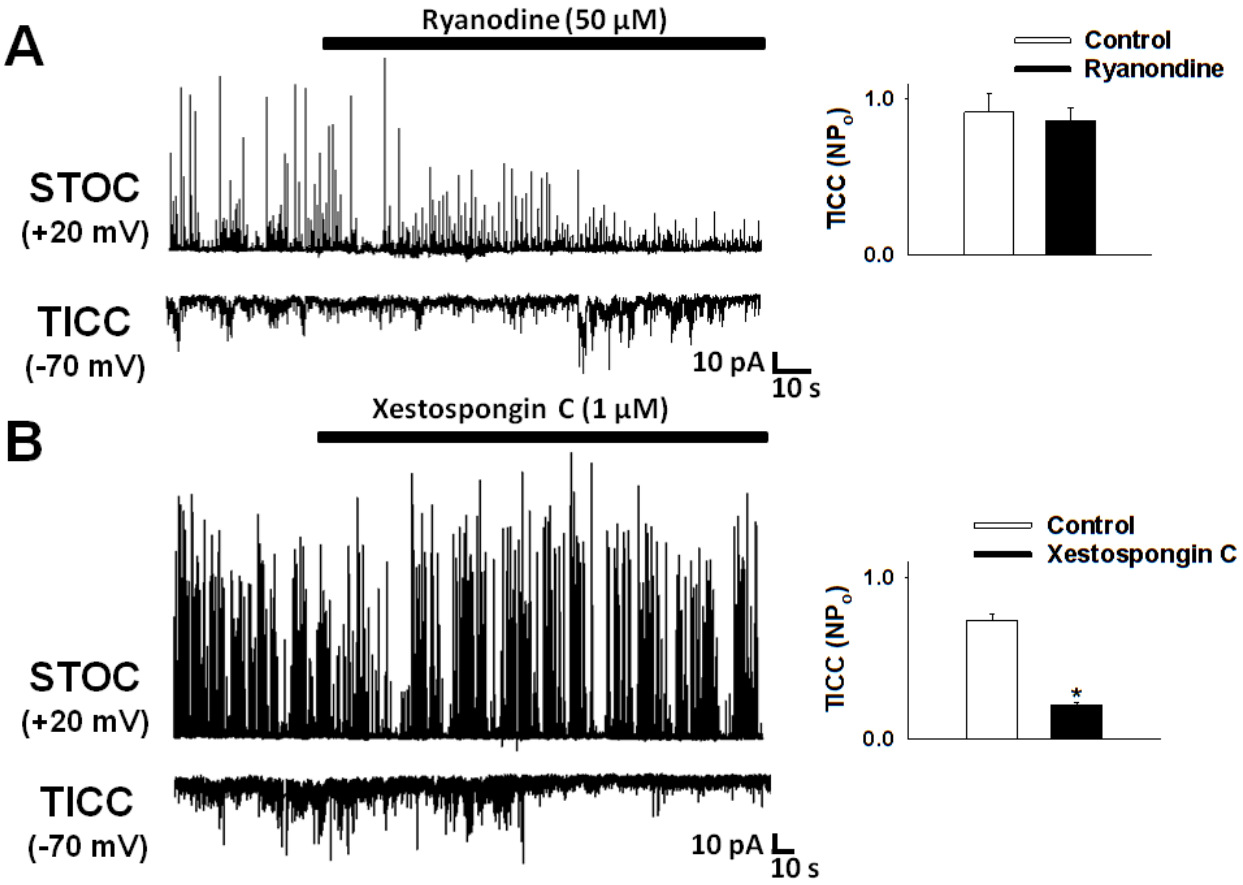

Figure 2.7: TICCs are Activated by IP_3R-dependent SR Ca^{2+} Release. A: Representative traces of STOC and TICC activity in the presence of the SR ryanodine receptor antagonist ryanodine (50 µM). Summary data of TICC NP_o (right, n=4). B: Representative traces of STOC and TICC activity in the presence of the IP_3R blocker Xestospongin C (1 µM). Summary data of TICC NP_o (right, n=5).

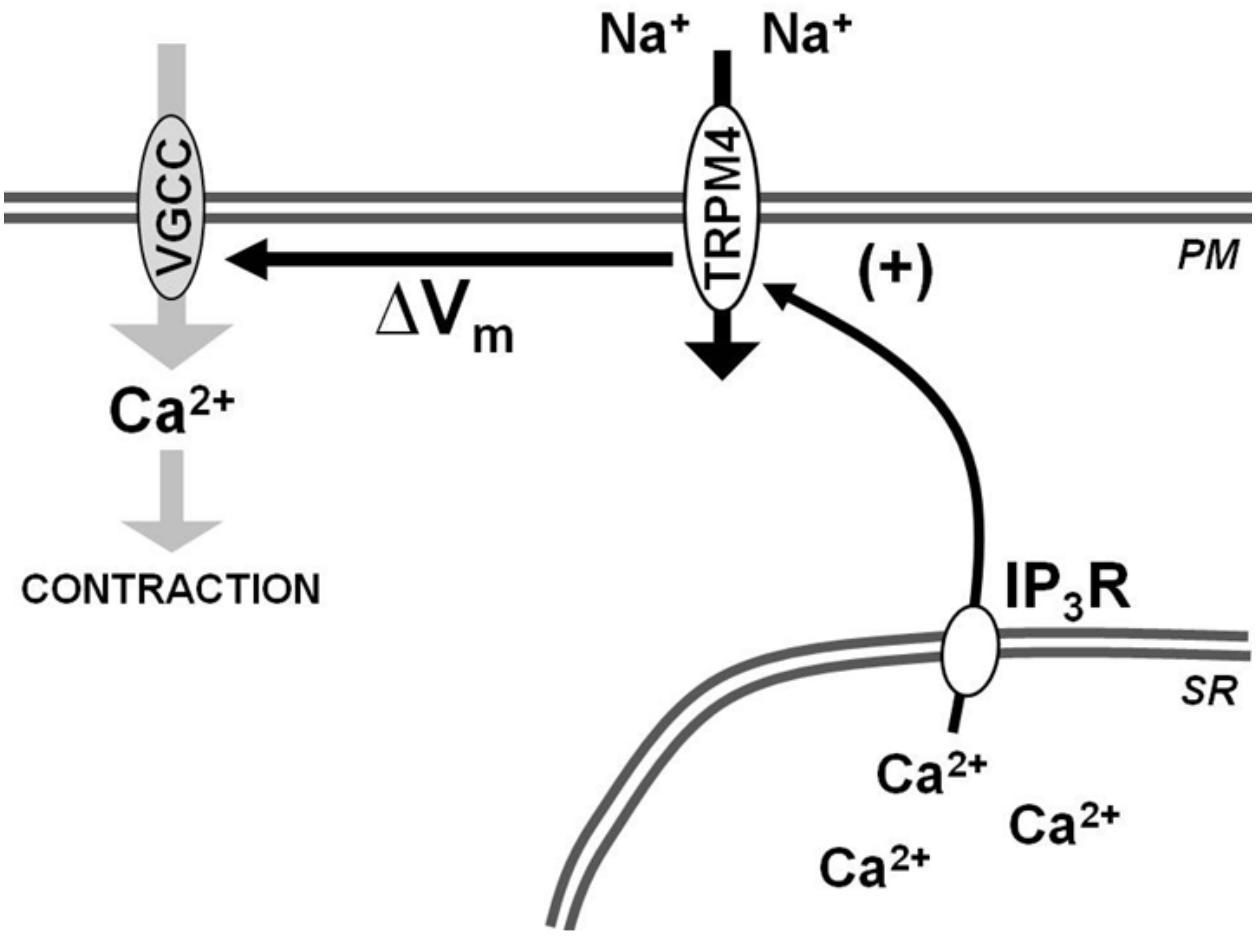

Figure 2.8: Activation of TRPM4 by IP_3R-Mediated SR Ca^{2+}. VGCC, voltage-gated calcium channels; ΔVm, change in membrane potential; TRPM4, transient receptor potential melastatin 4; PM, plasma membrane; SR, sarcoplasmic reticulum; IP_3R, inositol 1,4,5-trisphosphate receptor.

CHAPTER 3

Endogenous Cytosolic Ca^{2+} Buffering is Necessary for TRPM4 Activity in Cerebral Artery Smooth Muscle Cells

INTRODUCTION

The melastatin (M) Transient Receptor Potential (TRP) channel TRPM4 is a crucial mediator of pressure-induced vascular smooth muscle membrane depolarization and vasoconstriction, and is essential for autoregulation of cerebral blood flow (43, 58). High levels of intracellular Ca^{2+} (1-10 μM) are required for activation of TRPM4 (128), and under inside-out (28, 40, 43) or traditional whole cell patch configuration (40, 125), Ca^{2+} is introduced in order to activate and record TRPM4 currents. However, under these conditions TRPM4 also undergoes fast, Ca^{2+}-dependent inactivation, and currents decay to baseline levels within 3 minutes (40, 43, 94, 126, 132). TRPM4 channel activity can be rescued from inactivation by inhibition of phospholipase C (PLC) activity or by inclusion of the membrane phospholipid phosphatidylinositol 4,5-bisphosphate (PIP_2) in the intracellular solution (125, 202). These findings suggest that high global levels of Ca^{2+} used to record TRPM4 currents in traditional whole cell and inside-out patch clamp configurations activate a Ca^{2+}-dependent PLC isoform (153) that inactivates the channel by depleting PIP_2. It is possible that Ca^{2+}-dependent inactivation precludes observation of TRPM4 currents during patch clamp experiments, leading to under-estimation of channel activity under native conditions. We recently identified Transient Inward Cation Currents (TICCs) as sustained TRPM4 channel activity in freshly isolated smooth muscle cells (55). These currents can be

continuously recorded for as long as 30 minutes using the whole cell perforated patch clamp configuration (55), a method that restricts cell dialysis and causes minimal disruption of the intracellular environment, allowing global and local Ca^{2+} dynamics to function naturally. Thus, Ca^{2+}-dependent inactivation of TRPM4 may not be an inherent property of the channel itself but is a consequence of recoding methods. However, the mechanisms underlying this phenomenon are not clear. The goal of the current study is to determine how Ca^{2+}-dependent activation of TRPM4 currents is maintained in cerebral artery smooth muscle cells under native conditions.

Subcellular regions with Ca^{2+} levels much greater than the global [Ca^{2+}] result from Ca^{2+} influx from the extracellular space (115, 165) or from Ca^{2+} released from intracellular stores (15, 78, 79, 107, 201). The temporal and spatial characteristics of these small Ca^{2+} domains are shaped by the magnitude and duration of the initial Ca^{2+} signal, and by Ca^{2+} removal and intrinsic Ca^{2+} buffering within the cytosol (99). For example, the plasma membrane Ca^{2+}-ATPase (PMCA), the Na^{+}/Ca^{2+} exchange system, the sarco(endo)plasmic reticulum Ca^{2+}-ATPase (SERCA), and Ca^{2+} sequestering in the mitochondria and nucleus (99) all actively remove Ca^{2+} from the intracellular space. Additionally, cytosolic proteins, such as calmodulin, calpain, and troponin C, bind Ca^{2+} and limit the availability of free intracellular Ca^{2+} (184). These Ca^{2+} buffering mechanisms are essential for insuring the transient nature of intracellular Ca^{2+} signaling events by limiting spatial spread and preventing prolonged high cytosolic Ca^{2+} levels.

Localized, transient increases in cytosolic Ca^{2+} can directly activate Ca^{2+}-sensitive ion channels (78, 192) in vascular smooth muscle cells. Our laboratory

recently reported loss of TRPM4 channel activity following specific inhibition of the SR inositol Ca^{2+} release channel, 1,4,5-trisphosphate receptor (IP_3R) (55), suggesting that subcellular cytosolic Ca^{2+} domains also activate TRPM4 channels in the plasma membrane in native smooth muscle cells. However, the role of endogenous Ca^{2+} buffering in regulation of TRPM4 activity has not been reported. We hypothesized that under conventional whole cell conditions, loss of intrinsic cytosolic Ca^{2+} buffering following cellular dialysis contributes to Ca^{2+}-dependent inactivation of TRPM4 channels. To test this hypothesis, we examined the consequences of manipulating intracellular Ca^{2+} buffering on TRPM4 activity in freshly isolated cerebral myocytes. In the absence of cytosolic Ca^{2+} buffering, we found that TICC activity quickly dissipated with the same inactivation kinetics as recombinant TRPM4 activity recorded in the presence of high global Ca^{2+} under conventional whole cell conditions. Using conventional whole cell patch clamp electrophysiology, we recorded sustained, TICC-like currents (whole-cell TICCs) with ethylene glycol-bis(2-aminoethylether)-N,N,N′,N′-tetraacetic acid (EGTA) or 2-bis(o-aminophenoxy)ethane-N,N,N',N'-tetraacetic acid (BAPTA) added to the intracellular recording solution at concentrations (10 and 0.1 mM, respectively) that mimic the effects of endogenous Ca^{2+} buffering. These currents were pharmacologically and biophysically identical to TRPM4-dependent currents recorded under perforated patch clamp conditions. Higher concentrations of BAPTA abolished these currents, demonstrating that TRPM4 channels are present on the plasma membrane very near, but not physically coupled to, IP_3Rs. This conclusion is supported by TRPM4 and IP_3R immunolabeling experiments. This study demonstrates that intact

endogenous Ca^{2+} buffering is required to maintain TRPM4 channel activity in smooth muscle cells.

MATERIAL AND METHODS

Animals

Male Sprague-Dawley rats (250–350 g; Harlan) were used for these studies. Animals were deeply anesthetized with pentobarbital sodium (50 mg ip) and euthanized by exsanguination according to a protocol approved by the Institutional Animal Care and Use Committees (IACUC) of Colorado State University. Brains were isolated in cold 3-(N-morpholino) propanesulfonic acid (MOPS)-buffered saline (in mM): 3 MOPS (pH 7.4), 145 NaCl, 5 KCl, 1 $MgSO_4$, 2.5 $CaCl_2$, 1 KH_2PO_4, 0.02 EDTA, 2 pyruvate, and 5 glucose and 1% bovine serum albumin. Cerebral and cerebellar arteries were dissected from the brain, cleaned of connective tissue, and stored in MOPS-buffered saline prior to further manipulation.

A7r5 Cell Culture and Transient DNA Transfection

A7r5 cells (ATCC) were cultured in Dulbecco's 1X High Glucose Modified Eagle Medium (Gibco) supplemented with 10% fetal bovine serum (Gibco) and 0.5% penicillin-streptomycin (Gibco). Cells were maintained at 37°C with 6% CO_2, media was changed every two to three days, and cells were sub-cultured when confluent using 0.25% trypsin-EDTA (Gibco). A7r5 cells were transiently transfected with a plasmid encoding a TRPM4-GFP fusion protein (23) with the aid of Effectene Transfection Reagent (Qiagen) according to manufacturer's instructions for adherent cells. Media was

changed 24 hours after transfection, and cells were cultured for 1-2 days prior to electrophysiology experiments.

Isolation of Cerebral Artery Smooth Muscle Cells

Vessels were placed on ice in a magnesium-based physiological saline solution (Mg-PSS) containing (in mM) 5 KCl, 140 NaCl, 2 $MgCl_2$, 10 HEPES, and 10 glucose. Arteries were initially digested in 0.6 mg/mL papain (Worthington) and 1 mg/mL dithioerythritol at 37°C for 17 minutes, followed by a 15 minute incubation at 37°C in 1.0 mg/ml type II collagenase (Worthington). The digested segments were washed three times in ice-cold Mg-PSS solution and incubated on ice for 30 minutes. Following this incubation period, vessels were triturated to liberate smooth muscle cells and stored in ice-cold Mg-PSS for use. Smooth muscle cells were studied within 6 hours following isolation.

RNAi and Reversible Permeabilization

Small interfering RNAs (siRNA) against TRPM4 were used to down-regulate expression of the channel in isolated cerebral arteries (55). siRNA molecules purchased from Qiagen (1027280 [AllStars Negative Control], SI02868292 [Rn_Trpm4_1], and SI02868313 [Rn_Trpm4_4]) were dissolved as instructed at a concentration of 20 μM in siRNA Suspension Buffer. Control siRNA or TRPM4 siRNA molecules were introduced into intact cerebral arteries using a reversible permeabilization procedure. To permeabilize the arteries, segments were first incubated for 20 minutes at 4^{o}C in the following solution (in mM): 120 KCl, 2 $MgCl_2$, 10

EGTA, 5 Na_2ATP, and 20 TES; (pH 6.8). Arteries were then placed in a similar solution containing siRNA (40 nM) for 3 hours at 4°C and then transferred to a third siRNA-containing solution with elevated $MgCl_2$ (10 mM) for 30 minutes at 4°C. Permeabilization was reversed by placing arteries in a MOPS-buffered physiological siRNA-containing solution consisting of (in mM): 140 NaCl, 5 KCl, 10 $MgCl_2$, 5 glucose, and 2 MOPS; (pH 7.1) for 30 minutes at room temperature. Ca^{2+} was gradually increased in the latter solution from nominally Ca^{2+}-free to 0.01, 0.1, and 1.8 mM over a 45 minute period. Following these procedures, arteries were cultured for two to three days in D-MEM/F-12 culture media supplemented with L-glutamine (2 mM) (Gibco), and 0.5% penicillin-streptomycin (Gibco). Arteries were then used for smooth muscle cell isolation.

Immunocytochemistry and Membrane Staining.

Cells were enzymatically dissociated from cerebral vessels as described above, and allowed to adhere to glass slides for 20 minutes at 4°C. Cells were fixed with 4% formaldehyde for 10 minutes, permeabilized with cold methanol (-80°C), blocked with 2% bovine serum albumin, and incubated with primary antibodies overnight at 4°C. The following primary antibodies were used as appropriate: goat anti-TRPM4 at 1:50 (sc-27540, Santa Cruz) and rabbit anti-IP3R at 1:50 (AB1622, Chemicon). Cells were subsequently washed and incubated with appropriate fluorescent secondary antibody for 2 hours at room temperature. The following secondary antibodies were used as appropriate; anti-rabbit conjugated to Texas Red, (sc-2780, Santa Cruz) and anti-goat conjugated to FITC, (sc-2704, Santa Cruz). Membrane specific fluorescent staining

was performed using 5 µg/mL ER-Tracker™ Green (Invitrogen), 5 µg/mL ER-Tracker™ Red (Invitrogen), or 5 µg/mL CellMask™ Deep Red (Invitrogen). For specific plasma membrane staining, cells were incubated in CellMask™ Deep Red in Mg-PSS for 10 minutes at 37°C. For specific SR membrane staining, cells were incubated in ER-Tracker™ Green or ER-Tracker™ Red in MgPSS for 30 minutes at 37°C. For dual membrane staining, the cells were incubated in ER membrane stain, washed, and incubated in plasma membrane stain. For simultaneous immunocytochemistry and membrane staining, fixed cells were first immunolabeled for the appropriate protein and then incubated in the specific membrane stain. Fluorescent images were obtained using a spinning disk confocal microscope (Andor) and a 100x oil immersion objective. Excitation of Texas Red and FITC was by illumination with the 543-nm line and 488-nm line, respectively. Immunofluorescence was not detected in cells probed with secondary antibody alone. All images were acquired at 1024x1024 pixels and were analyzed using Volocity 6.0 (PerkinElmer).

General Electrophysiological Recordings

Currents were recorded using an AxoPatch 200B amplifier equipped with an Axon CV 203BU headstage (Molecular Devices). Recording electrodes (1-3 MΩ) were pulled, polished, and coated with wax to reduce capacitance. Currents were filtered at 1 kHz, digitized at 40 kHz, and stored for subsequent analysis. Clampex and Clampfit versions 10.2 (Molecular Devices) were used for data acquisition and analysis, respectively. All experiments were performed at room temperature (22°C).

Electrophysiological Recording Solutions

Macroscopic whole cell currents from HEK 293 cells transfected with TRPM4-GFP were recorded in external bathing solution containing (in mM): 146 NaCl, 5 $CaCl_2$, 10 HEPES, and 10 Glucose (pH = 7.4). The bathing solution was supplemented with the potassium channel blocker TEA (10 mM). The pipette solution contained (in mM): 146 CsCl, 1 $MgCl_2$, 10 HEPES and 0.1$CaCl_2$. TICC activity recorded under perforated patch clamp conditions was performed in external bathing solution containing (in mM): 134 NaCl, 6 KCl, 1 $MgCl_2$ 2 $CaCl_2$, 10 HEPES, and 10 glucose at pH 7.4 (NaOH). The pipette solution contained (in mM): 110 K-aspartate, 1 $MgCl_2$, 30 KCl, 10 NaCl, 10 HEPES, and 5 µM EGTA at pH 7.2 (NaOH). TICC activity recorded under whole-cell patch clamp conditions was performed in external bathing solution containing (in mM): 140 NaCl, 5 CsCl, 2 $CaCl_2$, 1 $MgCl_2$, 10 HEPES, and 10 glucose at pH of 7.4 (NaOH). The pipette solution contained (in mM): 20 CsCl, 87 K-aspartate, 1 $MgCl_2$, 5 MgATP, and 10 HEPES (pH 7.2, CsOH). External solution with the K^+ channel blocker tetraethylammonium (TEA) contained (in mM): 130 NaCl, 10 TEA, 5 CsCl, 2 $CaCl_2$, 1 $MgCl_2$, 10 HEPES, and 10 glucose at pH 7.4. Additional external solutions include, Na^+-free external solution containing (in mM): 140 N-methyl-D-glucamine (NMDG), 5 $CsCl_2$, 1 $MgCl_2$, 2 $CaCl_2$, 10 HEPES, 10 glucose at pH 7.4 (HCl); and Ca^{2+} free external solution containing (in mM): 130 NaCl, 5 $CsCl_2$ 1 $MgCl_2$ 0.73 $CaCl_2$, 1 EGTA, 10 HEPES, and 10 glucose at pH 7.4 (NaOH).

Electrophysiological Recordings from TRPM4-Expressing A7r5 Cells

Conventional whole cell patch clamp studies were conducted using non-transfected A7r5 cells or cells transiently transfected with TRPM4-GFP (23). Transfected cells were identified by the presence of green fluorescence. Cells were initially held at a membrane potential of 0 mV. Currents were measured during voltage ramps between -100 and +100 mV (time of ramp) repeated every 4 seconds.

Electrophysiological Recordings from Isolated Smooth Muscle Cells

Freshly isolated cerebral artery smooth muscle cells were placed into a recording chamber (Warner Instruments) and allowed to adhere to glass coverslips for 20 minutes at room temperature. GΩ seals were obtained in Mg-PSS. For perforated whole cell patch clamp recordings, amphotericin B (40 μM) was included in the pipette solution. Perforation was deemed acceptable if series resistance was less than 50 MΩ. For conventional whole cell patch clamp recordings, isolated smooth muscle cells were voltage clamped at a membrane potential (E_m) of -70 mV. In our recording solutions, the calculated reversal potential for total monovalent cations is 7.7 mV and -48.9 mV for monovalent anions (Cl^-). TICC activity at -70 mV was calculated as the sum of the open channel probability (NP_o) of multiple open states with unitary amplitude of 1.75 pA (i.e. 1 open state). This value was based on the reported unitary conductance of TRPM4 (25 pS).

Channel open probability (NP_o) was calculated using the following equation:

$$NP_o = \sum_{j=1}^{N} \frac{(t_j \cdot j)}{T}$$

Where:

t_j = time spent in seconds with j = 1,2,….N channels open

N = max number of channels observed

T = duration of measurement.

Calculations and Statistics

All data are means ± SE. Values of n refer to the number of cells for patch clamp experiments. Data were compared as indicated using paired t-tests or one-way repeated measures analysis of variance (ANOVA). A level of $P \leq 0.05$ was accepted as statistically significant for all experiments. All peak amplitude histograms were constructed using Origin 8.1 (OriginLab Corp.).

RESULTS

Disruption of the Intracellular Environment Leads to Ca^{2+}-Dependent TRPM4 Inactivation.

Under traditional whole cell patch clamp configurations, TRPM4 currents recorded from recombinant channels expressed in HEK 293 cells, or from native channels in freshly isolated cerebral artery myocytes, exhibit rapid, Ca^{2+}-dependent inactivation (40, 128). To better characterize the time course of TRPM4 inactivation we compared recombinant macroscopic TRPM4 currents from smooth muscle-derived A7r5

cells and native TRPM4 channel activity in freshly-isolated smooth muscle cells. Currents were obtained from A7r5 cells transfected with TRPM4-GFP (23) using the conventional whole cell configuration with 100 μM Ca^{2+} included in the patch pipette solution. As expected, in the presence of high cytosolic Ca^{2+} levels, cation currents exhibited outward rectification and rapid inactivation (Figure 1A). Peak TRPM4-GFP currents (black arrowhead, n=5) decreased by 26 ± 6% at 8 seconds (grey arrowhead) and 60 ± 5% at 60 seconds (white arrowhead). These findings are consistent with previous reports of TRPM4 channel activity in HEK 293 cells (40, 128) and demonstrate that recombinant TRPM4 channel currents in A7r5 cells quickly dissipate following prolonged exposure to high global Ca^{2+}.

In native cerebral artery smooth muscle cells patch clamped under perforated patch conditions (leaving the intracellular environment undisturbed), TRPM4 currents manifest as TICCs. TICCs can be recorded under perforated patch conditions for as long as seal integrity can be maintained. We recorded TICC activity under perforated patch clamp conditions (PP, Figure 3.1B) and TICC-like currents under conventional whole cell patch clamp (WC, Figure 3.C) configuration without the addition of Ca^{2+} to the pipette solution. TICCs recorded under perforated patch conditions did not inactivate, while under whole cell conditions we observed time-dependent decay of TICC-like activity. Activity decreased by 16 ± 10% at 10 seconds and by 64 ± 6% at 60 seconds following cellular dialysis. The time course of inactivation of whole cell TRPM4 currents recorded from A7r5 cells (Figure 3.1A) and the decay of TICC activity in native cerebral artery smooth muscle cells (Figure 3.1B) are identical (Figure 3.1C), suggesting that inactivation results from a common mechanism. Furthermore, these

findings are consistent with the hypothesis that in freshly isolated smooth muscle cells patch clamped under whole cell conditions, cytosolic Ca^{2+} levels are increased following cellular dialysis, disruption of the intracellular environment, and loss of intrinsic Ca^{2+} buffering.

EGTA Emulates Endogenous Cytosolic Ca^{2+} Buffering.

To examine the hypothesis that loss of intracellular Ca^{2+} buffering capacity during cellular dialysis under conventional whole cell conditions results in TRPM4 inactivation, we used established software (CalC version 6.0, (102)) to model the effects of different concentrations of the slow Ca^{2+} buffer EGTA on the linear spread of Ca^{2+}released from a single IP_3R (Ca^{2+} puff). The current strength and on- and off-times of Ca^{2+} puffs were assumed to be 0.2 pA, 17 ms, and 100 ms, respectively, (18, 171) and resting, free global Ca^{2+} was assumed to be 200 nM with a diffusion coefficient of 200 μMs^{-1} (5). Ca^{2+} movements during three buffering states were modeled: no buffering, endogenous smooth muscle cell buffering, and buffering with EGTA. As a first order approximation, we modeled endogenous cytosolic Ca^{2+} buffering capacity of a cell with the mean of reported values (Table 1) for the most abundant Ca^{2+} binding protein calmodulin (CaM) at a reported concentration of 40 µM in smooth muscle cells (203). Additionally, our model used the reported values for the diffusion coefficient, Ca^{2+} affinity, dissociation constant, and Ca^{2+} on- and off-rates for CaM and EGTA (Table 1) (5, 47, 112, 164, 203) and compared the diffusion of free Ca^{2+} within model cells containing different concentrations of EGTA with those of cells with endogenous buffering.

In cells modeled with endogenous Ca^{2+} buffering, Ca^{2+} levels decreased logarithmically with distance from the Ca^{2+} source (Figure 3.2). Cells modeled with no Ca^{2+} buffering elicit a nearly linear relationship between [Ca^{2+}] and the distance traveled from the Ca^{2+} source (Figure 3.2). Thus, in the absence of Ca^{2+} buffering, Ca^{2+} levels are greater at any given point away from the Ca^{2+} source than what is predicted for native endogenous buffering conditions. The no buffer condition models the conventional whole-cell patch clamp conditions used for the recording shown in Figure 3.1B, resulting in time-dependent inactivation of TRPM4 currents. Thus, it is possible that TRPM4 inactivation under these conditions results from loss of endogenous Ca^{2+} buffering. The effects of EGTA were also examined in our modeling experiments. These findings predict that at a concentration of 10 mM the buffering capacity of EGTA has the same effect on the spatial spread of Ca^{2+}, up to 100 nm, as projected for endogenous intracellular Ca^{2+} buffers (Figure 3.2).

Sustained TRPM4 Currents Under Conventional Whole Cell Patch Clamp Conditions.

To test the hypothesis that depletion of Ca^{2+} buffering contributes to Ca^{2+}-dependent inactivation of TRPM4, we compared channel activity recorded in cerebral arterial myocytes under perforated and conventional whole cell configuration with EGTA (10 mM) included in the pipette. Under perforated patch clamp conditions, TICCs have a frequency of 20.1 ± 1.6 Hz (n = 5) (Figure 3.3A). To better characterize the channel activity, a peak amplitude histogram was constructed (Figure 3.3B) and 5 peaks (solid line) were identified at -1.70, -3.43, -5.02, -6.5, and -8.49 pA and are consistent with the calculated unitary current amplitude for 1 (-1.7 pA), 2 (-3.4 pA), 3 (-5.1 pA), 4 (-6.8 pA),

and 5 (-8.5 pA) TRPM4 channel openings as well as our previous findings (55). These currents were compared to those recorded using the whole cell configuration with 10 mM EGTA added to the pipette solutions. Currents recorded under these conditions (Figure 3.3C) are reminiscent of TICCs recorded under perforated patch clamp conditions (Figure 3.3A). For clarity, we refer to TICC-like currents recorded using the conventional whole cell configuration as “whole-cell TICCs”. Whole-cell TICCs have a frequency of 20.1 ± 2.0 Hz (n = 5) (Figure 3.3C). A peak amplitude histogram was constructed (Figure 3.3D) and 4 peaks (solid line) were identified with the calculated current amplitude for multiple TRPM4 channel openings. The peaks in the histogram occur at -1.7, -3.3, -5.1, and -6.8 pA and are consistent with the calculated unitary current amplitude for TRPM4 and peaks we observed under perforated patch clamp conditions (Figure 3.3B). The correspondence of event frequency and peak amplitude histograms between the two methods suggests that whole-cell TICCs are identical to TICCs recorded under the perforated patch clamp conditions.

Biophysical properties of whole-cell TICCs were compared with those of TICCs recorded under perforated patch clamp conditions and TRPM4 currents recorded using conventional whole cell and inside-out configurations. To rule out the influence of K^+ channels, recordings were made in the presence of the broad-spectrum K^+ channel blocker tetraethylammonium (TEA, 10 mM). TEA had no effect on the total open probability (NP_o) of current activity (n=4), demonstrating that these cation currents are independent of K^+ channel activity (Figure 3.4A). Whole-cell TICCs were eliminated when Na^+ in the bathing solution was replaced with the non-permeable cation N-methyl-D-glucamine (NMDG) (Figure 3.4B), indicating that currents are conducted by Na^+ ions,

consistent with the selectivity of TRPM4 for monovalent cations. To examine the voltage dependence of whole-cell TICCs, currents were recorded in the presence of TEA and at different holding potentials, with the mean current amplitude (I) plotted as a function of membrane potential (V). Similar to the I/V relationships reported for TRPM4 obtained under conventional conditions (40, 128), whole-cell TICCs displayed modest inward and outward rectification, and reversed at 5-10 mV, consistent with the reversal potential for monovalent cations (7.7 mV) calculated for solutions used in these experiments (Figure 3.4C).

Pharmacological TRPM4 inhibitors were employed to provide further evidence that whole-cell TICCs result from TRPM4 channel activity. Fluflenamic acid reportedly inhibits TRPM4 (EC_{50} = 2.8 µM) and TRPM5 (EC_{50} = 24.5 µM) currents (186). Whole-cell TICC activity was diminished following the administration of fluflenamic acid (10 µM) (Figure 3.5A). The selective TRPM4 blocker 9-phenanthrol (30 µM) also attenuated whole-cell TICC activity (Figure 3.5B). At the concentration used for this study, 9-phenanthrol inhibits TRPM4 and not TRPM5 (60), TRPC3, TRPC6, BK_{Ca}, K_{IR}, K_V, and L-type Ca^{2+} channels (58). These findings demonstrate that whole-cell TICC activity is suppressed by TRPM4 blockers, suggesting that these currents are carried by TRPM4 channels.

To provide additional evidence for a link between TRPM4 and whole-cell TICCs, TRPM4 expression was silenced using siRNA. We previously reported that TRPM4 siRNA specifically downregulates TRPM4 mRNA and protein expression but had no effect on TRPC3 or TRPC6 expression (55). We found that whole-cell TICCs were present in arterial smooth muscle cells isolated from arteries treated with control siRNA,

whereas treatment with TRPM4-specific siRNA nearly abolished these currents (Figure 3.5C). Thus, whole-cell TICCs have properties similar to TICCs recorded under perforated patch clamp conditions and TRPM4 currents recorded using conventional methods. Furthermore, whole-cell TICC activity is attenuated by TRPM4 blockers and diminished in cells treated with TRPM4 siRNA. These finding indicate that the molecular identity of the channel responsible for whole-cell TICCs in native smooth muscle cells is TRPM4. More importantly, our findings indicate that restoration of intracellular Ca^{2+} buffering to endogenous levels is sufficient to prevent Ca^{2+}-dependent inactivation of TRPM4, suggesting that endogenous Ca^{2+} buffers are essential for preventing TRPM4 channel inactivation in smooth muscle cells under native conditions.

Whole-Cell TICCs are Activated by IP_3R-dependent SR Ca^{2+} Release.

A prior study from our lab showed that in cerebral artery smooth muscle cells patch clamped in the perforated patch configuration, TRPM4 is activated by Ca^{2+} release from IP_3R (55). To examine Ca^{2+}-dependent activation of TRPM4 channels under cytosolic EGTA-buffered conditions, we recorded whole-cell TICC activity following the removal of extracellular Ca^{2+} and during pharmacological manipulation of SR Ca^{2+} stores. Removal of extracellular Ca^{2+} did not acutely disrupt whole-cell TICC activity, but extended exposure (3 minutes) to Ca^{2+}-free bathing solution resulted in decreased activity (Figure 3.6A). Following disruption of SR Ca^{2+} stores by the inhibition of SERCA pumps with cyclopiazonic acid (CPA, 30 µM), we observed a decrease in whole-cell TICC activity (Figure 3.6B), suggesting that SR Ca^{2+} release is still necessary for activation of TRPM4 channels under these conditions. Consistent

with our previous report (55), inhibition of ryanodine receptors by ryanodine (50 μM) had no effect (Figure 3.6D), while blocking IP_3R with Xestospongin C (1 μM) greatly attenuated whole-cell TICC activity (Figure 3.6C). To further characterize the role of IP_3R, we employed the membrane permeable IP_3 analog, Bt-IP_3 (200) to activate IP_3R. We observed a dose-dependent increase in TICC activity in the presence of Bt-IP_3 (Figure 3.6E), which was blocked in the presence of Xestospongin C. These data provide additional evidence for the activation of TRPM4 by Ca^{2+} released from IP_3R. Overall, these findings suggest that inclusion of EGTA (10 mM) in the pipette solution does not disrupt activation of TRPM4 by IP_3R-mediated Ca^{2+} release but does provide sufficient buffering capacity to prevent rapid Ca^{2+}-dependent inactivation of the channel.

Whole-Cell TICC Activity is Modulated by the Cytosolic Buffering with BAPTA.

Our findings show that the activation of plasma membrane TRPM4 channels by Ca^{2+} released from IP_3Rs on the SR membrane is not blocked when EGTA (10 mM) is included in the intracellular solution, suggesting that the two channels are in close proximity. The effectiveness of Ca^{2+} buffers within a given volume is dependent on the Ca^{2+} affinity, binding rates, and mobility of the buffer (112). EGTA and BAPTA have similar mobility and steady-state binding affinities for Ca^{2+} (Table 1) and differ only in the binding kinetics, i.e. BAPTA binds Ca^{2+} approximately 100 times faster than EGTA (116). Comparing the buffering effectiveness of BAPTA versus an identical concentration of EGTA has previously been used to estimate the volume buffered within the range of tens of nanometers (46, 116). To further characterize the Ca^{2+} domains between IP_3Rs and TRPM4, we modeled the effects of different concentrations of

BAPTA on the linear spread of Ca^{2+} released from a single IP_3R, as described above. We used buffering parameters previously reported for the diffusion coefficient, Ca^{2+} affinity, dissociation constant, and Ca^{2+} on- and off-rates for BAPTA (Table 1) (112). With an intracellular [BAPTA] of 0.1 mM, our model predicts that the spatial spread of Ca^{2+} from a point source will be nearly identical to that of an endogenous buffering environment, whereas when [BAPTA] was increased to 10 mM, our model predicts that the spatial spread of Ca^{2+} is much more restricted (Figure 3.7).

To test the predictions of our cytosolic Ca^{2+} buffering model we examined Ca^{2+}-dependent activation and inactivation of TRPM4 channel activity. Different concentrations of EGTA and BAPTA were included in the pipette solution, and whole-cell TICC activity was recorded from freshly isolated cerebral artery myocytes. A graphical representation of the hypothesized effects of these buffering conditions on Ca^{2+} levels at the plasma membrane and TRPM4 activity is shown in Figure 3.8B. We found that when EGTA (10 mM) and BAPTA (0.1 mM), which emulate the effects of endogenous Ca^{2+} buffering (Figure 3.8B), were included in the pipette solution, whole-cell TICC activity did not differ from that observed when cells were patch clamped under perforated patch conditions (Figure 3.8A). When EGTA was included in the patch pipette at concentrations lower than 10 mM, whole-cell TICC activity was significantly less than that recorded under perforated patch conditions (Figure 3.8A), suggesting that buffering under these conditions was insufficient to prevent Ca^{2+}-dependent inactivation of TRPM4 channel activity (Figure 3.8B). Inclusion of BAPTA at 1 or 10mM diminished channel activity (Figure 3.8A), suggesting that TRPM4 channels are located very near to, but are not physically coupled with IP_3Rs (2, 3). Our model predicts that

the spatial spread of Ca^{2+} is restricted under these conditions (Figure 3.8B), suggesting that Ca^{2+} levels within the plasma membrane and SR junctions are insufficient to activate channel activity. These data demonstrate, in agreement with our modeling predictions, that EGTA (10 mM) and BAPTA (0.1 mM) are sufficient to restore endogenous Ca^{2+} buffering lost during cellular dialysis under whole cell patch clamp conditions and can prevent rapid Ca^{2+}-dependent inactivation of the channel.

TRPM4 and IP_3R are Proximate.

Our functional electrophysiological data suggest that the activation of plasma membrane TRPM4 channels by Ca^{2+} released from IP_3Rs on the SR membrane requires that the two channels and membranes be in close proximity. To test this idea and assess the relative localization of TRPM4 and IP_3R in cerebral artery myocytes, isolated cells were immunolabeled with TRPM4 and IP_3R-specific antibodies, and the SR and plasma membranes were fluorescently stained with selective dyes. In cells stained with selective dyes, the SR membrane is plainly visible and is clearly separated from the plasma membrane, demonstrating dye specificity and the close proximity of the two membranes (Figure 3.9A, insert a). Separation of the SR membrane from the plasma membrane is apparent in intensity plots along a line segment as distinct fluorescence peaks corresponding to the plasma (red) and SR (green) membranes (Figure 3.9A, insert b). When immunolabeling and membrane staining are combined, we observe that TRPM4 channels are localized to the plasma membrane, and IP_3Rs are expressed in the SR membrane approaching the plasma membrane (Figure 3.9B-E). Dual immunolabeling experiments confirm the proximal localization of TRPM4

channels and IP_3R at distinct junction sites (Figure 3.9F, inserts a and b). These findings demonstrate the presence of SR to plasma membrane (SR/PM) junctions where IP_3R channels are present in the SR membrane proximal to TRPM4 channels localized in the plasma membrane.

DISCUSSION

The current study demonstrates the importance of endogenous intracellular Ca^{2+} buffering for maintaining TRPM4 activity in cerebral artery myocytes. Our major findings are: (1) restoration of endogenous Ca^{2+} buffering capacity lost when native smooth muscle cells are dialyzed under conventional whole cell conditions prevents time-dependent inactivation of whole-cell TICCs; (2) the biophysical properties of whole-cell TICCs are consistent with those of TICCs recorded using the perforated patch clamp configuration and TRPM4 currents recorded using conventional methods; (3) the pharmacological and molecular profile of currents recorded under whole-cell conditions indicates that these novel currents are conducted by TRPM4 channels; and (4) high concentrations of BAPTA can extinguish the Ca^{2+} signaling required for the activation of TRPM4, suggesting that TRPM4 channels are not physically coupled to IP_3R but are located within 50 nm. These findings demonstrate for the first time that cytosolic Ca^{2+} buffering influences membrane excitability by maintaining and modulating TRPM4 channel activity in native cerebral artery smooth muscle cells.

Many of the biophysical and pharmacological characteristics of the novel whole-cell TICCs reported here are identical to those we previously reported for TICCs recorded under perforated patch clamp conditions (55), and those described for TRPM4 channels recorded under conventional patch clamp conditions. For example, whole-cell

TICCs recorded from native cerebral artery myocytes have the same frequency of occurrence (20.1 ± 2.0 Hz, n = 5) as TICCs recoded under perforated patch clamp conditions (20.1 ± 1.7 Hz, n = 5) and are in agreement with the reported unitary conductance of TRPM4 (134, 138, 199). Whole-cell TICCs reversed at a membrane potential near 0 mV in symmetrical cationic solutions and substitution of Na^+ with the impermeant cation NMDG in the bathing solution completely blocked channel activity, consistent with TRPM4's selectivity for monovalent cations (40, 128). We also found that whole-cell TICC activity was significantly less following administration of TRPM4 blockers, including the selective compound 9-phenanthrol (55, 58, 60), and in cells isolated from arteries treated with TRPM4-specific siRNA. Thus, we conclude that TICCs recorded under our whole cell conditions represent authentic TRPM4 activity in native cerebral artery myocytes.

The current findings indicate that the I/V relationship of TRPM4 is strongly influenced by the patch clamp configuration. Single channel recordings for TRPM4 obtained from inside-out patches in symmetrical cation solutions have a linear current to voltage relationship (43), while currents obtained using the conventional whole-cell configuration with similar solutions are dually rectifying (40, 128). In our previous work, we reported that under perforated patch clamp conditions with physiological bathing solution, TICCs exhibited modest inward rectification at negative potentials and a small non-rectifying outward current at positive potentials (55). In the current study, whole-cell TICC activity exhibits dual rectification, similar to that observed under conventional whole cell recording conditions. These discrepancies are likely a result of cellular dialysis. TRPM4 currents are blocked by the endogenous polyamine spermine (133),

which is removed by dialysis under whole cell conditions. Polyamine block is responsible for rectification of inwardly-rectifying K^+ (K_{IR}) channels in vascular smooth muscle cells (135, 175), and we propose that this effect accounts for TRPM4 current rectification under native conditions.

TRPM4 activity is necessary for pressure-induced smooth muscle vasoconstriction *in vitro* (40, 43, 58) and autoregulation of cerebral blood flow *in vivo* (151), demonstrating that the channel is a critical mediator of vascular function. However, rapid Ca^{2+}-dependent desensitization of TRPM4 currents when recorded under conventional whole cell and inside-out patch clamp conditions hindered our understanding of the regulatory mechanisms of the channel under native conditions. TRPM4 activity can be prolonged by inhibition of PLC or by inclusion of the PIP_2 in the intracellular solution (126, 202). These findings suggest that high intracellular Ca^{2+}levels (10-100 μM) typically used to initiate and record TRPM4 current in conventional whole cell and inside-out configurations activates a Ca^{2+}-dependent PLC isoform, leading to TRPM4 inactivation by depleting PIP_2 levels. Additionally, TRPM4 activity does not inactivate when recorded under perforated patch clamp conditions when the cytosolic environment is maintained (55, 71). In the current study, we investigated the role of endogenous Ca^{2+} buffering in this process and found that when Ca^{2+} buffers are not present in the intracellular solution, whole-cell TICCs exhibit time-dependent inactivation with kinetics similar to those observed for TRPM4-expressing cultured cells patch clamped using the whole cell configuration and with 100 μM free Ca^{2+} included in the intracellular solution (Figure 3.1). We hypothesized that when endogenous free Ca^{2+} buffering mechanisms are disrupted during cell dialysis under

conventional whole cell conditions, increases in cytosolic [Ca^{2+}] resulting from intrinsic Ca^{2+} influx or release from the SR can also cause Ca^{2+}-dependent inactivation of TRPM4. To test this possibility, we modeled the effects of endogenous Ca^{2+} buffers on the spatial spread of Ca^{2+} from a point source. The endogenous and exogenous buffering parameters used for our model are based on values reported in the literature, which have a wide range and may over- or under-estimate buffering capacity. Additionally, the model is based on buffering parameters for whole cell conditions, which may differ from those within specific subcellular nano or microdomains. Lastly, as a first order approximation, we only considered the endogenous buffering parameters of the most abundant Ca^{2+} binding protein, calmodulin, at a total intracellular concentration of 40 µM (159, 203). However, even with the possible inaccuracies of our model, we were able to accurately predict that addition of 10 mM EGTA or 0.1 mM BAPTA to the intracellular solution restores TRPM4 activity to that observed under native Ca^{2+} buffering conditions in the perforated patch configuration. Thus, these findings suggest that levels of calmodulin, and perhaps other Ca^{2+}-binding proteins like calpain and troponin C, together would equal a buffering capacity similar to 10 mM EGTA. Furthermore, if only free Ca^{2+} binding proteins are lost during cellular dialysis under whole cell conditions, our findings suggest that anchored Ca^{2+} homeostasis-important ion channels like PMCA, Na^+/Ca^{2+} exchangers, and SERCA pumps play a minor role in preventing the Ca^{2+}-dependent inactivation of TRPM4 channels under physiological conditions. Additionally, physical interaction of calmodulin with the c-terminus of TRPM4 is essential for Ca^{2+} sensitivity and activation of the channel in physiological range of intracellular Ca^{2+} concentrations (131). Our ability to rescue channel activity

following cell dialysis suggests that calmodulin required for channel activation is constitutively bound to the channel itself and not free within the cytoplasm. This is consistent with work from Nilius *et al.*, reporting five possible Ca^{2+}-dependent calmodulin interacting domains on TRPM4, two at the n-terminus and three at the c-terminus (131). Our findings clearly demonstrate that maintenance of TRPM4 activity is a novel role for free endogenous Ca^{2+} buffering proteins, a property that may regulate critical features of smooth muscle cell excitability and contractility.

Proper maintenance of SR Ca^{2+} stores is necessary for many cellular functions. SERCA pumps actively siphon Ca^{2+} from the cytoplasm back into the SR lumen, refilling internal Ca^{2+} stores. This process of recycling Ca^{2+} is important for maintaining the transmembrane Ca^{2+} gradient of low cytosolic and high SR lumen Ca^{2+} levels. Inhibition of the SERCA pumps by CPA disrupts the Ca^{2+} refilling of the SR, and Ca^{2+} is leaked from internal stores into the cytoplasm, disrupting the Ca^{2+} gradient. In many types of cells, SR Ca^{2+} store depletion activates store operated Ca^{2+} entry channels (SOCs) (146). However, in the current study, we did not record SOC activity following the depletion of internal Ca^{2+} stores with CPA. This observation is consistent with prior studies that failed to demonstrate SOC activity in contractile cerebral artery smooth muscle cells (87, 147, 158, 197, 200). Consistent with our previous reports using perforated patch clamp (55), whole-cell TICC activity quickly decreased following the pharmacological inhibition of SERCA pumps by CPA (30 μM). It seems likely that depletion of SR Ca^{2+} stores translates to a loss of Ca^{2+} release and decreased activation of Ca^{2+}-sensitive ion channels. For example, the large conductance Ca^{2+}-activated potassium channel (BK_{Ca}) is stimulated by Ca^{2+} release from ryanodine

receptors located on the SR membrane to produce spontaneous transient outward currents (STOCs) (79, 121). Store depletion significantly decreases Ca^{2+} dependent activation of BK_{Ca} channels and STOC activity is abolished within 40-120 seconds following CPA administration (20, 170, 179). Thus, the time required for BK_{Ca} inactivation in response to CPA is similar to that observed for TRPM4 inactivation following this treatment in the current study, suggesting that loss of TRPM4 activity results from diminished SR Ca^{2+}-release. Alternatively, it is possible that CPA-induced Ca^{2+} leak from internal stores elevates $[Ca^{2+}]$ within small cytoplasmic spaces proximal to the plasma membrane to levels that lead to Ca^{2+}-dependent inactivation of TRPM4 channels. Consistent with this possibility, reports using fluorescent Ca^{2+} indicators in smooth muscle cells show an immediate increase in cytosolic Ca^{2+}, presumably due to Ca^{2+} leak from the SR, reaching maximum $[Ca^{2+}]_i$ within 40 - 300 seconds (65, 80). This subsequent increase in global calcium may lead to TRPM4 channel inactivation and the relative rapid loss of TICC activity. Regardless of the exact mechanisms, our findings clearly show that intact SR Ca^{2+} stores are required for TRPM4 activity in native cerebral artery myocytes.

Differential modulation of TRPM4 channel activity by the slow Ca^{2+} buffer EGTA and the fast Ca^{2+} buffer BAPTA provides strong evidence that TRPM4 channels are proximal and functionally coupled with IP_3R through Ca^{2+} signaling events. BAPTA and EGTA have similar steady-state Ca^{2+} binding affinities, but significantly different binding rate constants (Table 1) (5). Based on this divergence, comparison of BAPTA- and EGTA-dependent disruptions of Ca^{2+}-dependent processes can be used to classify localized regions of elevated Ca^{2+} as "Ca^{2+} nanodomains" or "Ca^{2+} microdomains" (7,

46, 116). Ca^{2+} microdomains, with a Ca^{2+} source-to-sensor distance of greater than 50 nm, are defined by Ca^{2+}-dependent responses that are equally disrupted by identical concentrations of BAPTA and EGTA (7, 116). In contrast, Ca^{2+} nanodomains, with a Ca^{2+} source-to-sensor distance less than 50 nm, are defined by Ca^{2+}-dependent responses that are significantly interfered with by BAPTA, but not by equal concentrations of EGTA (7, 116). Our findings demonstrating that whole-cell TICC activity can be recorded in the presence of 10 mM EGTA but not in 10 mM BAPTA suggest that IP_3R-mediated activation of TRPM4 channels occur in Ca^{2+} nanodomains, and that TRPM4 channels and IP_3R are less than 50 nm apart. The current estimate of the junctional spaces between plasma membrane caveolae and SR membrane projections is 15 ± 7 nm (53, 145). Therefore, our findings suggest that IP_3R and TRPM4 channels are localized within these small spaces. Additionally, recent studies have reported physical coupling of IP_3R and the canonical TRP channel, TRPC3, through the caveolae scaffolding protein caveolin-1 in smooth muscle cells (2, 3, 200). Inhbition of whole-cell TICCs by Ca^{2+} chelation with BAPTA provides electrophysiological evidence that plasma membrane TRPM4 channels are not physically coupled to IP_3R located in the SR, but rather are activated by Ca^{2+} release events from IP_3R located less than 50 nm away from TRPM4 channels on the plasma membrane.

In conclusion, our findings suggest that endogenous intracellular Ca^{2+} buffering and SR Ca^{2+} recycling are essential for maintenance of TRPM4 channels activity in cerebral artery smooth muscle cells. Furthermore, we demonstrate that IP_3R-mediated activation of TRPM4 channels occur within Ca^{2+} nanodomains created by SR/plasma

membrane junctions. Lastly, the regulation of smooth muscle cytosolic Ca^{2+} buffering and the SR/plasma membrane architecture play integral roles in excitability and arterial function through modulation of TRPM4 channel activity.

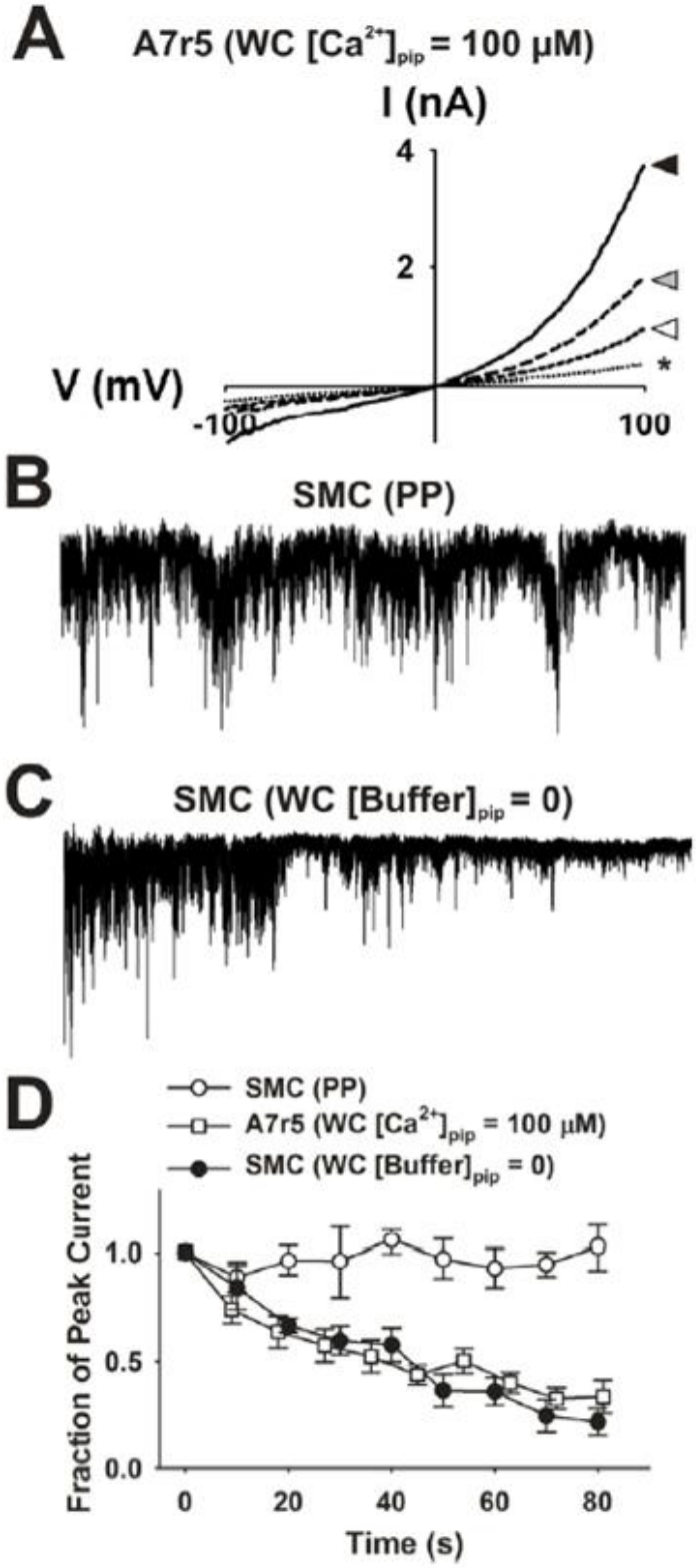
A
A7r5 (WC [Ca2+]pip = 100 µM)
I (nA)
4
2
V (mV)
-100
100
*
B
SMC (PP)
C
SMC (WC [Buffer]pip = 0)
D
SMC (PP)
A7r5 (WC [Ca2+]pip = 100 µM)
SMC (WC [Buffer]pip = 0)
Fraction of Peak Current
1.0
0.5
0.0
0
20
40
60
80
Time (s)

Figure 3.1: The Kinetics of Ca^{2+}-Dependent TRPM4 Desensitization are Similar in A7r5 and Freshly Isolated Smooth Muscle Cells. A: Current/Voltage (I/V) relationship showing total current at 8 (grey arrowhead) and 60 seconds (white arrowhead) after peak (black arrowhead) in A7r5 cells expressing TRPM4-GFP and non-transfected cells (*). Cells were recorded under conventional whole cell patch clamp conditions (WC) with 100 µM Ca^{2+} added to the pipette solution. B: Representative trace of Transient Inward Cation Currents (TICC) activity recorded from a freshly isolated cerebral artery smooth muscle cell (SMC) under perforated whole cell patch clamp conditions (PP). Membrane potential = -70 mV. C: Representative trace of TICC-like activity recorded from a freshly isolated cerebral artery smooth muscle cell under conventional whole cell patch clamp conditions when no Ca^{2+} buffer is present in the intracellular solution. Membrane potential = -70 mV. D: Time course of inactivation of TRPM4 currents (at +70 mV) in A7r5 cells (n=6), TICC activity recorded under perforated patch clamp conditions (n=8), and TICC-like currents recorded under whole-cell conditions in native myocytes (n=5) as a fraction of the peak current following cellular dialysis.

Table 3.1. Modeling Buffering Parameters

Parameters	Endogenous	BAPTA	EGTA
Diffusion Coefficient ($\mu m^2 s^{-1}$)	20	220	200
Ca^{2+} affinity (K_d) (nM)	200	150	150
Dissociation constant β_F/α_F (μM)	10	0.22	0.15
Ca^{2+} On-rate α_F ($\mu M^{-1} s^{-1}$)	1	400	5
Ca^{2+} Off-rate β_F (s^{-1})	10	80	0.75

References: (5, 25, 47, 72, 84, 112, 164)

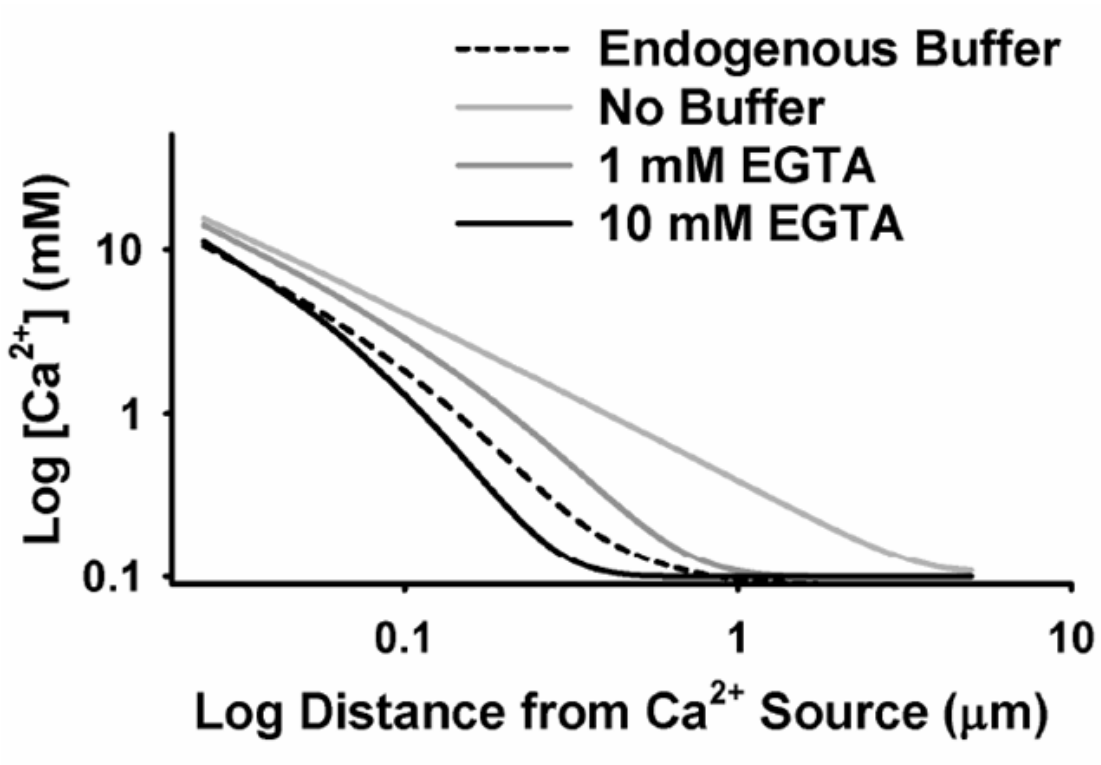

Figure 3.2: Endogenous Ca^{2+} Buffering Can be Mimicked with EGTA. Modeling the effects of endogenous buffering capacity and different concentrations (1 and 10 mM) of the slow Ca^{2+} chelator EGTA on $[Ca^{2+}]$ as a function of distance from a single IP_3R Ca^{2+} release site.

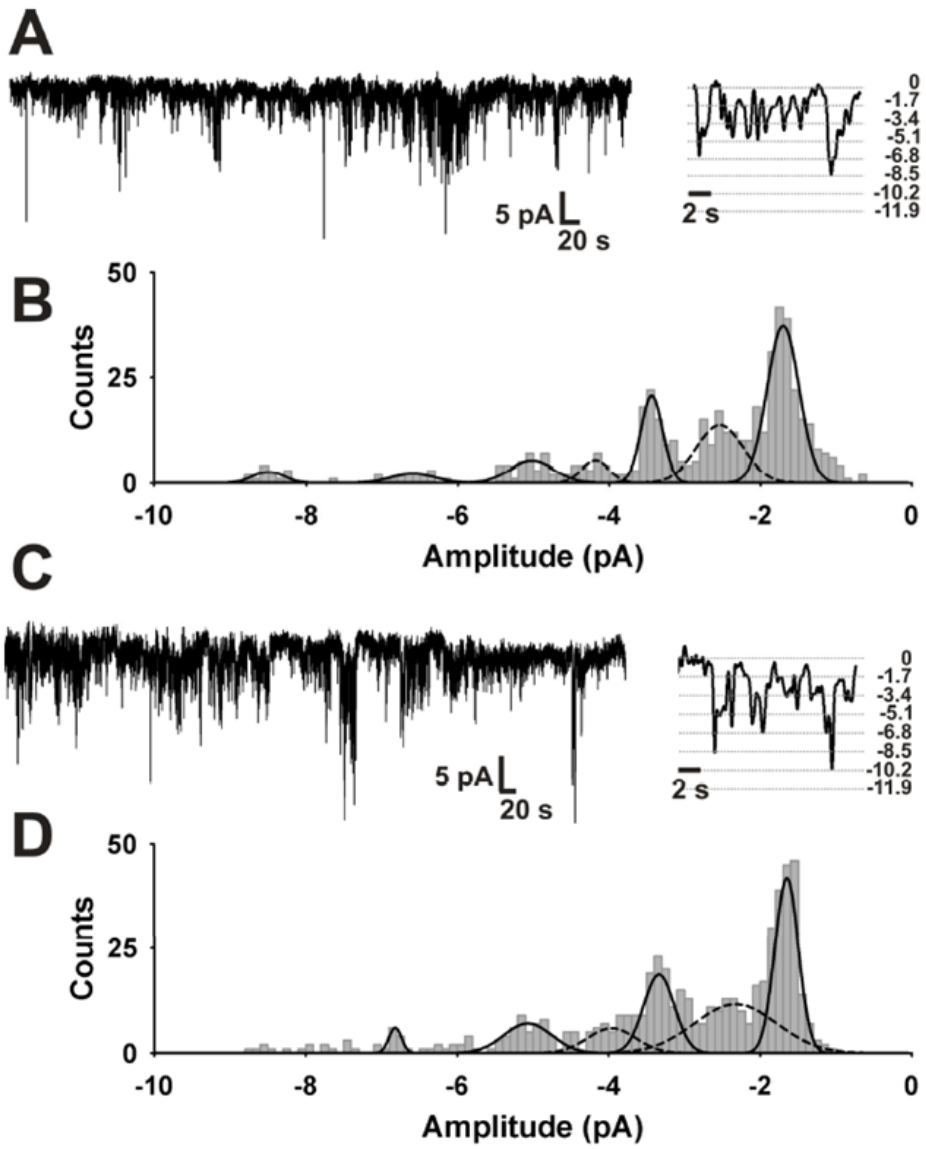

Figure 3.3: Sustained Transient Cation Channel Activity in Freshly Isolated Smooth Muscle Cells. A: Representative perforated patch clamp recordings of Transient Inward Cation Currents (TICC) obtained using the amphotericin B perforated patch configuration. Representative of 5 cells. Insert shows expanded time scale. B: Peak amplitude histogram of TICC activity recorded from freshly isolated smooth muscle (0.1 pA bins) under perforated patch clamp conditions. Data are fitted with multiple Gaussian functions. The solid-line peaks match calculated current amplitude for TRPM4 channel openings. The dash-line peaks do not match with calculated current amplitude for TRPM4 channel openings. C: Representative conventional whole cell patch clamp recording of whole-cell TICC activity with 10 mM EGTA included in the pipette solution. D: Peak amplitude histogram of whole-cell TICC activity recorded from freshly isolated smooth muscle (0.1 pA bins) with 10 mM EGTA in the pipette solution. Data are fitted with multiple Gaussian functions, with the solid-line and dash-line peaks matching and not matching, respectively, with the calculated current amplitude for TRPM4 channel openings.

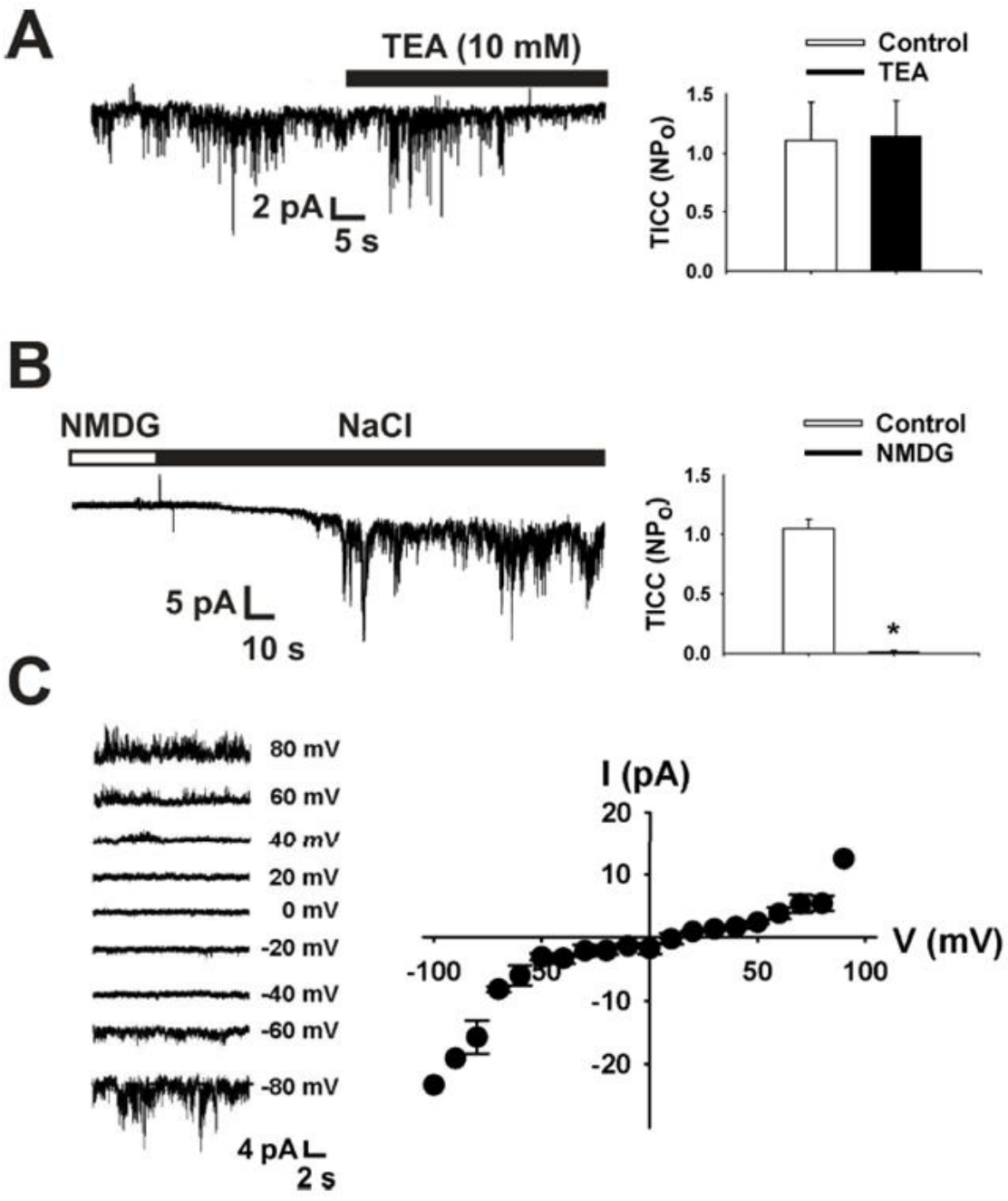

Figure 3.4: Biophysical Properties of Whole-Cell TICC Activity. A: Representative trace and summary data of whole-cell TICC activity in the presence of the tetraethylammonium (TEA) (10 mM, n=4). B: Representative trace and summary data of whole-cell TICC activity with Na^+ replaced with the non-permeabale cation N-methyl-D-glucamine (NMDG), n=9, *P≤0.05 vs. Control. C: Sample traces of whole-cell TICC recordings obtained at holding potentials (V_H) from +80 to -70 mV in the presence of TEA. Average current amplitude to voltage relationship (I/V) for cells (n=3-5) with symmetrical total cations solutions under whole cell patch clamp conditions.

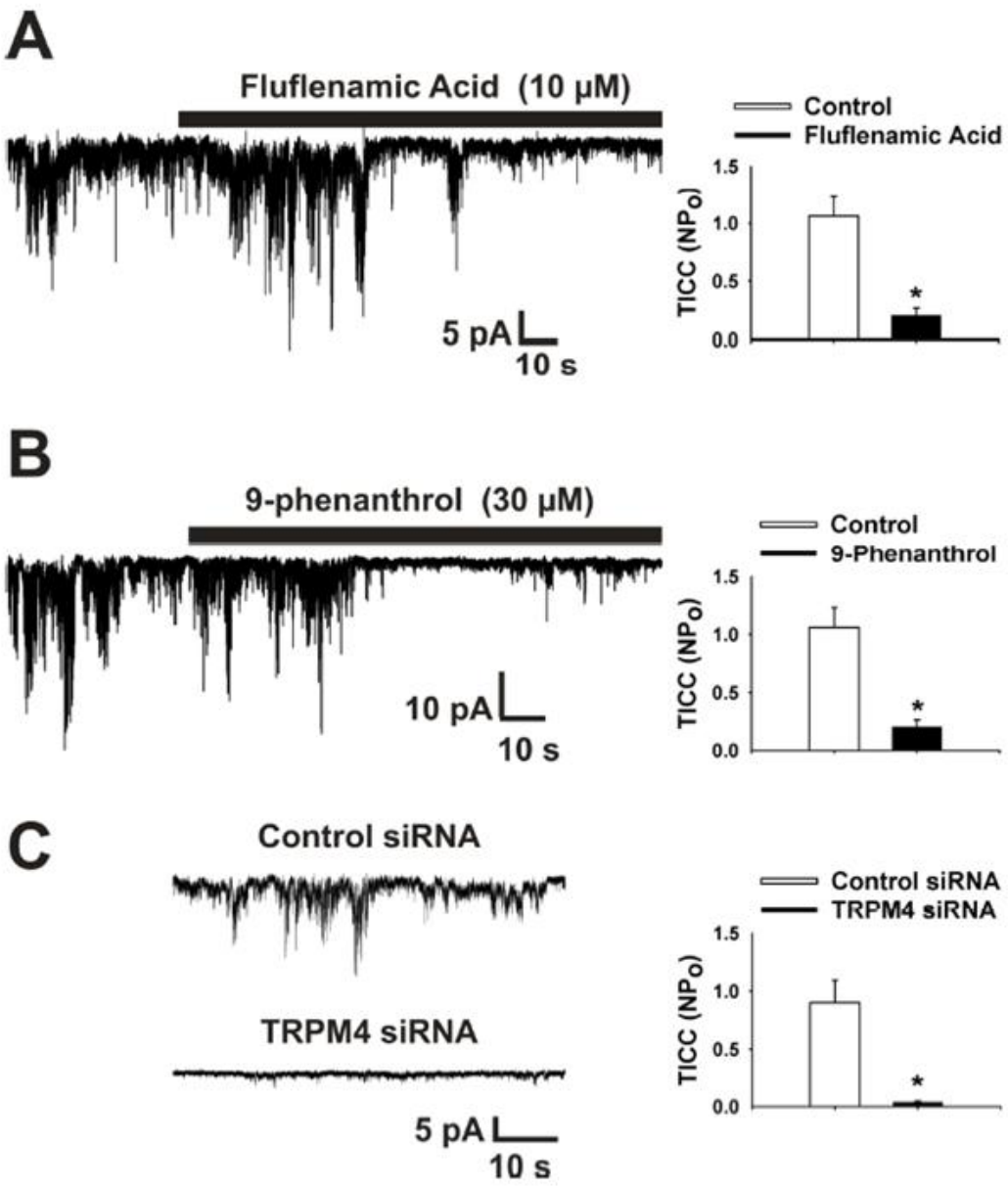

Figure 3.5: Whole-Cell TICCs Represent TRPM4 Channel Activity. A: Representative trace and summary data of whole-cell TICC activity in the presence of fluflenamic acid (10 µM, n=3), a blocker of TRPM4 activity. B: Representative traces and summary data of whole-cell TICC activity in the presence of the selective TRPM4 blocker 9-phenanthrol (30 µM, n=3). *P≤0.05 vs. control. C: Representative recordings and summary data of whole-cell TICC activity from a cell isolated from arteries treated with control (top; n=10) and TRPM4 (bottom n=10) siRNA. *P≤0.05 vs. control siRNA.

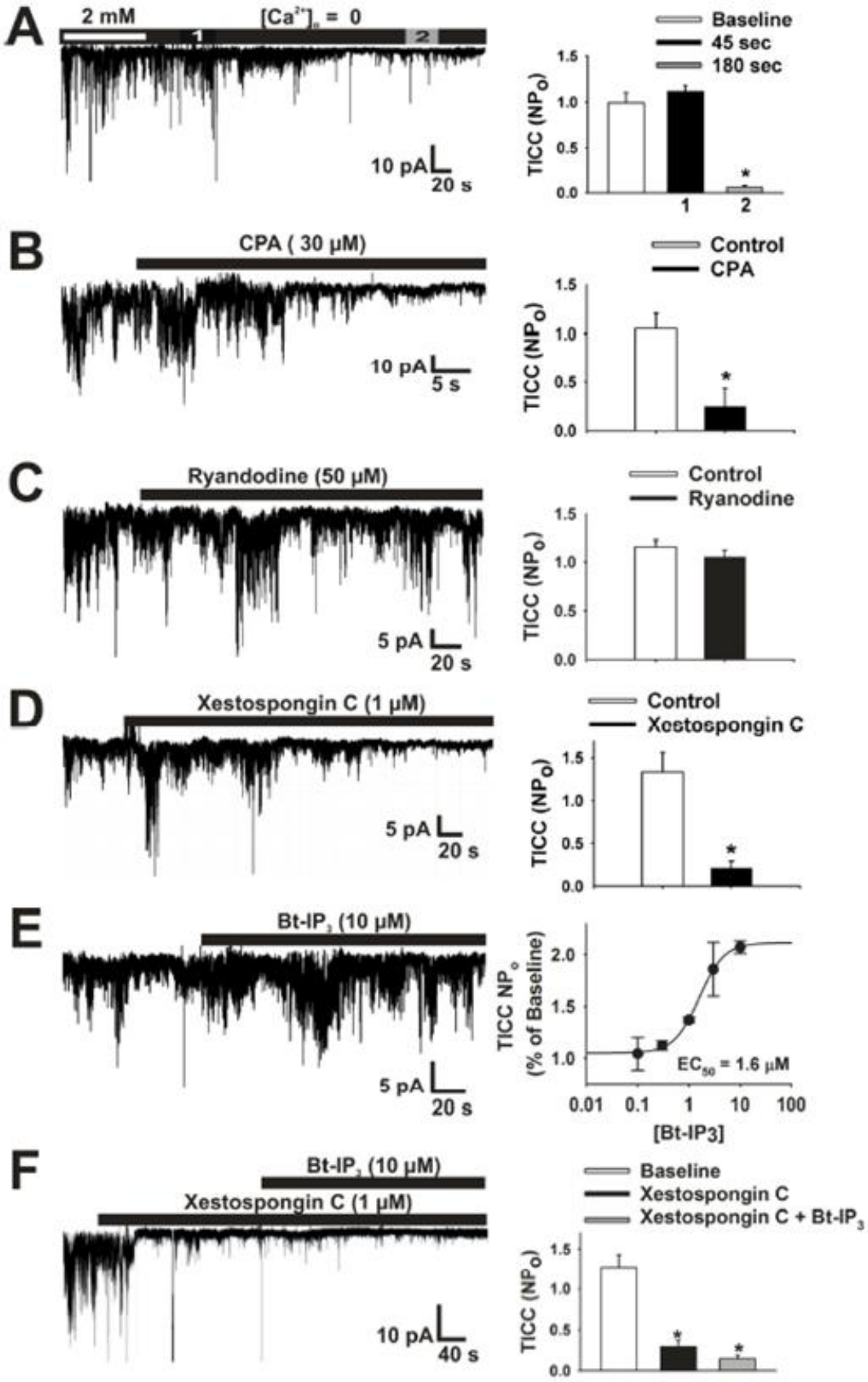
A
2 mM
[Ca2+]o = 0
1
2
10 pA
20 s
Baseline
45 sec
180 sec
TICC (NPo)
1.5
1.0
0.5
0.0
*
1
2
B
CPA (30 µM)
10 pA
5 s
Control
CPA
TICC (NPo)
C
Ryandodine (50 µM)
5 pA
20 s
Control
Ryanodine
D
Xestospongin C (1 µM)
5 pA
20 s
Control
Xestospongin C
E
Bt-IP3 (10 µM)
5 pA
20 s
TICC NPo
(% of Baseline)
2.0
EC50 = 1.6 µM
0.01
0.1
1
10
100
[Bt-IP3]
F
Bt-IP3 (10 µM)
Xestospongin C (1 µM)
10 pA
40 s
Baseline
Xestospongin C
Xestospongin C + Bt-IP3

Figure 3.6: Whole-Cell TICCs are Activated by IP_3R-dependent SR Ca^{2+} Release. A: Representative trace and summary data of whole-cell TICC activity in the presence of extracellular Ca^{2+} (n=4) and at 45 sec [1] (n=4) and ~3 minutes [2] (n=3) after extracellular Ca^{2+} is removed. B: Representative trace and summary data of whole-cell TICC activity in the presence of the SERCA pump blocker cyclopiazonic acid (CPA, 30 µM, n=3). C: Representative trace and summary data of whole-cell TICC activity in the presence of the specific ryanodine receptor blocker ryanodine (50 µM, n=3). D: Representative trace and summary data of whole-cell TICC activity in the presence of the specific IP_3R blocker Xestospongin C (1 µM, n=3). *P≤0.05 vs. control. E: Representative trace and dose response of the effects of the membrane permeable IP_3 analog, Bt-IP_3 (10 µM) on whole-cell TICC activity (EC_{50} = 1.6 µM); n = 3-5 per dose. F: Representative trace and summary data of whole-cell TICC activity in the presence of Xestospongin C (1 µM, n=3), and Bt-IP_3 (10 µM, n=4). *P≤0.05 vs. control.

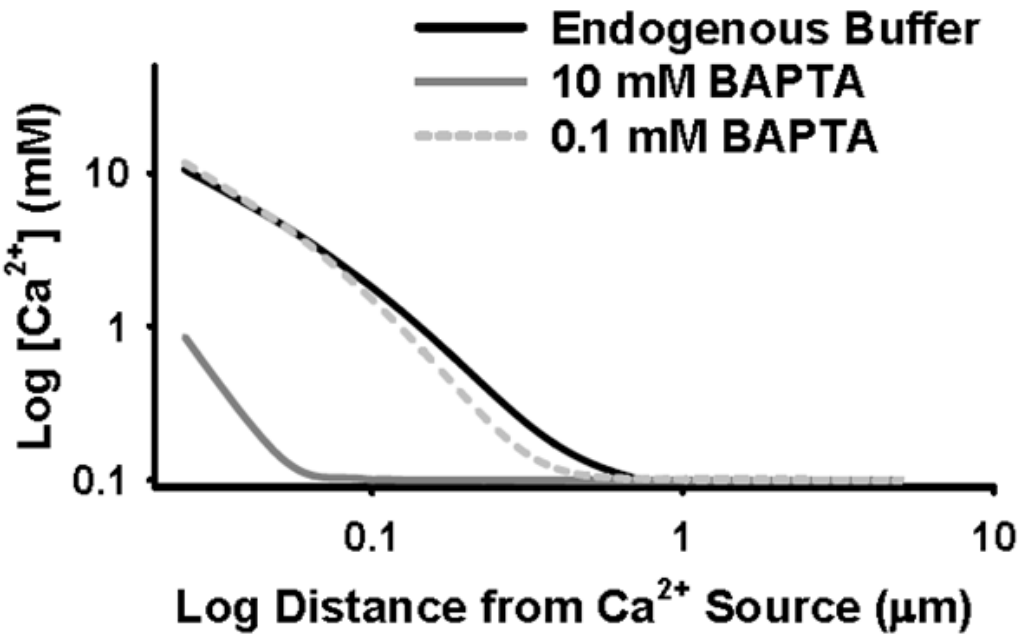

Figure 3.7: Endogenous Ca^{2+} Buffering Can be Mimicked with BAPTA. Modeling the effects of endogenous buffering capacity and different concentrations (0.1 and 10 mM) of the fast Ca^{2+} chelator BAPTA on $[Ca^{2+}]$ as a function of distance from a single IP_3R Ca^{2+} release site.

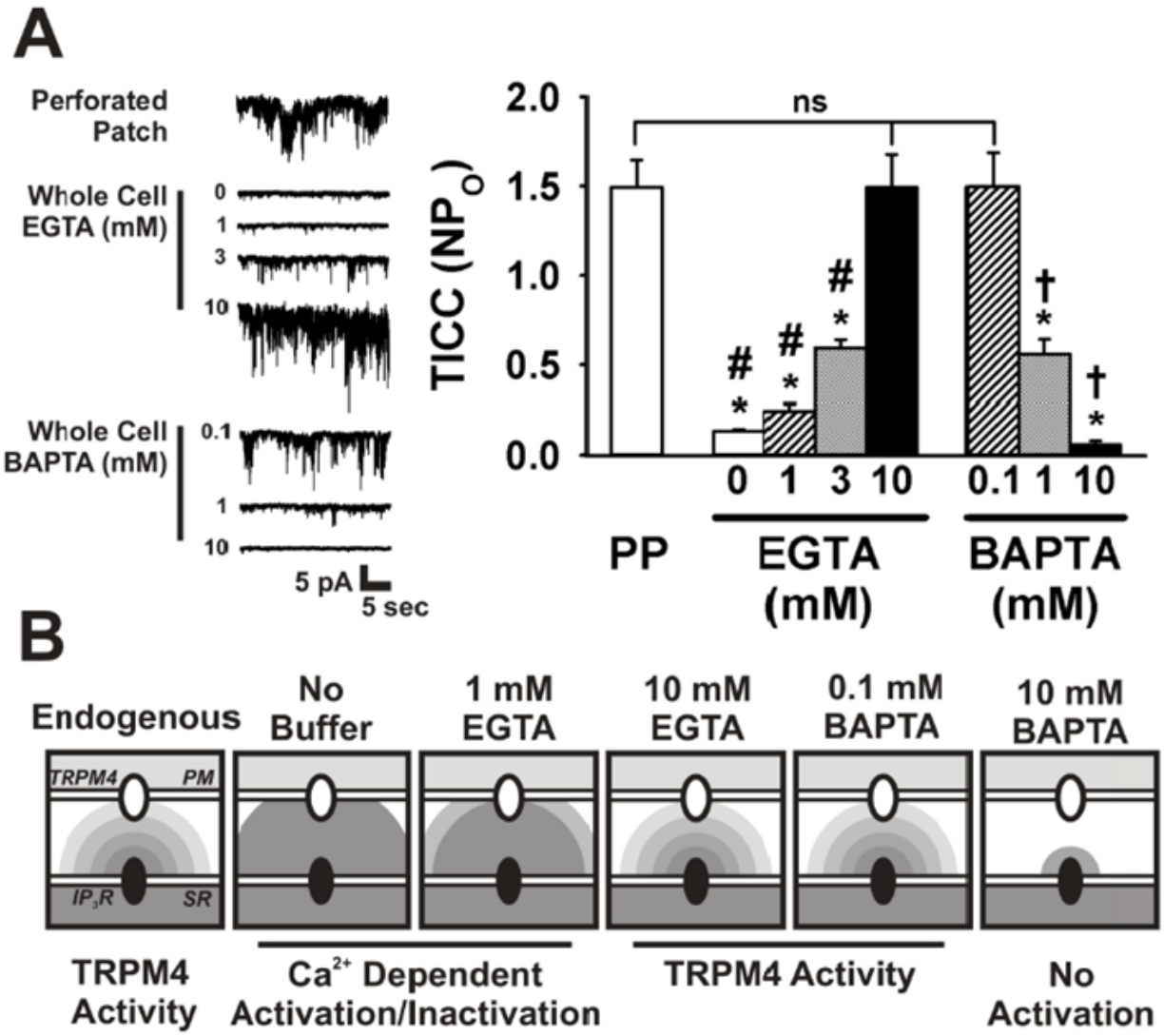

Figure 3.8: Effects of Buffer Concentration on Whole-Cell TICC Activity. A: Representative traces of channel activity from recordings under perforated patch clamp (PP) and whole-cell configuration with different concentration of EGTA or BAPTA added to the pipette solution. B: Summary data showing average total open probabilities (NP_o) of whole-cell TICC activity at different concentrations of Ca^{2+} buffers; n = 5-7 per group. *P≤0.05 vs. PP, #P≤0.05 vs. 10 mM EGTA, and †P≤0.05 vs. 0.1 mM BAPTA. C: Schematic representation of the Ca^{2+} spread and hypothetical activation and inactivation of TRPM4 following the Ca^{2+} release from a single IP_3R.

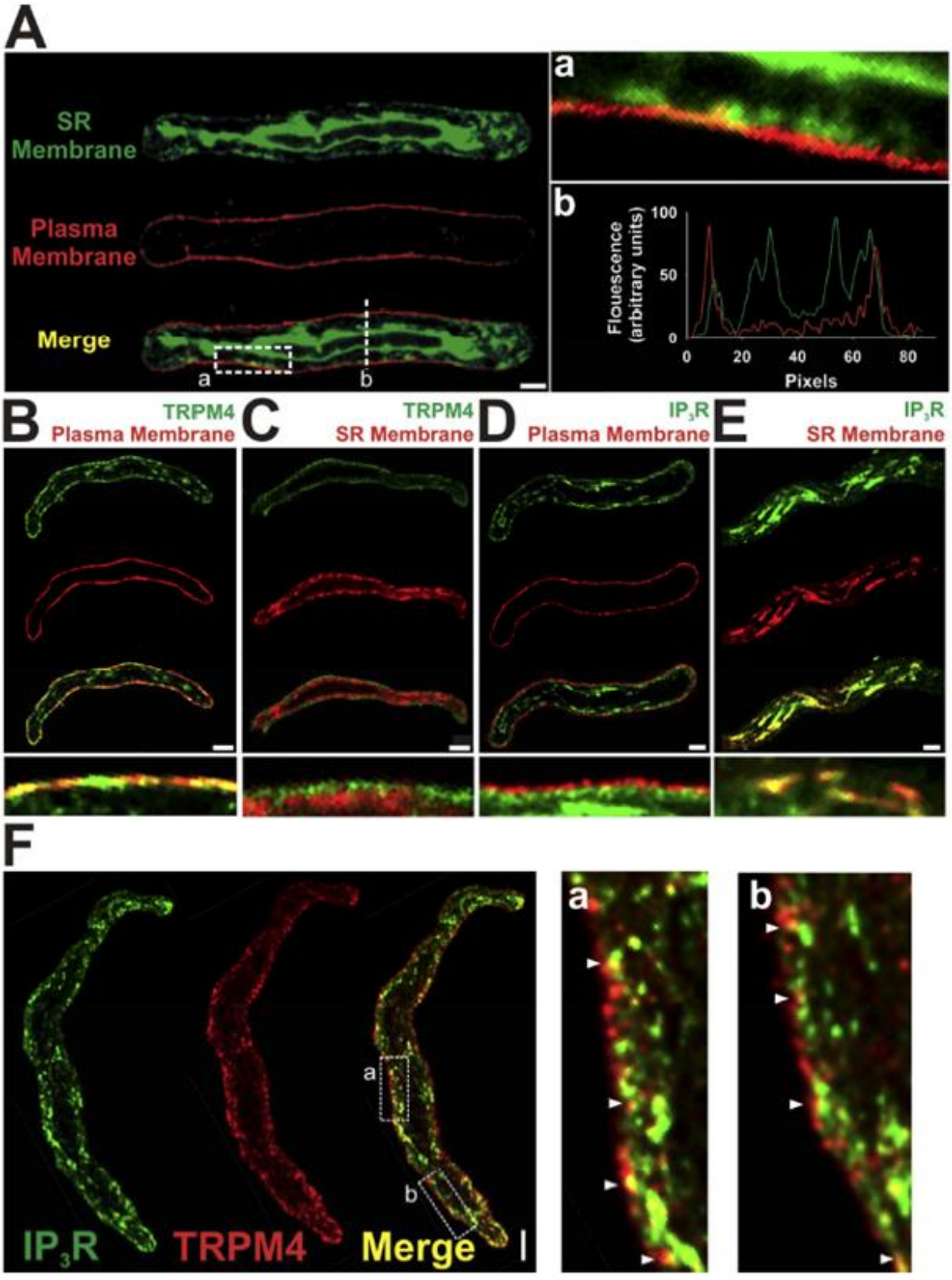
A
SR Membrane
Plasma Membrane
Merge
a
b
Flouescence (arbitrary units)
100
50
0
0
20
40
60
80
Pixels
B TRPM4 Plasma Membrane
C TRPM4 SR Membrane
D IP3R Plasma Membrane
E IP3R SR Membrane
F
IP3R
TRPM4
Merge

Figure 3.9: Localization of TRPM4 and IP3R in Freshly Isolated Smooth Muscle Cells. A: Representative images demonstrate the specific fluorescent staining of the sarcoplasmic reticulum (SR, green) and plasma membrane (red) in a freshly isolated smooth muscle cell. Merged image shows little overlap of the SR and plasma membrane. Bar = 5 µm. (a) Higher magnification of insert illustrating specific staining of SR and plasma membrane. (b) Intensity profile of SR and plasma membrane fluorescence along the line segment. B: Representative images of an isolated smooth muscle cell immunolabeled for TRPM4 (green) and stained for the plasma membrane (red). Bar = 10 µm. Bottom: High magnification insert demonstrating the co-localization (yellow) of TRPM4 with the plasma membrane. C: Representative images of an isolated smooth muscle cell immunolabeled for TRPM4 (green) and stained for the SR membrane (red). Bar = 10 µm. Bottom: High magnification insert demonstrating separation of TRPM4 and the SR membrane. D: Representative images of an isolated smooth muscle cell immunolabeled for IP_3R (green) and stained for the plasma membrane (red). Bar = 10 µm. Bottom: High magnification insert demonstrating separation of IP_3R and the plasma membrane. E: Representative images of an isolated smooth muscle cell immunolabeled for IP_3R (green) and stained for the SR membrane (red) Bar = 10 µm. Bottom: High magnification insert demonstrating the co-localization of IP_3R with the SR membrane (yellow). F: Representative images of an isolated smooth muscle cell immunolabeled for IP_3R (green) and TRPM4 (red). Bar = 10 µm. (a and b) High magnification of inserts illustrating specific localization of TRPM4 (red, outside) and IP_3R (green, inside). Notice the distinct points of co-localization (arrowhead).

CHAPTER 4

Pharmacological Inhibition of TRPM4 Hyperpolarizes Vascular Smooth Muscle

INTRODUCTION

Smooth muscle cell membrane potential is central to the regulation of arterial tone. Receptor-dependent vasoconstrictor agonists and intraluminal pressure depolarize vascular smooth muscle and open voltage-dependent Ca^{2+} channels (VDCCs), causing intracellular [Ca^{2+}] to rise and contractility to increase. The resting membrane potential of arterial myocytes is established by the relative magnitude of hyperpolarizing and depolarizing influences. K^+ efflux tend to drive the membrane potential to the K^+ equilibrium potential (E_K at 37ºC ≈ -90 mV) (68, 121) whereas cation influx directs the membrane to depolarized potentials (E_{Na} at 37ºC ≈ +60 mV, E_{Ca2+} ≈ +150 mV) (68, 121). K^+ channel-dependent hyperpolarization of smooth muscle membrane potential has been studied extensively (121) but much less in known about the cation channels that contribute to membrane depolarization.

Several members of the transient receptor potential (TRP) superfamily of cation channels are present in vascular smooth muscle cells and contribute to the regulation of smooth muscle membrane potential and contractility (36, 40, 43, 151, 152, 194). Antisense-mediated gene silencing has been used to demonstrate that expression of TRPM4 (39, 40, 151) and TRPC6 (194) channels are required for pressure-induced smooth muscle cell depolarization and myogenic vasoconstriction of cerebral arteries. TRPC3 channels mediate receptor-dependent responses in these vessels(152). Further

investigation into the regulation of TRP channels and how they influence vascular function has been hampered by the lack of selective pharmacological inhibitors. Recently, it was reported that the hydroxytricyclic compound 9-hydroxyphenanthrene (9-phenanthrol) blocks TRPM4 channels in an HEK cell expression system with a half-maximal inhibitory concentration (IC_{50}) of 16.7±4.5 μM under conventional whole-cell patch clamp conditions (60). The related channel TRPM5 is not inhibited by 9-phenanthrol at a concentration of 100 μM, suggesting that the compound has selectivity for TRPM4 (60). However, the effects of the compound on other TRP, K^+, and Ca^{2+} channels involved in smooth muscle cell function have not been previously reported. Therefore, the goals of the current study were to further examine the selectivity of 9-phenanthrol and to determine the effects of the compound on cerebral artery smooth muscle cell membrane potential and contractility.

We find that 9-phenanthrol blocks sustained TRPM4 currents in freshly isolated cerebral artery myocytes with an IC_{50} that is consistent with the value reported for recombinant TRPM4 channels expressed in HEK cells. In addition, we find that 9-phenanthrol is without effect on TRPC3 and TRPC6 currents in HEK expression systems. Our studies also demonstrate that 9-phenanthrol is without effect on K^+ and VDCCs that are involved in the regulation of smooth muscle membrane potential and contractility, suggesting that the compound may be useful for investigation of the physiological function of TRPM4 in these cells. Block of TRPM4 currents with 9-phenantrol in intact cerebral vessels at physiological intraluminal pressure results in substantial hyperpolarization of vascular smooth muscle cell membrane potential and dilation of arteries with myogenic tone. These findings show that TRPM4 currents play a

major role in establishing the membrane potential of arterial myocytes and maintaining myogenic tone.

MATERIALS AND METHODS

Animals

Male Sprague-Dawley rats (300-350 g; Harlan, Indianapolis, Indiana, USA) were used for these studies. Animals were deeply anesthetized with sodium pentobarbital (50 mg/kg. i.p.) and euthanized by exsanguination according to a protocol approved by the Institutional Animal Care and Use Committee (IACUC) of Colorado State University. Brains were isolated in ice-cold MOPS-buffered saline (in mM): 3 MOPS (pH 7.4), 145 NaCl, 5 KCl, 1 $MgSO_4$, 2.5 $CaCl_2$, 1 KH_2PO_4, 0.02 EDTA, 2 pyruvate, 5 glucose and 1% bovine serum albumin. Cerebral and cerebellar arteries were dissected from the brain, cleaned of connective tissue, and stored in MOPS-buffered saline on ice prior to further manipulation.

Cerebral Artery Smooth Muscle Cell Preparation

To isolate smooth muscle cells, vessels were cut into 2-mm segments and placed in the following Mg^{2+}-based physiological saline solution (Mg-PSS) (in mM): 140 NaCl, 5 KCl, 2 $MgCl_2$, 10 glucose, and 10 HEPES; (pH 7.2). Arterial segments were initially incubated at room temperature in 0.6 mg/mL papain (Worthington) and 1 mg/ml dithiothreitol (DTT) for 17 min, followed by a 15 min incubation at 37 ºC in 1 mg/mL type II collagenase (Worthington). Digested segments were washed three times in Mg-PSS

and triturated to release smooth muscle cells. Cells were stored on ice in Mg-PSS for use the same day.

Human Embryonic Kidney (HEK) Cell Culture

Human embryonic kidney (HEK) 293 cells were cultured in Dulbecco's 1X High Glucoses Modified Eagle Medium (Gibco) supplemented with 10% fetal bovine serum (Gibco) and 0.5% penicillin-streptomycin (Gibco). Cells were incubated at 37°C with 6% CO_2, media was changed every 2-3 days, and cells were sub-cultured when confluent using 0.25% Trypsin-EDTA (Gibco).

General Patch Clamp Electrophysiology

Currents were recorded using an AxoPatch 200B amplifier equipped with an Axon CV 203BU headstage (Molecular Devices). Recording electrodes (1-3 MΩ) were pulled, polished, and coated with wax to reduce capacitance. GΩ seals were obtained in Mg-PSS. Currents were filtered at 1 kHz, digitized at 40 kHz, and stored for subsequent analysis. Clampex and Clampfit versions 10.2 (Molecular Devices) were used for data acquisition and analysis, respectively. All patch clamp experiments were performed at room temperature (22 - 25°C).

TRPC3 and TRPC6 Currents in HEK Cells

The pipette solution used to record both TRPC3 and TRPC6 currents contained (mM) 130 CsOH, 110 aspartic acid, 15 CsCl, 1 $MgCl_2$, 3.6 $CaCl_2$, 10 EGTA, 10 HEPES (pH 7.4). The extracellular bath solution for TRPC3 contained (mM) 140 NaCl, 5 CsCl,

0.1 $MgCl_2$, 0.05 $CaCl_2$, 10 Glucose, 10 HEPES (pH 7.4). HEK cells were co-transfected by electroporation with a plasmid that encodes TRPC3 channels tagged with Yellow Fluorescent Protein (TRPC3-YFP) and with a second plasmid encoding the Angiotension II (AngII) AT_1 receptor. Transfected cells were plated on 12 mm glass cover slips and allowed to adhere for ~2-3 hours at 37°C, 6% CO_2. Transfected cells expressing TRPC3-YFP were identified using fluorescent microscopy, initially voltage clamped at 0 mV, and voltage ramps from -100 mV to +100 mV were applied every 4 seconds. After baseline currents were recorded, AngII (10 nM) was administered to induce receptor-mediated TRPC3 currents. When the evoked current reached a steady state, 9-phenanthrol (30 μM) was administered to examine the effect of the compound on TRPC3 currents.

The extracellular bath solution used to record TRPC6 currents contained (in mM) 150 NaCl, 0.08 KCl, 0.8 $MgCl_2$, 5.4 $CaCl_2$, 10 Glucose, 10 HEPES (pH 7.4). HEK cells transiently transfected with a TRPC6 expression plasmid (ChanTest, Inc.) and non-transfected cells were plated on glass cover slips and allowed to adhere for ~12 hours at 37°C, 6% CO_2. Using the same voltage protocol used to record TRPC3 currents, conventional whole-cell currents were recorded from TRPC6-expressing cells and compared to currents recorded from non-transfected cells. 9-phenanthrol (30 μM) was administered to TRPC6-expressing cells to assess the effects of the compound on TRPC6 currents.

The calculated reversal potential for monovalent cations is 0 mV for the TRPC3 solutions and 0.9 mV for the TRPC6 solutions. For divalent cations, the reversal potentials are -43.2 mV for the TRPC3 solutions and 3.8 mV for the TRPC6 solution.

Reversal potentials for monovalent anions are 1.6 mV for the TRPC3 solution and -1 mV for the TRPC6 solution.

Large conductance Ca^{2+}-activated K^+ (BK_{Ca}) and TRPM4 Currents in Smooth Muscle Cells

Spontaneous transient outward currents (STOCs) result from activation of numerous BK_{Ca} channels following transient release of Ca^{2+} from ryanodine receptors located on the sarcoplasmic reticulum (SR) and represent BK_{Ca} activity under physiological conditions in smooth muscle cells (118). Transient inward cation currents (TICCs) are the result of activation of TRPM4 channels by SR Ca^{2+} released from inositol trisphosphate receptors (IP_3R) (54). For the current study, both STOCs and TICCs were recorded using the perforated patch clamp configuration. Isolated smooth muscle cells were transferred to a recording chamber (Warner Instruments) and allowed to adhere to glass coverslips for 20 min at room temperature. Amphotericin B (40 µM) was included in the pipette solution to perforate the membrane. Acceptable perforation was determined by a series resistance of less than 50 MΩ. STOCs and TICC activity were recorded in normal external bathing solution containing (in mM) 134 NaCl, 6 KCl, 1 $MgCl_2$, 2 $CaCl_2$, 10 HEPES, and 10 glucose at pH of 7.4 (NaOH). The pipette solution contained (in mM) 110 K-aspartate, 1 $MgCl_2$, 30 KCl, 10 NaCl, 10 HEPES, 5 (µM) EGTA at pH 7.2 (NaOH). STOCs were recorded at a membrane potential of +20 mV and TICCs were recorded at -70 mV. The calculated reversal membrane potential for the perforated patch solutions is is -1.8 mV for total monovalent cations and -30.6 mV for monovalent anions (Cl^-). STOCs were defined as a transient event greater than 10

pA (more than one BK_{Ca} channel), and the frequency was calculated by dividing the number of events by the time between the first and last event. TICC activity at -70 mV was calculated as the sum of the open channel probability (NP_o) of multiple open states of 1.75 pA. This value was based on the reported unitary conductance of TRPM4 (25 pS).

Channel open probability (NP_o) was calculated using the following equation:

$$NP_o = \sum_{j=1}^{N} \frac{(t_j \cdot j)}{T}$$

Where:

t_j = time spent in seconds with j = 1,2,….N channels open

N = max number of channels observed

T = duration of measurement.

Voltage-Dependent K^+ (K_V) Currents in Smooth Muscle Cells

The conventional whole-cell patch clamp configuration was used to examine the effects of 9-phenanthrol on K_v currents in smooth muscle cells. The extracellular bath solution contained (mM) 5 KCl, 140 NaCl, 2 $MgCl_2$, 10 Glucose, and 10 HEPES. The pipette solution contained (mM) 87 K^+ aspartate, 20 KCl, 1 $CaCl_2$, 1 $MgCl_2$, 10 HEPES, 10 EGTA, and 5 MgATP. Cells were initially voltage clamped at -80 mV and voltage steps from -80 mV to +30 mV were applied for 400 ms in 10 mV increments, followed with a step to -40 mV for 200 ms. Recordings were performed in the presence of paxilline (5 µM) to block BK_{Ca} activity. Recording were obtained in the presence of the vehicle for 9-phenanthrol (DMSO) and when 9-phenanthrol (30 µM) was present in the

superfusion bath. Average current density (pA/pF) during the steady state for each voltage step was used to generate current-voltage relationships.

Inwardly-Rectifying (K_{IR}) Currents in Smooth Muscle Cells

Conventional patch-clamp electrophysiology was used to measure whole-cell K_{IR} currents in isolated smooth muscle cells using a previously described method (172). The pipette solution for these experiments contained (mM): 5 NaCl, 35 KCl, 100 K^+ gluconate, 1 $CaCl_2$, 10 HEPES, 10 EGTA, 2.5 Tris-ATP and 0.2 GTP (pH 7.2). Cells were voltage clamped at −60 mV and equilibrated for 15 min in a bath solution containing (mM): 135 NaCl, 5 KCl, 0.1 $MgCl_2$, 10 HEPES, 5 glucose and 0.1 $CaCl_2$ (pH 7.4). Following equilibration, bath [K^+] was elevated from 5 to 60 mM by replacement of NaCl by KCl. Voltage ramp between −120 and 20 mV (0.047 mV ms^{-1}) were applied in the presence and absence of 30 μM BaCl, and K_{IR} (Ba^{2+}-sensitive) currents were calculated by current subtraction. K_{IR} currents recorded in the presence of 9-phenanthrol were compared to those recorded in the presence of vehicle (DMSO).

Voltage-Dependent Ca^{2+} Currents in Smooth Muscle Cells The conventional whole-cell patch clamp technique was used to record VDCCs in smooth muscle cells. Freshly prepared cerebral arterial myocyte suspensions were transferred to a recording chamber and the cells were allowed to adhere to glass cover slips for 20 minutes at room temperature. During experiments, cells were superfused with a solution containing (in mM): 120 $NMDG^+$, 5 CsCl, 1 $MgCl_2$, 10, glucose, 10 HEPES, and 20 $CaCl_2$ adjusted to pH 7.4 with HCl. Pipettes were filled with a solution composed of (in mM): 87 Cs-aspartate, 20 CsCl, 1 $MgCl_2$, 5 MgATP, 0.1 Na_2GTP, 1 NADPH, 10 HEPES, and 10

EGTA, adjusted to pH 7.2 with CsOH. Cells were initially voltage clamped at -70 mV and VDCC currents were evoked by stepping the membrane potential to +30 mV. Currents recorded in the presence of vehicle (DMSO) were compared to those recorded in the presence of 9-phenanthrol (30 μM).

Isolated Vessel Experiments

Arteries were harvested and transferred to a vessel chamber (Living Systems, Inc.). The proximal end of the vessel was cannulated with a glass micropipette and secured with monofilament thread. Blood was gently rinsed from the lumen, and the distal end of the vessel was cannulated and secured. Arteries were pressurized to 10 mmHg with physiological saline solution (PSS) (in mM): 119 NaCl, 4.7 KCl, 1.8 $CaCl_2$, 1.2 $MgSO_4$, 24 $NaHCO_3$, 0.2 KH_2PO_4, 10.6 glucose, 1.1 EthyleneDiamineTetraacetic Acid (EDTA) and superfused (5 mL/min) with warmed (37°C) PSS aerated with a normoxic gas mixture (21% O_2, 6% CO_2, balance N_2). Following a 15-minute equilibration period, intraluminal pressure was slowly increased to 110 mmHg, vessels were stretched to remove bends, and pressure was reduced to 10 mmHg for an additional 15-minute equilibration period. Inner diameter was continuously monitored using video microscopy and edge-detection software (Ionoptix). Arteries pressurized to 10 mmHg were exposed to isotonic PSS containing 60 mM KCl to assess viability of the preparation. Arteries were pressurized to 70 mmHg and stable myogenic tone was allowed to develop prior to the administration of 9-phenanthrol. To determine maximum (i.e. passive) diameter, vessels were superfused with Ca^{2+}-free PSS (in mM): 119 NaCl,

4.7 KCl, 1.2 $MgSO_4$, 24 $NaHCO_3$, 0.2 KH_2PO_4, 10.6 glucose, 1.1 EDTA, 3 EGTA, and 0.01 diltiazem.

Smooth Muscle Cell Membrane Potential

For measurement of smooth muscle cell membrane potential, cerebral arteries were isolated and pressurized to 70 mmHg, and smooth muscle cells were impaled through the adventitia with glass intracellular microelectrodes (tip resistance 100-200 MΩ). A WPI Intra 767 amplifier was used for recording membrane potential (E_m). Analog output from the amplifier was recorded using Ionwizard software (sample frequency 20 Hz). Criteria for acceptance of E_m recordings were: 1) an abrupt negative deflection of potential as the microelectrode was advanced into a cell; 2) stable membrane potential for at least 1 minute; and 3) an abrupt change in potential to approximately 0 mV after the electrode was retracted from the cell.

Calculations and Statistics

All data are mean ± SE. Values of *n* refer to number of arteries for isolated vessel experiments or number of cells for patch clamp experiments. Statistical methods conform to the recommendations of the editors of Circulation Research(189). A level of $P \leq 0.05$ was accepted as statistically significant for all experiments.

RESULTS

9-Phenanthrol Selectively Blocks Sustained TRPM4 Currents

A recent report from our laboratory demonstrates that TICCs, TRPM4 currents under near-physiological conditions, can be recorded from cerebral artery smooth muscle cells voltage clamped using the amphotericin B perforated patch configuration (54). TICC currents are diminished when TRPM4 expression is attenuated using siRNA, suggesting that TICCs represent TRPM4 activity under physiological conditions in cerebral artery smooth muscle cells (54). To characterize the effects of 9-phenanthol on native TRPM4 currents, we examined the concentration-response relationship for TICC inhibition. We find that 9-phenanthrol inhibits TICC activity in a concentration-dependent manner with an IC_{50} of 10.6 μM, (Figure 4.1A and B) in agreement with the prior report (16.7±4.5 μM for TRPM4 channel in an HEK expression system, whole-cell conditions (60)). These data indicate that 9-phenanthrol effectively blocks TRPM4 currents recorded under near-physiological conditions in native smooth muscle cells.

The effects of 9-phenanthrol on other ion channels involved in smooth muscle cell function have not been previously reported. We began our investigation into the specificity of the compound by examining its effects on TRPC3 and TRPC6 currents. These channels were selected because both are involved in the regulation of cerebral artery smooth muscle membrane potential and contractility (76, 152, 194). To study the effects of 9-phenanthrol on TRPC3 currents, recombinant TRPC3 channels and angiotensin II (AngII) AT_1 receptors were co-expressed in HEK cells. Transfected cells were patch clamped in the conventional whole-cell configuration. Currents in unstimulated cells were small (Figure 4.2A and B). However, large TRPC3-dependent

currents were evoked by administration of AngII (10 nM) (Figure 4.2A and B). These currents were not diminished by administration of 9-phenanthrol (30 μM) to the bathing solution (Figure 4.2A and B), indicating that TRPC3 channels are not blocked by the compound.

HEK cells transiently transfected with recombinant TRPC6 were also patch clamped in the conventional whole-cell configuration. Basal cation currents recorded from TRPC6-expressing cells were greater in magnitude than those recorded from untrasfected HEK cells (Figure 4.2C and D). 9-phenanthrol had no effect on these currents (Figure 4.2C and D), indicating that TRPC6 channels are not blocked by this compound. These experiments demonstrate that 9-phenanthrol effectively blocks TRPM4 channels but has no effect on TRPC3 or TRPC6 currents at a concentration sufficient to nearly eliminate TRPM4 currents.

9-Phenanthrol Does not Block BK_{Ca}, Kv, or K_{IR} Channels in Smooth Muscle Cells

To further examine the utility of 9-phenathrol for investigations into the role of TRPM4 channels in freshly-isolated vascular smooth muscle, we examined the effects of the compound on the major K^+ (BK_{Ca}, K_V, and K_{IR}) channels involved in the function of these cells. STOCs were recorded from smooth muscle cells using the perforated patch voltage clamp configuration. 9-phenanthrol (30 μM) had no effect on STOC frequency or amplitude (Figure 4.3A, B, and C), demonstrating that the compound does not alter BK_{Ca} channel activity or the ryanodine receptor-dependent SR Ca^{2+} release events (Ca^{2+} sparks) that generate STOCs.

The conventional whole cell patch clamp configuration was used to examine the effects of 9-phenanthrol (30 μM) on K_v and K_{IR} channel activity. K_v currents evoked by voltage steps did not differ between control and 9-phenanthrol treated cells (Figure 4.3D and E), indicating that the compound is without effect on these channels. K_{IR} channels were isolated using $BaCl_2$, according to a method described by Smith et al. (172). Ba^{2+}-sensitive currents did not differ when recorded in the presence or absence of 9-phenanthrol (30 μM), demonstrating that the compound does not alter the activity of K_{IR} channels (Figure 4.3F-H).

Voltage-Dependent Ca^{2+} Channels are not Blocked by 9-Phenanthrol

VDCCs are the major Ca^{2+} influx pathway in cerebral artery myocytes. Conventional whole-cell patch clamp was used to investigate the effects of 9-phenanthrol on VDCC activity in native cerebral artery smooth muscle cells. To evoke VDCC currents, cells were voltage clamped at -70 mV and then stepped to +30 mV. Whole cell Ca^{2+} currents recorded (I_{Ca}) under these conditions did not differ between vehicle and 9-phenanthrol (30 μM) treated cells (Figure 4.4A and B), demonstrating that the compound is without effect on VDCCs at this concentration.

9-Phenanthrol Hyperpolarizes Vascular Smooth Muscle Cells

Knockdown of TRPM4 expression diminishes pressure-induced smooth muscle depolarization (42), but the acute effects of TRPM4 inhibition on resting membrane potential have not been reported. 9-phenanthrol was used to examine the contribution of TRPM4-dependent current to the resting membrane potential of vascular smooth

muscle cells in isolated cerebral and cerebellar arteries. Arteries were pressurized to physiological levels (70 mmHg) and smooth muscle membrane potential was measured using intracellular microelectrodes before and after 9-phenanthrol (30 μM) was administered via the superfusion bath, and again after the drug was washed out of the recording chamber. Prior to 9-phenanthrol administration, the resting membrane potential of arterial myocytes was -39.0 ± 1.9 mV (n=4) (Figure 4.5A and B). In the presence of 9-phenanthrol, the membrane potential was significantly hyperpolarized (-73.1 ± 8.3 mV; n=4) (Figure 4.5A and B). Following washout of the drug, resting membrane potential did not differ from that recorded prior to 9-phenanthrol administration (-36.4 ± 1.2 mV; n=3), demonstrating that the effects of the drug are reversible (Figure 4.5A and B). In theory, 9-phenanthrol-induced membrane hyperpolarization could result from inhibition of an inward cation current or from activation of an outward K^+ current. However, we find that 9-phenanthrol does not alter K^+ currents in smooth muscle cells, indicating that the compound hyperpolarizes the membrane by blocking an inward cation current. 9-phenanthrol does not block TRPC6 or TRPC3 currents at this concentration, suggesting that a block of a TRPM4-dependent Na^+ current is responsible for hyperpolarization of the smooth muscle membrane. These data demonstrate that TRPM4 is an important depolarizing influence in cerebral artery smooth muscle cells.

9-Phenanthrol Dilates Pressurized Cerebral Arteries

9-phenanthrol blocks TRPM4 currents and hyperpolarizes vascular smooth muscle cells in pressurized cerebral arteries. Hyperpolarization of the arterial myocyte

membrane causes vasodilation by closing VDCCs and decreasing intracellular [Ca^{2+}]. To determine the effects of 9-phenanthrol on smooth muscle contractility, isolated cerebral arteries were pressurized to 70 mmHg and allowed to develop spontaneous myogenic tone. Luminal diameter was continuously recorded as 9-phenanthrol was added to the superfusion bath. Administration of 9-phenanthrol (30 μM) significantly dilated pressurized cerebral arteries (Figure 4.6A-C). Myogenic tone decreased by approximately 75% in the presence of 30 μM 9-phenanthrol and was essentially eliminated by a concentration of 100 μM (Figure 4.6A-C). The effects of the drug were reversible and myogenic tone redeveloped after 9-phenanthrol was washed from the superfusion bath (Figure 4.6A and B). The IC_{50} for 9-phenanthrol-induced dilation of cerebral arteries with myogenic tone is 2.6 μM (Figure 4.6C), comparable with the IC_{50} of this compound for block of sustained TRPM4 currents in smooth muscle cells (10.6 μM) (Figure 4.1B).

We also found that administration of 9-phenanthrol (30 μM) did not alter vasoconstriction in response to elevated levels of extracellular KCl (60 mM) (Figure 4.6D). This finding provides further evidence that the compound does not block depolarization-induced Ca^{2+} influx. Furthermore, these data suggest that 9-phenanthrol does not interfere with membrane depolarization resulting from diminished K^+ efflux or directly inhibit smooth muscle contraction in isolated resistance arteries. Our findings indicate that 9-phenanthrol causes arterial dilation by blocking depolarizing TRPM4 currents to hyperpolarize smooth muscle cell membrane potential and decrease voltage-dependent Ca^{2+} influx.

DISCUSSION

The current study examined the specificity of the TRPM4 blocker 9-phenanthrol and investigated the effects of the compound on the resting membrane potential and contractility of cerebral artery smooth muscle cells. The major findings of this study are: 1) 9-phenanthrol inhibits sustained TRPM4 currents in cerebral artery vascular smooth muscle cells; 2) At a concentration that nearly abolishes sustained TRPM4 currents, 9-phenanthrol does not alter the activity of TRPC3, TRPC6 K_V, BK_{Ca}, K_{IR}, or VDCC channels; 3) 9-phenanthrol reversibly hyperpolarizes the smooth muscle cell membrane potential in pressurized cerebral arteries; and 4) 9-phenanthrol reversibly dilates cerebral arteries with myogenic tone. These findings demonstrate for the first time that 9-phenanthrol blocks native TRPM4 channels in cerebral artery myocytes without affecting the activity of other channels that are important for smooth muscle function. More importantly, these findings show that TRPM4-dependent cation currents are a primary depolarizing influence in cerebral artery smooth muscle cells under physiological conditions and are critical for establishment and maintenance of myogenic tone.

Selective pharmacological inhibitors are invaluable tools for elucidating the functional impact of the many ion channels present in vascular smooth muscle cells. Few TRP channels inhibitors with significant specificity are currently available and studies of these channels have relied on molecular techniques, such as antisense (40, 43) or siRNA-mediated (54) downregulation of channel expression. Although these methods are useful, limitations, such as phenotypic changes during culture and possible off-target effects of the inhibitory molecules complicate interpretation of the data. It is

also impossible to examine the acute effects and reversibility of channel inhibition using these methods. Antisense-mediated downregulation experiments suggest that TRPM4 is an important mediator of pressure-(42) and protein kinase C-dependent (41) vasoconstriction and autoregulation of cerebral blood flow in vivo (151). To better understand the significance of this channel, we sought a pharmacological inhibitor that was without significant off-target effects. Prior studies demonstrate that 9-phenanthrol effectively blocks TRPM4 under whole-cell (60), inside out (60), and amphotericin B perforated patch configurations (54). Grand et al. also report that 9-phenanthrol does not affect the function of the CFTR Cl^- transporter or TRPM5 channels (60). However, the effects the compound on cation, K^+, and Ca^{2+} channels that are important regulators of smooth muscle cell membrane potential and contractility have not been previously reported. Current findings demonstrate that 9-phenanthrol does not inhibit TRPC3 or TRPC6 channels at a concentration (30 μM) that essentially abolishes TRPM4 currents in smooth muscle cells. Furthermore, this concentration of the compound does not alter STOC activity in cerebral myocytes, demonstrating that 9-phenanthrol is without effect on BK_{Ca} channels and Ca^{2+} sparks generated by release of Ca^{2+} from ryanodine receptors on the SR. We also find that 9-phenanthrol does not alter the activity of K_v or K_{IR} currents. Our findings also show that 9-phenanthrol does not block VDCC activity. These data are in agreement with the lack of effect of the compound on arterial constriction in response to elevated extracellular K^+, demonstrating that the compound does not interfere with voltage-dependent Ca^{2+} influx in intact arteries. In addition, this experiment shows that 9-phenanthrol does not interfere with myosin light chain kinase activity or other components of the vascular smooth muscle contractile apparatus.

Taken together, these findings demonstrate that 9-phenanthrol is a useful reagent for studying TRPM4 function in cerebral artery smooth muscle cells.

Contractility of arterial smooth muscle is largely regulated by graded changes in smooth muscle cell membrane potential (85). Membrane depolarization activates VDCCs, stimulating Ca^{2+} influx and enhancing contractility by increasing the activity of myosin light chain kinase (85). The resting membrane potential of cerebral artery smooth muscle cells (~-40 mV) under physiological levels of intraluminal pressure (~70 mmHg) (85) is depolarized compared to the K^+ equilibrium potential (~-90 mV) and is hyperpolarized compared with the equilibrium potentials for cations (E_{Na} at 37ºC ≈ +60 mV, E_{Ca2+} ≈ +150 mV) and Cl^- (-30 mV) (121). Thus, cerebral arterial membrane potential and contractility are ultimately determined by the relative magnitudes of hyperpolarizing and depolarizing currents. Increases in outward K^+ currents via BK_{Ca}, K_V, and K_{IR} channels hyperpolarize the smooth muscle plasma membrane and cause arterial relaxation (121). Cl^- efflux could theoretically have a depolarizing effect on the arterial myocyte plasma membrane, but there is no convincing evidence demonstrating that Cl^- currents are significant for pressure-dependent regulation of cerebral artery smooth muscle membrane potential or arterial tone. Furthermore, Ca^{2+}-activated Cl^- channels are not present in cerebral artery smooth muscle (192), and swelling-activated mechanosensitive currents in these cells are dependent on cation channel activity (193). In contrast, significant evidence suggests that TRPC3, TRPC6, and TRPM4 cation currents contribute to agonist and pressure-induced membrane potential depolarization and constriction of cerebral arteries (39, 151, 152, 194). In the presence of 9-phenanthrol, smooth muscle membrane potential in pressurized cerebral arteries is

significantly hyperpolarized and myogenic tone is nearly abolished. 9-phenanthrol does not activate K^+ currents or inhibit TRPC3, TRPC6, or VDCC channels, suggesting that membrane hyperpolarization and loss of myogenic tone resulting from 9-phenanthrol administration is due to inhibition of TRPM4 cation currents. Treatment with 9-phenanthrol (30 μM) hyperpolarized smooth muscle cells in cerebral arteries pressurized to 70 mmHg to ~-70 mV, whereas, following antisense-mediated downregulation of TRPM4, smooth muscle cell membrane potential in cerebral arteries pressurized to 80 mmHg expression was ~-50 mV (42). Differences in membrane potential between arteries exposed to TRPM4 antisense and 9-phenanthrol may be due to incomplete knockdown in antisense-treated arteries. Previous work from our lab using reversible permeabilization suggests that ~80% of smooth muscle cells take up TRPM4 siRNA(55), and the cells that do not take up TRPM4 siRNA exhibit normal levels of TRPM4 expression (55). Taken together, these findings indicate that TRPM4 currents are a major depolarizing influence in cerebral artery smooth muscle cells and likely influence contractility by increasing Ca^{2+} influx via VDCC. It is also possible that TRPM4-mediated Na^+ influx could decrease Ca^{2+} efflux by the Na^+/Ca^{2+} exchanger, increasing intracellular [Ca^{2+}] and force generation. In either case, our findings demonstrate that TRPM4 channels significantly influence myocyte contractility and arterial tone.

TRPM4 and TRPC6 have been linked to pressure-dependent smooth muscle membrane depolarization and myogenic vasoconstriction of cerebral arteries (43, 194). The current findings shed light on the relative importance of these channels in this important physiological response (9). We find that a concentration of 9-phenanthrol (30

μM) that inhibits ~75% of TRPM4 activity under perforated patch clamp conditions but does not block TRPC6 activity, considerably hyperpolarizes the smooth muscle cell membrane and nearly abolishes myogenic tone. These data suggest that TRPM4 is the primary mediator of pressure-induced responses in cerebral artery smooth muscle cells and that TRPC6 channels play a secondary or regulatory role. It is possible that TRPC6 channels could act upstream of TRPM4 to mediate myogenic constriction by influencing intracellular Ca^{2+} dynamics. TRPM4 requires high levels of intracellular Ca^{2+} for activation (95, 124). We recently reported that in native cerebral artery smooth muscle cells, TRPM4 channels are activated by release of Ca^{2+} from SR stores through IP_3 receptors (54). TRPC6 is permeable to Ca^{2+}, and it is possible that Ca^{2+} influx through the channel could potentiate IP_3-dependent Ca^{2+} signals required for TRPM4 activity (54) by a Ca^{2+} induced-Ca^{2+} release mechanism. Interestingly, TRPC6 channels may be inherently mechanosensitive (173) and could be directly activated by increases in intraluminal pressure. However, a report from another lab did not find TRPC6 channels to be mechanosensitive (59), and further experiments are required to test this hypothesis and clarify the role of TRPC6 in the development of myogenic tone. While the involvement of TRPC6 remains uncertain, the findings of the current study clearly demonstrate that TRPM4 channels are required for the maintenance as well as the development of myogenic tone. The prior work using antisense oligonucleotides to silence TRPM4 prevented the development of myogenic tone and autoregulation of cerebral blood flow (42, 151), but because of the limitations of the molecular approach, did not investigate the role of the channel in maintaining arterial tone. The current findings show that 9-phenanthrol reverses spontaneous myogenic tone when applied to

pressurized arteries and that tone redevelops when the drug is removed. Thus, we conclude that TRPM4 activity is required for both the development and maintenance of myogenic tone in cerebral arteries and is a central regulator of vascular function.

In summary, our findings demonstrate that 9-phenanthrol is useful for investigating the functional significance of TRPM4 channels in vascular smooth muscle cells. Using this compound, we find that TRPM4 is a major depolarizing influence regulating smooth muscle cell membrane potential and that activity of the channel is necessary for the development and maintenance of myogenic tone. Our findings may stimulate the development of new therapeutic strategies for the treatment of cardiovascular diseases, such as systemic and pulmonary hypertension, that are associated with smooth muscle cell membrane depolarization. It is possible that derivatives of 9-phenanthrol or other selective TRPM4 inhibitors may reverse this effect and prove useful in controlling these conditions.

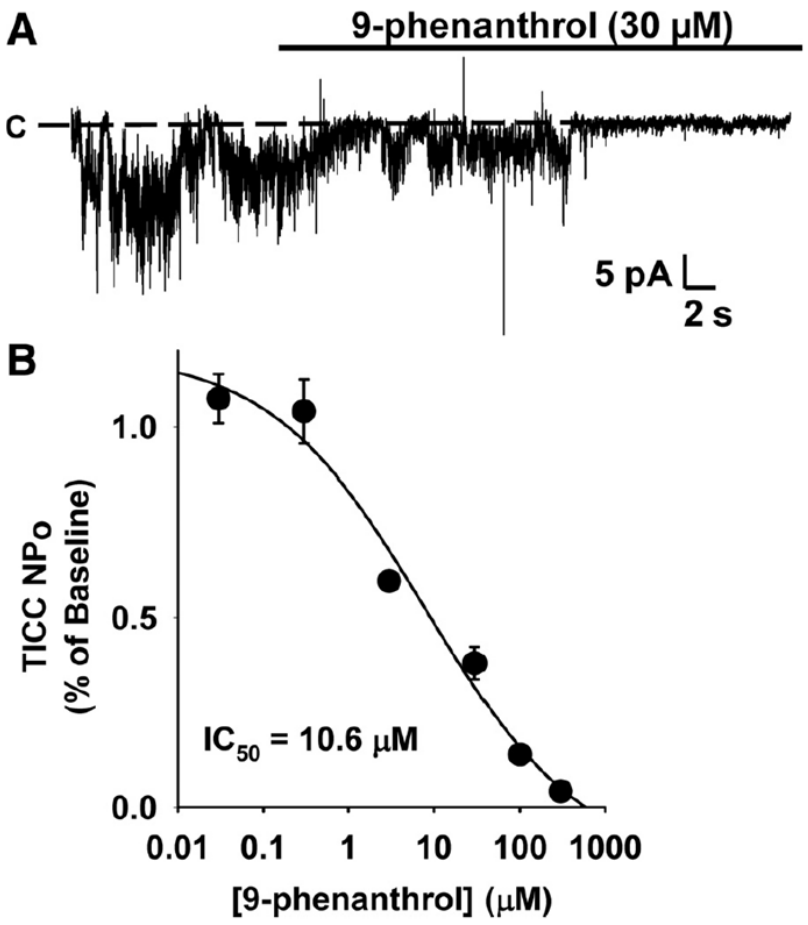

Figure 4.1: 9-Phenanthrol Inhibits Sustained TRPM4 Currents in Native Cerebral Artery Smooth Muscle Cells. *A*: representative recording of sustained transient inward cation current (TICC) activity in cerebral artery myocytes during administration of 9-phenanthrol (30 μM). C, closed state. *B*: dose response of 9-phenanthrol-mediated inhibition of TICC open channel probability (NP_o) (IC_{50} = 10.6 μM); *n* = 3–5 cells per dose.

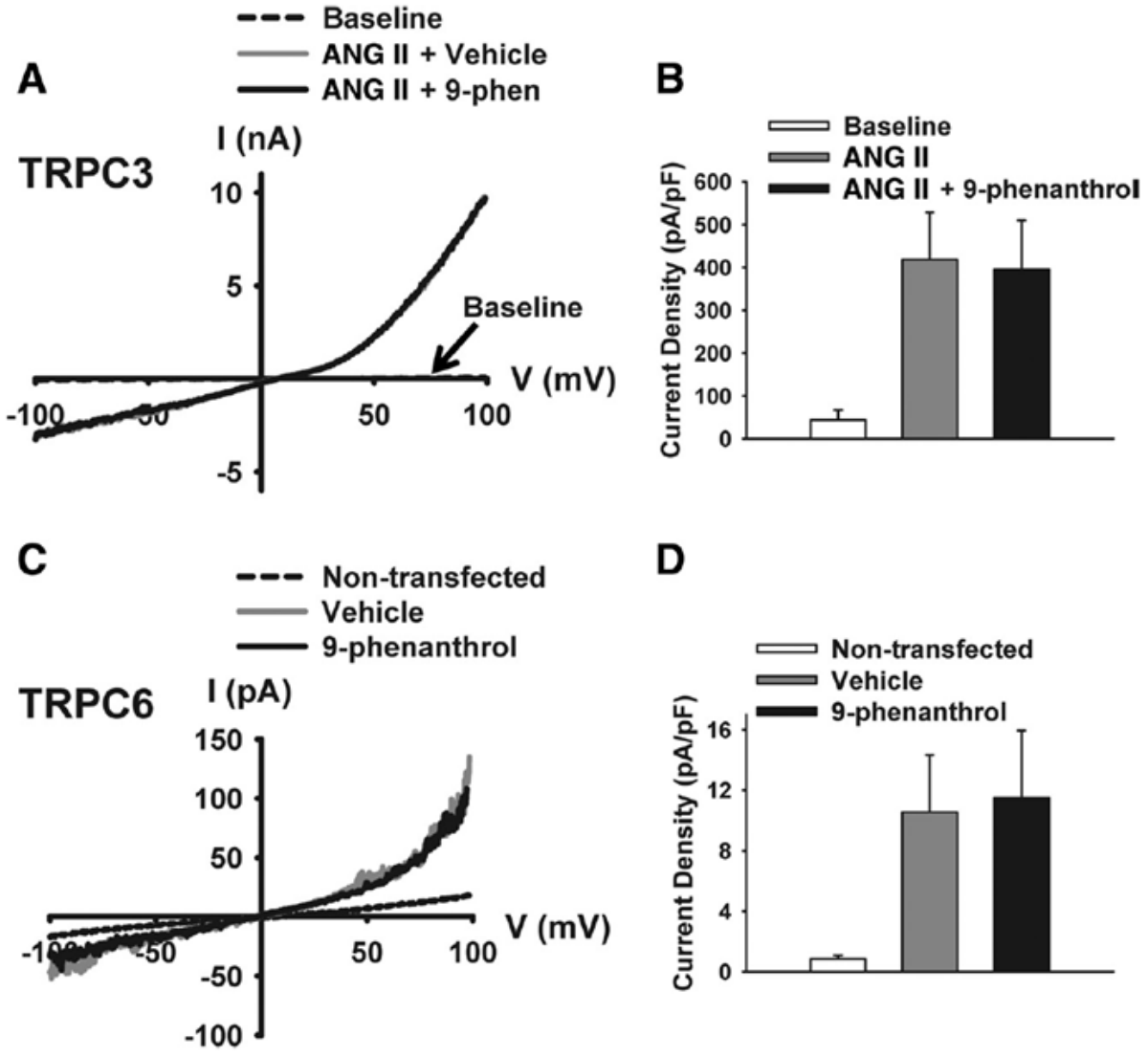

Figure 4.2: TRPC3 and TRPC6 Currents are Not Blocked by 9-phenanthrol. *A*: current (*I*) vs. voltage (*V*) relationship of baseline and angiotensin II (ANG II)-induced currents in human embryonic kidney (HEK) cells overexpressing TRPC3 recorded in absence and presence of 9-phenanthrol (9-phen; 30 μM). Note that the current recorded in the presence of 9-phenanthrol is obscured by the current recorded in the presence of vehicle. *B*: summary data of average current density at +85 mV before and following ANG II (10 nM) stimulation and after administration of 9-phenanthrol (30 μM) in the presence of ANG II; $n = 4$. *C*: *I* vs. *V*relationship of whole cell currents recorded from nontransfected HEK cells and TRPC6-expressing cells in absence and presence of 9-phenanthrol (30 μM). *D*: summary data of average current density at +85 mV for nontransfected cells and TRPC6-expressing cells in absence and presence of 9-phenanthrol (30 μM); $n = 6$.

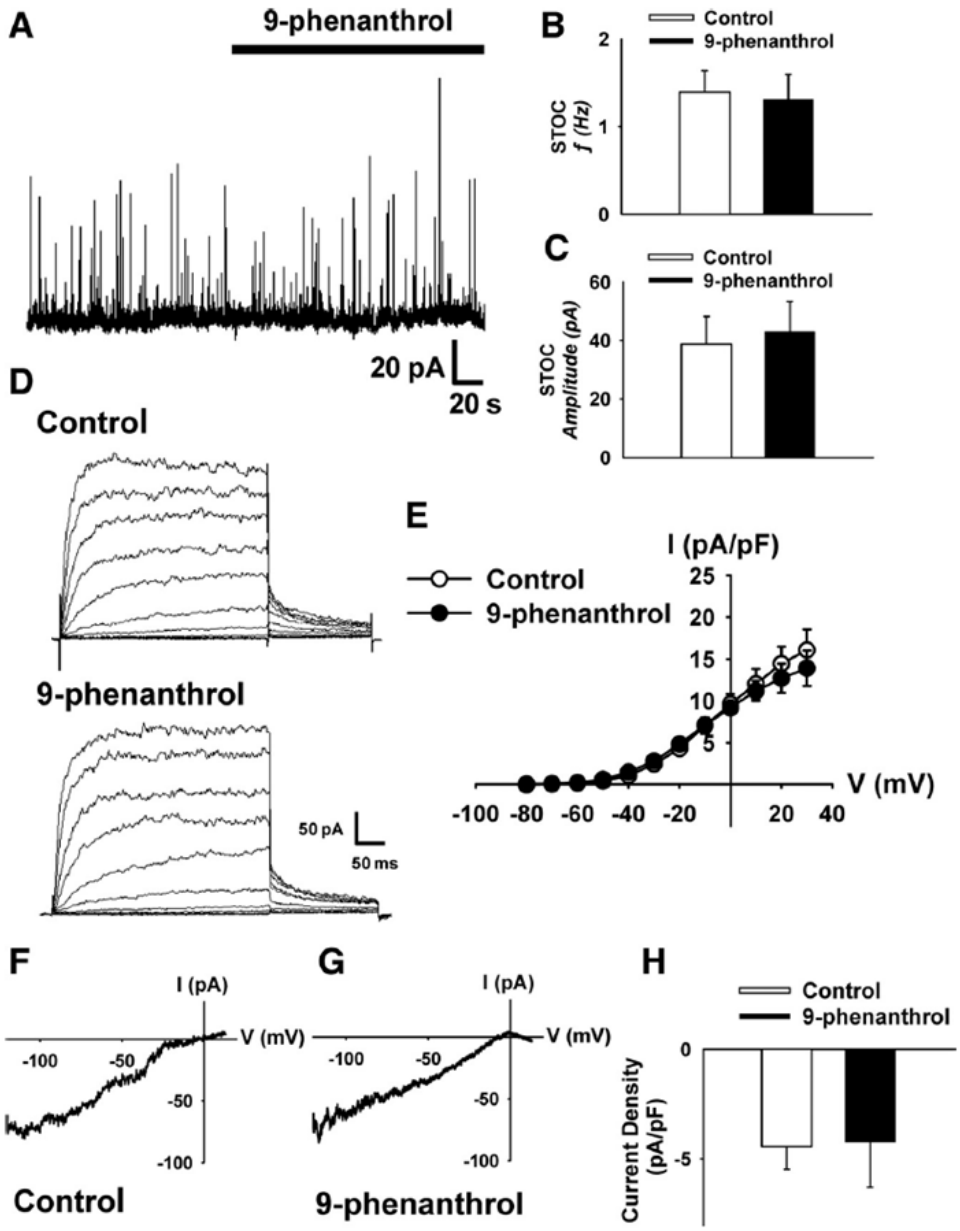

Figure 4.3: K^+ Currents in Cerebral Artery Smooth Muscle Cells are Not Altered by 9-phenanthrol. *A*: representative spontaneous transient outward current (STOC) activity following administration of 9-phenanthrol (30 μM). *B* and *C*: STOC frequency (*f*; in Hz; *B*) and amplitude (pA; *C*) in presence and absence of 9-phenanthrol;*n* = 6. *D*: representative voltage-dependent K^+ (K_V) currents in absence and presence of 9-phenanthrol (30 μM). *E*: summary of mean current density (pA/pF) vs. voltage relationship of K_V currents in vascular smooth muscle cells in absence and presence of 9-phenanthrol (30 μM); *n* = 5. *F* and *G*: representative inwardly rectifying K^+ (K_{IR}) currents in absence and presence of 9-phenanthrol (30 μM). *H*: summary of mean current density (pA/pF) at −80 mV for K_{IR} currents in vascular smooth muscle cells in the presence and absence of 9-phenanthrol (30 μM); *n* = 4 for control; *n* = 3 for 9-phenanthrol.

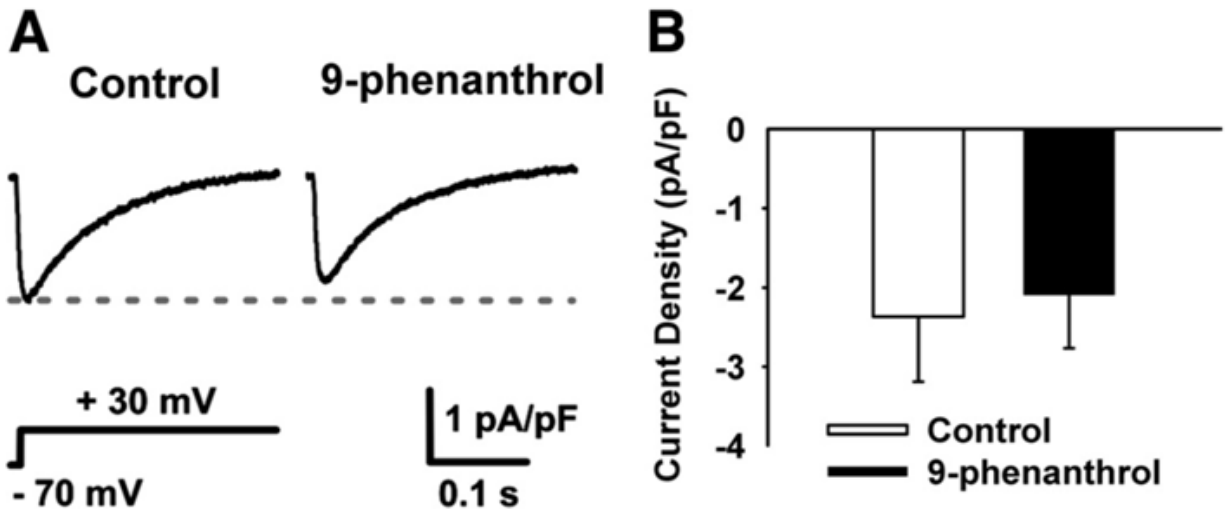

Figure 4.4: 9-Phenanthrol Does Not Inhibit Voltage-dependent Ca^{2+} Currents (I_{Ca}) in Cerebral Arterial Smooth Muscle Cells. *A*: representative voltage-dependent I_{Ca} at +30 mV recorded from cerebral arterial smooth muscle cells before (*left*) and after (*right*) administration of 9-phenanthrol (30 μM).*B*: summary of I_{Ca} current densities before and after administration of 9-phenanthrol; $n = 4$.

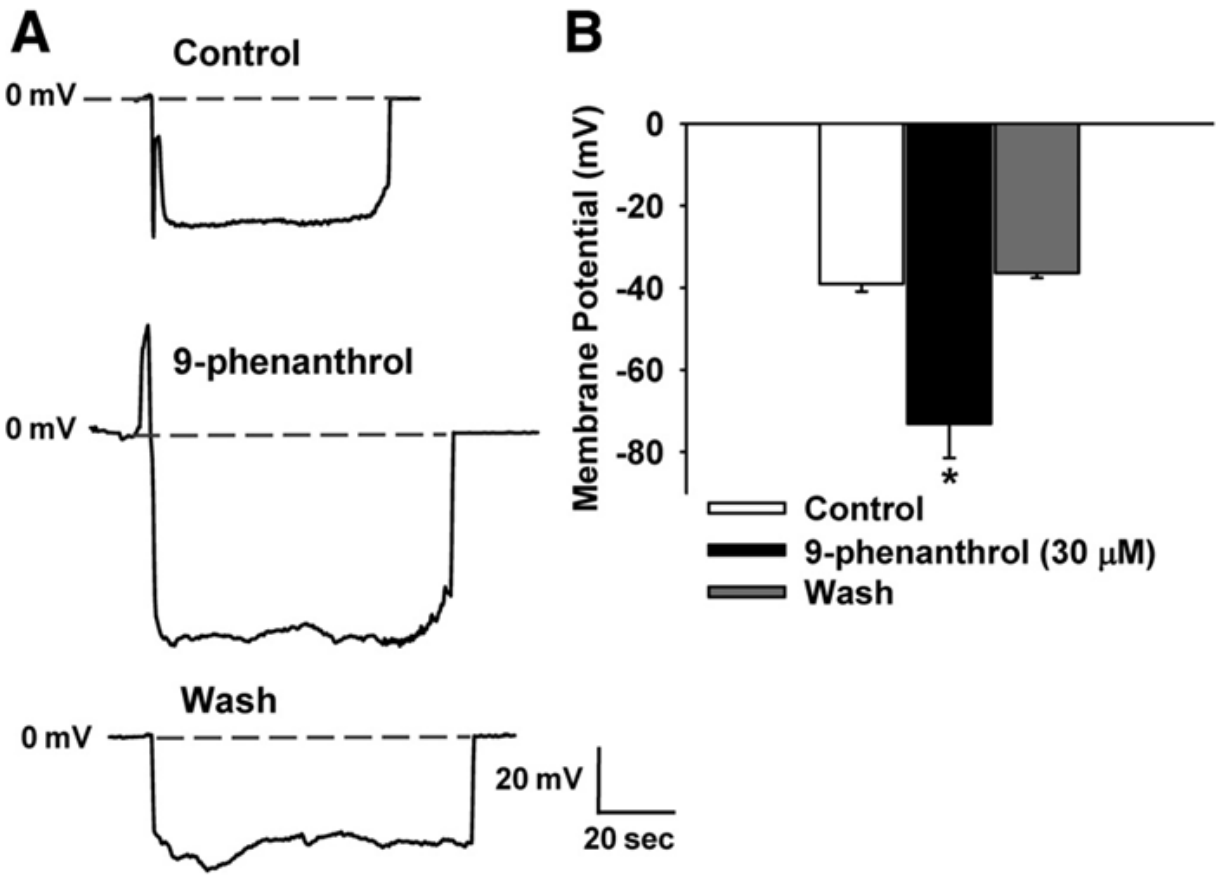

Figure 4.5: 9-Phenanthrol Hyperpolarizes Vascular Smooth Muscle Cells in Pressurized Cerebral Arteries. *A*: representative recordings of smooth muscle cell membrane potential in cerebral arteries pressurized to 70 mmHg under control conditions, following administration of 9-phenanthrol (30 μM), and after the compound was washed out of the superfusion bath. *B*: summary data showing the effects of 9-phenanthrol on smooth muscle cell membrane potential; $n = 4$ for control and 9-phenanthrol; $n = 3$ for Wash. *$P \leq 0.05$ vs. all other groups.

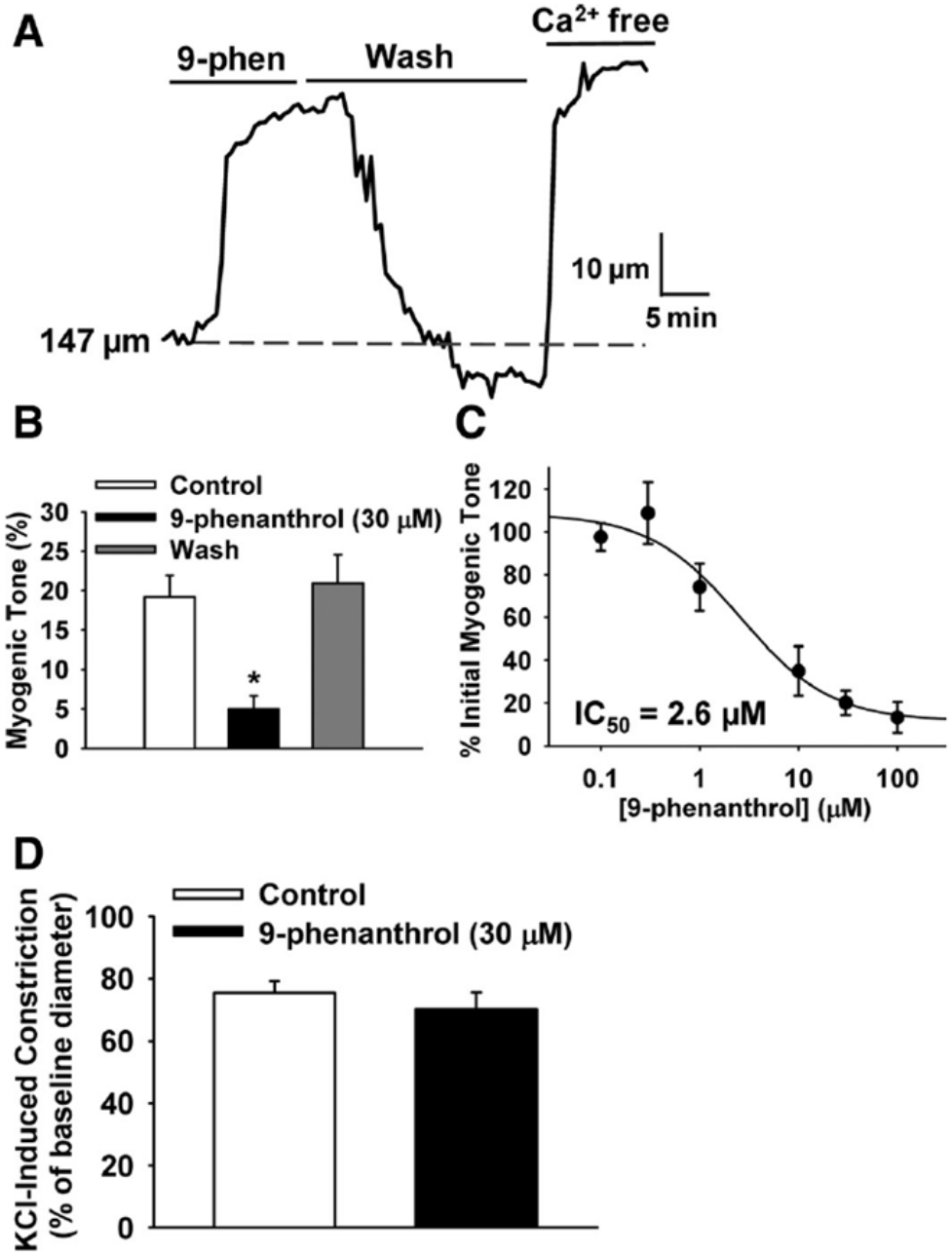

Figure 4.6: 9-Phenanthrol Dilates Pressurized Cerebral Arteries. *A*: representative recoding of luminal diameter of a cerebral artery pressurized to 70 mmHg demonstrating the reversible effects of 9-phenanthrol (30 µM) on myogenic tone. *B*: summary data of myogenic tone for pressurized cerebral arteries (70 mmHg) under control conditions, following treatment with 9-phenanthrol (30 µM), and after the compound was washed out of the superfusion bath; $n = 4$. *C*: concentration response curve for the effects of 9-phenanthrol on cerebral artery myogenic tone. IC_{50} = 2.6 µM; n = 4–7 arteries at each concentration. *D*: summary data showing the effects of 9-phenanthrol on KCl (60 mM)-induced constriction of cerebral arteries; $n = 4$. *$P \leq 0.05$ vs. all other groups.

CHAPTER 5

Summary and Perspective

TRPM4 IN CEREBRAL ARTERY SMOOTH MUSCLE CELLS

TRPM4 channels are present and functionally critical for the regulation of cerebral artery tone (43). Inside-out patch clamp recordings from freshly isolated cerebral artery smooth muscle cells in symmetrical cation solutions demonstrate a monovalent cation-selective and Ca^{2+}-dependent (EC_{50} = 200 μM) current with unitary conductance suggestive for TRPM4 (~24 pS) (43). Single channel activity exhibited a linear voltage dependency, with inward currents at negative potentials, reversal at 0 mV, and outward currents at positive potentials (43). Ion substitution experiments revealed the channel to be selective for Na^+ ions (43), and suppression of TRPM4 expression via antisense technology decreased channel activity, establishing the molecular identity of these currents as TRPM4 (43). Downregulation of TRPM4 impaired smooth muscle depolarization and myogenic constriction of isolated cerebral arteries (43). In addition, *in vivo* knockdown of TRPM4 expression impaired autoregulation of cerebral blood flow in living animals (151). Following suppression of the channel by infusion of antisense oligodeoxynucleotides targeting TRPM4 into rat cerebral spinal fluid, blood flow was recorded to be higher at resting and elevated mean arterial pressures (151). These were the first findings to demonstrate the functional significance of TRPM4 as a major contributor to cerebral blood flow regulation. The channel blocker 9-phenanthrol was employed to further and more acutely examine the role of TRPM4 in cerebral arteries. Blocking of TRPM4 currents with 9-phenanthrol reversibly hyperpolarizes smooth

muscle cells leading to dilation of cerebral arteries (58). Consistent with these findings, 9-phenanthrol was used to pharmacologically identify TRPM4 as the major contributor to resting membrane potential in human and monkey colonic smooth muscle cells (34). These findings demonstrate the functional significance of TRPM4 channels in the regulation of smooth muscle cell membrane potential.

In contrast with the findings discussed above, recent studies using TRPM4 knockout ($TRPM4^{-/-}$) mice reported no difference in myogenic tone in arteries from mouse hind limbs (101). One explanation is that the relationship between membrane potential and myogenic tone can vary between arteries of different vascular beds. In cerebral arteries, vascular tone as a function of membrane potential exhibits a near linear relationship (85), while in skeletal muscle arterioles this relationship is reported to be sigmoidal or non-linear (89). This difference between arteries of two vascular beds may suggest variations in the mechanism that regulate arterial tone. Alternatively, compensatory mechanisms may exist within knockout mouse systems. For example, TRPC6 deficient ($TRPC6^{-/-}$) mice exhibited a higher mean arterial blood pressure compared to controls, but this was associated with an upregulation of TRPC3 channels (31). Changes in expression levels of other TRP channels in $TRPM4^{-/-}$ mice were not reported, so possible compensation by other channels cannot be ruled out. Further experiments are warranted to resolve these issues.

Elucidation of cellular pathways that regulate TRPM4 channels in cerebral artery smooth muscle cells have been hampered by the channel's intrinsic and rapid Ca^{2+}-dependent inactivation (43, 57, 95). Micromolar concentrations of Ca^{2+} traditionally have been included in the recording pipette to activate TRPM4 channels following

cellular dialysis under conventional whole-cell recording conditions. Within a few minutes following exposure to high Ca^{2+}, TRPM4 activity rapidly inactivates (95, 128). Block of PLC activity or including PIP_2 in the recording pipette solution can rescue the channel from inactivation (125, 202). These observations suggest that loss of channel activity could be an artifact of conventional whole cell recording conditions. High intracellular concentrations of Ca^{2+} maintained following dialysis may over-stimulate Ca^{2+}-dependent PLC isoforms leading to depletion of local PIP_2 stores. To test this possibility, an amphotericin B perforated patch-clamp configuration was employed in which whole cell currents were recorded with minimal disruption of subcellular Ca^{2+} signaling pathways (71). This patch-clamp method allowed novel sustained inward cation currents to be recorded from native cerebral artery smooth muscle cells for as long as seal viability could be maintained (> 30 min). These currents are referred to as "transient inward cation currents" (TICCs) (55). TICCs have an apparent single channel conductance of ~25 pS, reverse near 0 mV in symmetrical cation solutions, and channel activity is lost following substitution of extracellular Na^+ with impermeant cation NMDG (55). TICC activity was inhibited by TRPM4-blockers flufenamic acid and 9-phenanthrol, and is attenuated by siRNA-mediated downregulation of TRPM4 expression in cerebral artery myocytes (55). These findings demonstrate that the molecular identity of the channel responsible for TICC activity is TRPM4. Recording of sustained TRPM4 currents under the perforated patch-clamp technique provides a novel method for further characterization of channel activity under near-physiological conditions in smooth muscle cells.

REGULATION OF TRPM4 IN CEREBRAL ARTERY SMOOTH MUSCLE CELLS

The ability to record sustained channel activity from native cells without major disruption of intracellular Ca^{2+} dynamics has allowed TRPM4 channel regulation to be characterized. TRPM4 requires [Ca^{2+}] above resting cystolic levels for activation. In freshly isolated cerebral artery smooth muscle cells, removal of extracellular Ca^{2+} did not acutely affect TRPM4 channel activity (55, 57). Blocking of the sarco(endo)plasmic reticulum Ca^{2+}-ATPase (SERCA) rapidly inhibited TICC activity, suggesting that Ca^{2+} released from internal stores activated the channel (55, 57). Inhibition of inositol trisphosphate receptors (IP_3R), but not ryanodine receptors, diminished TICC activity, suggesting that TRPM4 channels are activated by Ca^{2+} released from the sarcoplasmic reticulum (SR) via IP_3R (55, 57). In agreement with these findings, the membrane permeable inositol trisphosphate (IP_3) analog Bt-IP_3 increased TICC activity (57). This effect was lost when cells were pretreated with the IP_3R blocker xestospongin C (57), providing further evidence to the involvement of IP_3R in the activation of TRPM4 channels. The coupling between TRPM4 and IP_3R was also reported for the neonatal mouse preBötzinger complex, where the channels contribute to neuronal control of respiratory rhythms (24). These data suggest that a Ca^{2+} release event culminating from IP_3R within in the SR membrane activates TRPM4 channels located in the plasma membrane.

Changes in cytosolic Ca^{2+} dynamics influence IP_3R-dependent activation of TRPM4. Using immunocytochemistry and membrane specific staining, IP_3Rs in the SR membrane and TRPM4 channels located on the plasma membrane were found to be proximal (57). These findings were complemented by conventional whole cell patch

clamp experiments where the Ca^{2+} buffers ethylene glycol-bis(2-aminoethylether)-N,N,N′,N′-tetraacetic acid (EGTA) or bis-ethane-N,N,N′,N′-tetraacetic acid (BAPTA) were included in the pipette solution and dialyzed into the cell under the whole cell configuration. BAPTA and EGTA have identical steady-state kinetics and Ca^{2+} binding affinities, but significantly differ in their binding rate constants (5). BAPTA can bind free Ca^{2+} at a rate that is two orders of magnitude faster than EGTA (5). IP_3R-mediated activation of TRPM4 was observed when 10 mM EGTA but not 10 mM BAPTA (57) was included in the recording pipette. This difference in channel activity by equal concentrations of BAPTA or EGTA suggests that the IP_3R-mediated activation of TRPM4 occurs within spatially restricted domains. Ca^{2+} microdomains, with a Ca^{2+} source-to-sensor distance of greater than 50 nm, are defined by Ca^{2+}-dependent responses that are equally disrupted by identical concentrations of BAPTA and EGTA (112). In contrast, Ca^{2+} nanodomains, with a Ca^{2+} source-to-sensor distance less than 50 nm, are defined by Ca^{2+}-dependent responses that are significantly interfered with by BAPTA, but not by equal concentrations of EGTA (112). Therefore, the difference in channel activity in the presence of equal concentrations of BAPTA vs. EGTA, suggests that TRPM4 channels and IP_3Rs are located no more than 50 nm apart within Ca^{2+} nanodomains (Figure 5.1) Additionally, loss of TRPM4 channel activity following Ca^{2+} chelation with BAPTA provides electrophysiological evidence that the IP_3R-mediated activation of TRPM4 channels occurs via a Ca^{2+} release event and that these signaling events occur within nanodomains where the SR and plasma membranes are in close proximity.

Ca^{2+} is an important second messenger for multiple overlapping intracellular signaling pathways. TRPM4 channels are activated by micromolar levels of cytosolic Ca^{2+}, and recent work suggests that localized and transient release of Ca^{2+} from intracellular stores through IP_3R activates TRPM4 channels. IP_3Rs are also influenced by intracellular Ca^{2+}, but at much lower concentrations and exhibit a biphasic sensitivity where Ca^{2+} activates and inactivates the channel within a nanomolar range (300 nM) (73, 74). Ca^{2+} can excite or inhibit IP_3Rs directly at several distinct Ca^{2+} binding sites within the channel (for review see (113)) or indirectly by interfering with binding of IP_3 to the channel (11). Additionally, binding of IP_3 to IP_3R increases the Ca^{2+} sensitivity of channel (98) and the interplay between intracellular Ca^{2+} and IP_3 binding to IP_3R contributes to the versatility and hierarchical recruitment of observed Ca^{2+} signaling events. In response to increased levels of cytosolic $IP_{3,}$ individual IP_3Rs are activated giving rise to unitary events (Ca^{2+} blips) (16, 178), then clusters of IP_3Rs open together (Ca^{2+} puff) (150, 178, 182), and ultimately these events propagate from one cluster to another (Ca^{2+} waves) (110) . The particular IP_3R-mediated Ca^{2+} release event physiologically important for activation of TRPM4 in cerebral artery myocytes is still not known, but recordings of sustained TRPM4 channel activity from smooth muscle cells suggest that PLC-dependent generation of IP_3 and intracellular Ca^{2+} required for IP_3R activation are continuously present. Separation of the IP_3R-dependent Ca^{2+} release event from the Ca^{2+} signaling pathways initially regulating IP_3R function can be achieved through the difference of Ca^{2+} sensitivity between TRPM4 and IP_3R. Low levels of intracellular Ca^{2+} can modulate communication between IP_3Rs without affecting TRPM4 channel activity and smooth muscle membrane depolarization. Additionally,

signaling events initiated distal to SR/plasma membrane junctions can propagate between neighboring IP_3Rs towards nanodomains where IP_3R-dependent activation of TRPM4 channels occurs. These two tiers of Ca^{2+} sensitivity, with low nanomolar concentrations of Ca^{2+} stimulating IP_3Rs and higher micromolar concentrations activating TRPM4 channels, provides a separation and prevention of crosstalk between Ca^{2+} signaling events. This arrangement allows for multiple localized Ca^{2+} events to occur concurrently without stimulating TRPM4-mediated membrane depolarization and myogenic constriction.

In addition to TRPM4, other receptor-dependent and mechanosensitive TRP channels have been shown to play important roles in smooth muscle contractility, but the molecular mechanisms of how these channels may interact has yet to be addressed. IP_3Rs require on the presence of IP_3 and Ca^{2+} for activation, therefore IP_3R-mediated stimulation of TRPM4 depends on an initial source of localized Ca^{2+}. We propose that Ca^{2+} permeable TRP channels form upstream signaling complexes with IP_3R and TRPM4, whereas Ca^{2+} influx through these channels can stimulate IP_3R, leading to Ca^{2+}-induced Ca^{2+}-release dependent activation of TRPM4. Members of the TRPC, TRPM, and TRPV subfamilies have been reported to modulate receptor-activated calcium entry. Angiotensin II, a potent circulating vasoconstrictor, increases channel activity of TRPC1 and TRPC6 channels in rabbit mesenteric myocytes (48, 163). Additionally, TRPC6 currents also increase following exposure to phenylephrine (76), vasopressin (83), and reactive oxygen species (ROS) productions (32). In vascular smooth muscle cells, TRPC3 is activated by ET-1 (141) and UTP (152), with the latter causing membrane depolarization and vasoconstriction in cerebral arteries.

Activation of these agonist-sensitive TRP channels may lead to Ca^{2+} influx, stimulation of IP_3R, and activation of TRPM4 channels. Additionally, several TRP channels expressed in the vasculature, including TRPV4, TRPC1, 5, 6, TRPM4, 7, TRPA1, and TRPP2 (for review see (75)) are reported to have indirect or direct mechanosensitive currents, but their physiological relevance is still highly debated. Similar to the proposed upstream signaling of agonist-sensitive TRP channels, mechanosensitive TRP channels may be localized within signaling domains and allow for the indirect stretch-sensitive activation of TRPM4. Ca^{2+}-induced Ca^{2+}-release dependent signaling complexes have been previously reported in cerebral arterial myocytes, where Ca^{2+} conductance via TRPV4 channels contribute to smooth muscle hyperpolarization and arterial dilation (37). In response to endothelium-derived arachidonic acid metabolite 11, 12 epoxyeicosatrienoic acid (11, 12 EET), TRPV4-like currents are activated in mesenteric smooth muscle cells isolated from wild type but not from TRPV4 deficient mice (37). Ca^{2+} influx through TRPV4 leads to membrane hyperpolarization and arterial dilation through the formation of Ca^{2+} signaling complex with ryanodine receptors and BK_{Ca} channels. Ca^{2+} entry through TRPV4 stimulates ryanodine receptors in the SR membrane, which generates Ca^{2+} sparks, activates proximal BK_{Ca} channels, and leads to membrane hyperpolarization (37). The presence of these hyperpolarizing and depolarizing signaling complexes may act to amplify and integrate multiple TRP channel inputs of different external stimuli leading to modulations in smooth muscle membrane excitability and vasoconstrictor response.

Generation of myogenic tone requires PLC activity (136), but the mechanism behind PLC-dependent membrane depolarization and myocyte contraction is still not

clear. Recent findings showing that TRPM4-mediated membrane depolarization requires Ca^{2+} released from IP_3Rs in the SR which may provide insight to PLC-dependent vasoconstriction. Production of the endogenous IP_3R activator IP_3 occurs through the hydrolysis of PIP_2 by PLC, and, in arterial smooth muscle cells, the intracellular concentration of IP_3 (114) and PLC activity (136) are positively correlated with changes in arterial intraluminal pressure. Additionally, pharmacological inhibition of PLC results in smooth muscle membrane hyperpolarization and disruption of sustained pressure-induced constriction of arteries (82, 136). Therefore, tonic PLC activity could generate intracelluar IP_3 levels required for IP_3R activation and TRPM4-mediated smooth muscle membrane depolarization and maintenance of cerebral vascular tone. Multiple isoforms belonging to three families (β, γ, and δ) of PLC have been detected in vascular smooth muscle cells (97). Extracellular agonists bind to G protein-coupled receptors located on the plasma membrane and may activate PLCβ isoforms leading to receptor-mediated vasoconstriction. Early reports observed complete elimination of pressure- and agonist-induced tone following the inhibition of tyrosine kinases, upstream activators of PLCγ isoforms (30, 136). The direct influence of PLCβ or PLCγ isoforms on TRPM4 channel activity has not been shown, but generation of IP_3 and activation of sustained IP_3R-mediated TRPM4 currents could provide the depolarizing stimulus for PLC-dependent contractions. In addition, PLC has several upstream and downstream effects, expanding the possible interactions and molecular pathways that may influence TRPM4-mediated smooth muscle membrane depolarization and vasoconstriction.

PKC plays an important role in regulating basal arterial tone in cerebral arteries (41, 81, 156). Stimulation of PKC activity increases the Ca^{2+}-sensitive activation of TRPM4 currents (131), and in cerebral artery myocytes PMA elicits TRPM4-dependent membrane depolarization and arterial constriction (41). To further elucidate the mechanism of PKC-dependent increases in cation current, cell surface biotinylation and TIRF microscopy were used to examine the expression of TRPM4 protein in the plasma membrane (23). Following PKC stimulation, TRPM4 channels rapidly translocated (~5 minutes) to the plasma membrane in A7r5 cells, primary cerebral artery myocytes, and intact arteries (23). This effect was lost following selective inhibition of PKCδ, but not following blocking of PKCα and PKCβ (23). RNAi-mediated downregulation or pharmacological inhibition of PKCδ caused TRPM4 channels to translocate from the plasma membrane into the cytosol (52), suggesting that tonic PKCδ activity is required to maintain surface expression of TRPM4. Channel activity was inhibited following the administration of the PKCδ blocker rottlerin (52), and suppression of PKCδ expression hyperpolarized smooth muscle cells and impaired vessel constriction in response to both PMA and increases in intraluminal pressure in intact cerebral arteries (23). These findings provide a novel mechanism for the regulation of smooth muscle excitability through the dynamic trafficking of TRPM4 channels to and from the plasma membrane, and indicate that PKC-dependent increases in Ca^{2+} sensitivity of the channel may result from elevated levels of TRPM4 protein at the cell surface.

BK_{Ca} channels are a major hyperpolarizing influence in smooth muscle cells and recent evidence from our lab demonstrate that TRPM4 is a major depolarizing influence; therefore the resting membrane potential of smooth muscle cells is dependent on the

counteracting yet complimentary interactions of these two channels. The involvement of smooth muscle BK_{Ca} channels in the control of endothelial-dependent arterial tone has been well documented, but the participation of TRPM4 is still not known. Vasorelaxtion of many vascular beds in response to nitric oxide (NO) involves the activation of BK_{Ca} channels (51, 196). NO can stimulate guanylyl cyclase, elevate cyclic guanosine monophosphate (cGMP) levels, and activate cGMP-dependent protein kinase (PKG) (157). Additionally, beta-adrenergic stimulation of G_s-coupled proteins activate adenylyl cyclase and increase cyclic adenosine monophosphate (cAMP), resulting in the stimulation of cAMP-dependent protein kinase (PKA) (91, 169) . PKG and PKA activity mediates relaxation of many types of smooth muscle cells, in part, through the activation of BK_{Ca} channels, initiation of membrane hyperpolarization, and closing of L-type Ca^{2+} channels (92). As of now, there is no evidence of the physiological effect of NO, cGMP, cAMP, PKG, or PKA on TRPM4 channel currents, but the effect of these pathways on IP3R has been well studied. PKG- and PKA-dependent phosphorylation of IP_3R via an IP_3R-associated cGMP kinase substrate (IRAG) greatly attenuates channel function by directly regulating IP_3 sensitivity and indirectly by regulating IP_3 generation (111, 167). PKC/IRAG inhibition of IP_3R-dependent Ca^{2+} release relaxed colonic and aortic smooth muscle cells (111, 166). In tracheal smooth muscle cells, PKA activity attenuated IP_3R-mediated Ca^{2+} release by inhibiting the generation of IP_3 and reducing the number possible IP_3 binding sites (88). Inhibition of IP_3R-mediated Ca^{2+} release by PKG or PKA activity may result in a loss of TRPM4 channel activity. The possible negative effect of PKA and PKG on TRPM4-mediated membrane depolarization

compliments the positive effect they have on BK_{Ca} channel activity, ultimately leading to membrane hyperpolarization and relaxation of arteries.

TRPM4 IN HYPERTENSION

Smooth muscle hyperexcitability leading to increased peripheral resistance within the microvasculature contributes to the development of essential hypertension (50). In vascular smooth muscle cells, the regulation and permeability of K^+ and Ca^{2+} are altered during this disease, but involvement of TRPM4 channel activity has not been reported. In many hypertensive human and animal models, elevated vascular tone has been reported and is associated with a more depolarized resting membrane potential and disrupted Ca^{2+} handling (190). L-type Ca^{2+} current density in vascular smooth muscle cells from spontaneous hypertensive rats (SHR) is increased compared to their normotensive Wistar-Kyoto (WKY) controls (161, 191), leading to an increase in basal intracellular Ca^{2+} concentrations. In addition, BK_{Ca} channel activity is increased under hypertensive conditions (45, 160). The open probability of BK_{Ca} channels increases at more positive potentials, suggesting that increased channel activity during hypertension results from amplified depolarizing currents. TRPM4 is an intriguing potential contributor to this pathophysiological condition, as several of the molecular pathways that regulate its activity have also been shown to be altered under these conditions. For example, PLC activity and the generation of IP_3 increase in response to intraluminal pressures (114), and basal intracellular IP_3 concentrations are elevated in genetically hypertensive rats (13, 105, 154, 185, 187, 198). Although no difference in IP_3R expression or IP_3R-mediated Ca^{2+} release has been reported, an increase in intracellular IP_3 level together

with elevated cytosolic Ca^{2+} levels could increase tonic IP_3R-mediated TRPM4 channel activity and membrane depolarization. PKC activity has also been linked with pressure-dependent vasoconstriction and PMA-mediated activation of PKC enhances myogenic activity (109). Inhibition of PKC in cerebral arteries has a significantly greater effect on myogenic tone in cerebral arteries isolated from SHR rats compared to WKY controls (81), suggesting an increase in PKC activity during hypertension. Surface expression of TRPM4 channels is dynamically regulated by PKC (23) and the observed increase in PKC activity in SHR rats can lead to more channels localized in the plasma membrane. Interestingly, a missense mutation of TRPM4 impaired the endocytosis of channels leading to elevated channel density at the plasma membrane, contributing to the development of progressive familial heart block type 1 in humans (90). Mutations with similar effects on TRPM4 distibution in vascular smooth muscle cells could lead to higher tonic TRPM4 channel activity, increased membrane depolarization, and ultimately contribute to smooth muscle hyperexcitability, thereby contributing to hypertension. Additional studies investigating the involvement of TRPM4 in hypertension are needed to test this hypothesis.

CONCLUSION

The discovery of TRPM4 has unmasked the molecular identity of one type of NSC_{Ca} channels that were first described in 1981. TRPM4 processes biophysical properties and broad distribution reminiscent of NSC_{Ca} channels. In addition, TRPM4 channels are selective for monovalent cations, activated by, but impermeable to, Ca^{2+}, and are regulated by components of the PLC and PKC pathways (Figure 5.3).

Advancements in the ability to record TRPM4 channel activity in native smooth muscle cells has allowed for further insight to the signaling complexes that regulate the channel. It is apparent that TRPM4 is an essential ion channel for cerebral artery myocyte depolarization leading to contraction, but additional studies are needed to fully elucidate the possible complementary and integrative role it may play with other ion channels proposed to influence smooth muscle depolarization. More importantly, the pathophysiological role of TRPM4 in vascular dysfunction associated with hypertension, stroke, and other cardiovascular diseases warrants further investigation.

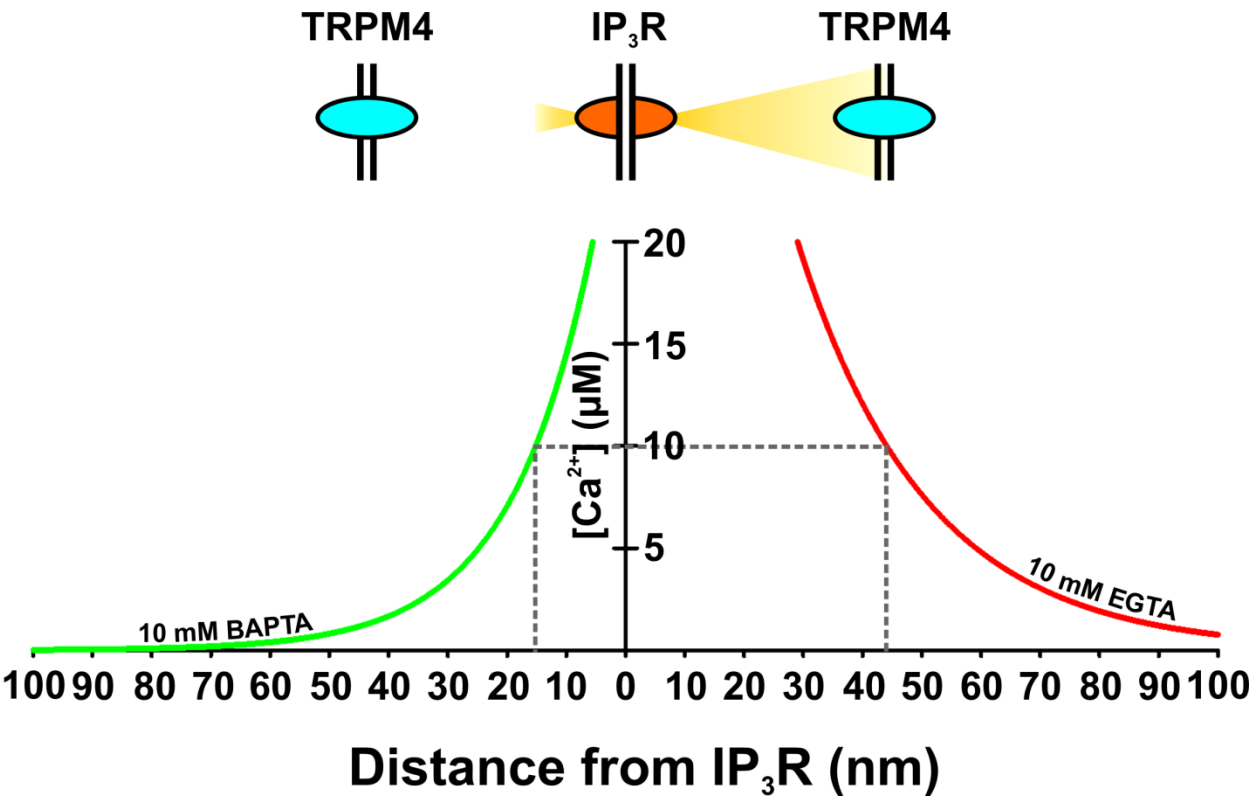

Figure 5.1: Simulation of TRPM4 by Ca^{2+} Nanodomain Created by Ca^{2+} released from the Sarcoplasmic Reticulum via IP_3R. In freshly isolated smooth muscles, TRPM4 activation requires Ca^{2+} released from the SR through proximal IP_3R. The Ca^{2+} concentration profile comparing the buffering capacity of the slow and fast Ca^{2+} chelators EGTA and BAPTA on $[Ca^{2+}]_i$ as a function of distance from a single IP_3R Ca^{2+} release site. Simulation data using CalC software v. 6.0 (102) was re-plotted from Gonzales and Earley (56).

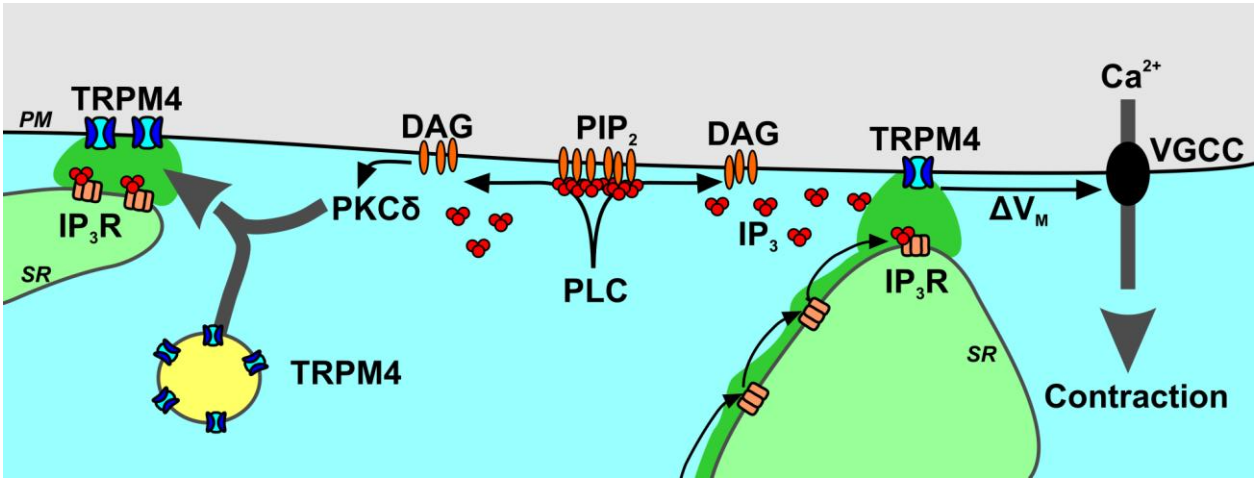

Figure 5.2: Regulation of TRPM4 Activity in Contractile Cerebral Artery Smooth Muscle Cells. PM, plasma membrane; SR, sarcoplasmic reticulum; PKCδ, protein kinase C; PIP_2, phosphatidylinositol 4, 5-bisphosphate; PLC, phospholipase C; IP_3, inositol triphosphate; IP_3R, inositol triphosphate receptor; V_M, membrane potential; and VGCC, voltage gated calcium channels.

REFERENCES

1. Aaroson PI, Bolton TB, Lang RJ, and MacKenzie I. Calcium currents in single isolated smooth muscle cells from the rabbit ear artery in normal-calcium and high-barium solutions. *J Physiol* 405: 57-75, 1988.

2. Adebiyi A, Narayanan D, and Jaggar JH. Caveolin-1 assembles type 1 inositol 1,4,5-trisphosphate receptors and canonical transient receptor potential 3 channels into a functional signaling complex in arterial smooth muscle cells. *J Biol Chem* 286: 4341-4348, 2011.

3. Adebiyi A, Zhao G, Narayanan D, Thomas-Gatewood CM, Bannister JP, and Jaggar JH. Isoform-selective physical coupling of TRPC3 channels to IP_3 receptors in smooth muscle cells regulates arterial contractility. *Circ Res* 106: 1603-1612, 2010.

4. Aickin CC and Brading AF. The effect of loop diuretics on Cl^- transport in smooth muscle of the guinea-pig vas deferens and taenia from the caecum. *J Physiol* 421: 33-53, 1990.

5. Allbritton NL, Meyer T, and Stryer L. Range of messenger action of calcium ion and inositol 1,4,5-trisphosphate. *Science* 258: 1812-1815, 1992.

6. Ashcroft SJ and Ashcroft FM. Properties and functions of ATP-sensitive K^+-channels. *Cell Signal* 2: 197-214, 1990.

7. Augustine GJ, Santamaria F, and Tanaka K. Local calcium signaling in neurons. *Neuron* 40: 331-346, 2003.

8. Bayguinov O, Hagen B, Bonev AD, Nelson MT, and Sanders KM. Intracellular calcium events activated by ATP in murine colonic myocytes. *Am J Physiol Cell Physiol* 279: C126-135, 2000.

9. Bayliss WM. On the local reactions of the arterial wall to changes of internal pressure. *J Physiol* 28: 220-231, 1902.

10. Bean BP, Sturek M, Puga A, and Hermsmeyer K. Calcium channels in muscle cells isolated from rat mesenteric arteries: modulation by dihydropyridine drugs. *Circ Res* 59: 229-235, 1986.

11. Benevolensky D, Moraru, II, and Watras J. Micromolar calcium decreases affinity of inositol trisphosphate receptor in vascular smooth muscle. *Biochem J* 299 (Pt 3): 631-636, 1994.

12. Benham CD, Hess P, and Tsien RW. Two types of calcium channels in single smooth muscle cells from rabbit ear artery studied with whole-cell and single-channel recordings. *Circ Res* 61: I10-16, 1987.

13. Bernier S and Guillemette G. Increased inositol 1,4,5-trisphosphate binding capacity in vascular smooth muscle of spontaneously hypertensive rats. *Am J Hypertens* 6: 217-225, 1993.

14. Berra-Romani R, Blaustein MP, and Matteson DR. TTX-sensitive voltage-gated Na^+ channels are expressed in mesenteric artery smooth muscle cells. *Am J Physiol Heart Circ Physiol* 289: H137-145, 2005.

15. Boittin FX, Coussin F, Morel JL, Halet G, Macrez N, and Mironneau J. Ca^{2+} signals mediated by Ins(1,4,5)P(3)-gated channels in rat ureteric myocytes. *Biochem J* 349: 323-332, 2000.

16. Bootman MD, Berridge MJ, and Lipp P. Cooking with calcium: the recipes for composing global signals from elementary events. *Cell* 91: 367-373, 1997.

17. Brayden JE and Nelson MT. Regulation of arterial tone by activation of calcium-dependent potassium channels. *Science* 256: 532-535, 1992.

18. Bruno L, Solovey G, Ventura AC, Dargan S, and Dawson SP. Quantifying calcium fluxes underlying calcium puffs in Xenopus laevis oocytes. *Cell Calcium* 47: 273-286, 2010.

19. Bulley S, Neeb ZP, Burris SK, Bannister JP, Thomas-Gatewood CM, Jangsangthong W, and Jaggar JH. TMEM16A Channels Contribute to the Myogenic Response in Cerebral Arteries. *Circ Res*, 2012.

20. Burdyga TV and Wray S. The effect of cyclopiazonic acid on excitation-contraction coupling in guinea-pig ureteric smooth muscle: role of the sarcoplasmic reticulum. *J Physiol* 517 (Pt 3): 855-865, 1999.

21. Corteling RL, Brett SE, Yin H, Zheng X-L, Walsh MP, and Welsh DG. The functional consequence of RhoA knockdown by RNA interference in rat cerebral arteries. *Am J Physiol Heart Circ Physiol* 293: H440-447, 2007.

22. Cox RH, Zhou Z, and Tulenko TN. Voltage-gated sodium channels in human aortic smooth muscle cells. *J Vasc Res* 35: 310-317, 1998.

23. Crnich R, Amberg GC, Leo MD, Gonzales AL, Tamkun MM, Jaggar JH, and Earley S. Vasoconstriction resulting from dynamic membrane trafficking of TRPM4 in vascular smooth muscle cells. *Am J Physiol Cell Physiol* 299: C682-694, 2010.

24. Crowder EA, Saha MS, Pace RW, Zhang H, Prestwich GD, and Del Negro CA. Phosphatidylinositol 4,5-bisphosphate regulates inspiratory burst activity in the neonatal mouse preBotzinger complex. *J Physiol* 582: 1047-1058, 2007.

25. Dargan SL, Schwaller B, and Parker I. Spatiotemporal patterning of IP_3-mediated Ca^{2+} signals in Xenopus oocytes by Ca^{2+}-binding proteins. *J Physiol* 556: 447-461, 2004.

26. Davis AJ, Shi J, Pritchard HA, Chadha PS, Leblanc N, Vasilikostas G, Yao Z, Verkman AS, Albert AP, and Greenwood IA. Potent vasorelaxant activity of the TMEM16A inhibitor T16A(inh) -A01. *Br J Pharmacol*, 2012.

27. Davis MJ, Donovitz JA, and Hood JD. Stretch-activated single-channel and whole cell currents in vascular smooth muscle cells. *Am J Physiol* 262: C1083-1088, 1992.

28. Demion M, Bois P, Launay P, and Guinamard R. TRPM4, a Ca^{2+}-activated nonselective cation channel in mouse sino-atrial node cells. *Cardiovasc Res* 73: 531-538, 2007.

29. Dhaka A, Viswanath V, and Patapoutian A. Trp ion channels and temperature sensation. *Annu Rev Neurosci* 29: 135-161, 2006.

30. Di Salvo J, Steusloff A, Semenchuk L, Satoh S, Kolquist K, and Pfitzer G. Tyrosine kinase inhibitors suppress agonist-induced contraction in smooth muscle. *Biochem Biophys Res Commun* 190: 968-974, 1993.

31. Dietrich A, Mederos YSM, Gollasch M, Gross V, Storch U, Dubrovska G, Obst M, Yildirim E, Salanova B, Kalwa H, Essin K, Pinkenburg O, Luft FC, Gudermann T, and

Birnbaumer L. Increased vascular smooth muscle contractility in TRPC6$^{-/-}$ mice. *Mol Cell Biol* 25: 6980-6989, 2005.

32. Ding Y, Winters A, Ding M, Graham S, Akopova I, Muallem S, Wang Y, Hong JH, Gryczynski Z, Yang SH, Birnbaumer L, and Ma R. Reactive oxygen species-mediated TRPC6 protein activation in vascular myocytes, a mechanism for vasoconstrictor-regulated vascular tone. *J Biol Chem* 286: 31799-31809, 2011.

33. Doughty JM, Miller AL, and Langton PD. Non-specificity of chloride channel blockers in rat cerebral arteries: block of the L-type calcium channel. *J Physiol* 507 (Pt 2): 433-439, 1998.

34. Dwyer L, Rhee PL, Lowe V, Zheng H, Peri L, Ro S, Sanders KM, and Koh SD. Basally activated nonselective cation currents regulate the resting membrane potential in human and monkey colonic smooth muscle. *Am J Physiol Gastrointest Liver Physiol* 301: G287-296, 2011.

35. Earley S. Vanilloid and melastatin transient receptor potential channels in vascular smooth muscle. *Microcirculation* 17: 237-249, 2010.

36. Earley S and Brayden JE. Transient receptor potential channels and vascular function. *Clin Sci (Lond)* 119: 19-36, 2010.

37. Earley S, Heppner TJ, Nelson MT, and Brayden JE. TRPV4 forms a novel Ca^{2+} signaling complex with ryanodine receptors and BKCa channels. *Circ Res* 97: 1270-1279, 2005.

38. Earley S, Reading S, and Brayden JE. Functional significance of transient receptor potential channels in vascular function. 2007.

39. Earley S, Resta TC, and Walker BR. Disruption of smooth muscle gap junctions attenuates myogenic vasoconstriction of mesenteric resistance arteries. *Am J Physiol Heart Circ Physiol* 287: H2677-2686, 2004.

40. Earley S, Straub SV, and Brayden JE. Protein kinase C regulates vascular myogenic tone through activation of TRPM4. *Am J Physiol Heart Circ Physiol* 292: H2613-2622, 2007.

41. Earley S, Straub SV, and Brayden JE. Protein kinase C regulates vascular myogenic tone through activation of TRPM4. *Am J Physiol Heart Circ Physiol* 292: H2613-2622, 2007.

42. Earley S, Waldron BJ, and Brayden JE. Critical role for transient receptor potential channel TRPM4 in myogenic constriction of cerebral arteries. *Circ Res* 95: 922-929, 2004.

43. Earley S, Waldron BJ, and Brayden JE. Critical role for transient receptor potential channel TRPM4 in myogenic constriction of cerebral arteries. *Circ Res* 95: 922-929, 2004.

44. Edwards FR, Hirst GD, and Silverberg GD. Inward rectification in rat cerebral arterioles; involvement of potassium ions in autoregulation. *J Physiol* 404: 455-466, 1988.

45. England SK, Wooldridge TA, Stekiel WJ, and Rusch NJ. Enhanced single-channel K^+ current in arterial membranes from genetically hypertensive rats. *Am J Physiol* 264: H1337-1345, 1993.

46. Fakler B and Adelman JP. Control of K(Ca) channels by calcium nano/microdomains. *Neuron* 59: 873-881, 2008.

47. Falke JJ, Drake SK, Hazard AL, and Peersen OB. Molecular tuning of ion binding to calcium signaling proteins. *Q Rev Biophys* 27: 219-290, 1994.

48. Fellner SK and Arendshorst WJ. Angiotensin II-stimulated Ca^{2+} entry mechanisms in afferent arterioles: role of transient receptor potential canonical channels and reverse Na^{+}/Ca^{2+} exchange. *Am J Physiol Renal Physiol* 294: F212-219, 2008.

49. Filosa JA, Bonev AD, Straub SV, Meredith AL, Wilkerson MK, Aldrich RW, and Nelson MT. Local potassium signaling couples neuronal activity to vasodilation in the brain. *Nat Neurosci* 9: 1397-1403, 2006.

50. Frohlich ED. Clinical significance of hemodynamic findings in hypertension. *Chest* 64: 94-99, 1973.

51. Fujino K, Nakaya S, Wakatsuki T, Miyoshi Y, Nakaya Y, Mori H, and Inoue I. Effects of nitroglycerin on ATP-induced Ca^{2+}-mobilization, Ca^{2+}-activated K^{+} channels and contraction of cultured smooth muscle cells of porcine coronary artery. *J Pharmacol Exp Ther* 256: 371-377, 1991.

52. Garcia ZI, Bruhl A, Gonzales AL, and Earley S. Basal protein kinase Cδ activity is required for membrane localization and activity of TRPM4 channels in cerebral artery smooth muscle cells. *Channels (Austin)* 5: 210-214, 2011.

53. Gherghiceanu M and Popescu LM. Caveolar nanospaces in smooth muscle cells. *J Cell Mol Med* 10: 519-528, 2006.

54. Gonzales AL, Amberg GC, and Earley S. Ca2+ Release from the Sarcoplasmic Reticulum is Required for Sustained TRPM4 Activity in Cerebral Artery Smooth Muscle Cells. *Am J Physiol Cell Physiol*, 2010.

55. Gonzales AL, Amberg GC, and Earley S. Ca2+ release from the sarcoplasmic reticulum is required for sustained TRPM4 activity in cerebral artery smooth muscle cells. *Am J Physiol Cell Physiol* 299: C279-288, 2010.

56. Gonzales AL and Earley S. Endogenous cytosolic Ca^{2+} buffering is necessary for TRPM4 activity in cerebral artery smooth muscle cells. *Cell Calcium* 51: 82-93, 2012.

57. Gonzales AL and Earley S. Endogenous cytosolic Ca(2+) buffering is necessary for TRPM4 activity in cerebral artery smooth muscle cells. *Cell Calcium* 51: 82-93, 2012.

58. Gonzales AL, Garcia ZI, Amberg GC, and Earley S. Pharmacological inhibition of TRPM4 hyperpolarizes vascular smooth muscle. *Am J Physiol Cell Physiol* 299: C1195-1202, 2010.

59. Gottlieb P, Folgering J, Maroto R, Raso A, Wood TG, Kurosky A, Bowman C, Bichet D, Patel A, Sachs F, Martinac B, Hamill OP, and Honore E. Revisiting TRPC1 and TRPC6 mechanosensitivity. *Pflugers Arch* 455: 1097-1103, 2008.

60. Grand T, Demion M, Norez C, Mettey Y, Launay P, Becq F, Bois P, and Guinamard R. 9-phenanthrol inhibits human TRPM4 but not TRPM5 cationic channels. *Br J Pharmacol* 153: 1697-1705, 2008.

61. Guinamard R, Demion M, and Launay P. Physiological roles of the TRPM4 channel extracted from background currents. *Physiology (Bethesda)* 25: 155-164, 2010.

62. Guinamard R, Salle L, and Simard C. The non-selective monovalent cationic channels TRPM4 and TRPM5. *Adv Exp Med Biol* 704: 147-171, 2011.

63. Harder DR. Pressure-dependent membrane depolarization in cat middle cerebral artery. *Circ Res* 55: 197-202, 1984.

64. He LP, Hewavitharana T, Soboloff J, Spassova MA, and Gill DL. A functional link between store-operated and TRPC channels revealed by the 3,5-bis(trifluoromethyl)pyrazole derivative, BTP2. *J Biol Chem* 280: 10997-11006, 2005.

65. Helli PB, Pertens E, and Janssen LJ. Cyclopiazonic acid activates a Ca^{2+}-permeable, nonselective cation conductance in porcine and bovine tracheal smooth muscle. *J Appl Physiol* 99: 1759-1768, 2005.

66. Henrion D, Laher I, Klaasen A, and Bevan JA. Myogenic tone of rabbit facial vein and posterior cerebral artery is influenced by changes in extracellular sodium. *Am J Physiol* 266: H377-383, 1994.

67. Hille B. Ionic channels in excitable membranes. Current problems and biophysical approaches. *Biophys J* 22: 283-294, 1978.

68. Hirst GD and Edwards FR. Sympathetic neuroeffector transmission in arteries and arterioles. *Physiol Rev* 69: 546-604., 1989.

69. Hirst GD, Silverberg GD, and van Helden DF. The action potential and underlying ionic currents in proximal rat middle cerebral arterioles. *J Physiol* 371: 289-304, 1986.

70. Hofmann T, Obukhov AG, Schaefer M, Harteneck C, Gudermann T, and Schultz G. Direct activation of human TRPC6 and TRPC3 channels by diacylglycerol. *Nature* 397: 259-263, 1999.

71. Horn R and Marty A. Muscarinic activation of ionic currents measured by a new whole-cell recording method. *J Gen Physiol* 92: 145-159, 1988.

72. Hulvershorn J, Gallant C, Wang CA, Dessy C, and Morgan KG. Calmodulin levels are dynamically regulated in living vascular smooth muscle cells. *Am J Physiol Heart Circ Physiol* 280: H1422-1426, 2001.

73. Iino M. Biphasic Ca^{2+} dependence of inositol 1,4,5-trisphosphate-induced Ca^{2+} release in smooth muscle cells of the guinea pig taenia caeci. *J Gen Physiol* 95: 1103-1122, 1990.

74. Iino M. Calcium dependent inositol trisphosphate-induced calcium release in the guinea-pig taenia caeci. *Biochem Biophys Res Commun* 142: 47-52, 1987.

75. Inoue R, Jian Z, and Kawarabayashi Y. Mechanosensitive TRP channels in cardiovascular pathophysiology. *Pharmacol Ther* 123: 371-385, 2009.

76. Inoue R, Okada T, Onoue H, Hara Y, Shimizu S, Naitoh S, Ito Y, and Mori Y. The transient receptor potential protein homologue TRP6 is the essential component of vascular $alpha_1$-adrenoceptor-activated Ca^{2+}-permeable cation channel. *Circ Res* 88: 325-332, 2001.

77. Jaggar JH, Porter VA, Lederer WJ, and Nelson MT. Calcium sparks in smooth muscle. *Am J Physiol Cell Physiol* 278: C235-256, 2000.

78. Jaggar JH, Wellman GC, Heppner TJ, Porter VA, Perez GJ, Gollasch M, Kleppisch T, Rubart M, Stevenson AS, Lederer WJ, Knot HJ, Bonev AD, and Nelson MT. Ca^{2+} channels, ryanodine receptors and Ca^{2+}-activated K^+ channels: a functional unit for regulating arterial tone. *Acta Physiol Scand* 164: 577-587, 1998.

79. Jaggar JH, Wellman GC, Heppner TJ, Porter VA, Perez GJ, Gollasch M, Kleppisch T, Rubart M, Stevenson AS, Lederer WJ, Knot HJ, Bonev AD, and Nelson MT. Ca2+ channels, ryanodine receptors and Ca(2+)-activated K+ channels: a functional unit for regulating arterial tone. *Acta Physiol Scand* 164: 577-587, 1998.

80. Janiak R, Wilson SM, Montague S, and Hume JR. Heterogeneity of calcium stores and elementary release events in canine pulmonary arterial smooth muscle cells. *Am J Physiol Cell Physiol* 280: C22-33, 2001.

81. Jarajapu YP and Knot HJ. Relative contribution of Rho kinase and protein kinase C to myogenic tone in rat cerebral arteries in hypertension. *Am J Physiol Heart Circ Physiol* 289: H1917-1922, 2005.

82. Jarajapu YP and Knot HJ. Role of phospholipase C in development of myogenic tone in rat posterior cerebral arteries. *Am J Physiol Heart Circ Physiol* 283: H2234-2238, 2002.

83. Jung S, Strotmann R, Schultz G, and Plant TD. TRPC6 is a candidate channel involved in receptor-stimulated cation currents in A7r5 smooth muscle cells. *Am J Physiol Cell Physiol* 282: C347-359, 2002.

84. Klingauf J and Neher E. Modeling buffered Ca^{2+} diffusion near the membrane: implications for secretion in neuroendocrine cells. *Biophys J* 72: 674-690, 1997.

85. Knot HJ and Nelson MT. Regulation of arterial diameter and wall [Ca2+] in cerebral arteries of rat by membrane potential and intravascular pressure. *J Physiol* 508 (Pt 1): 199-209, 1998.

86. Knot HJ and Nelson MT. Regulation of membrane potential and diameter by voltage-dependent K^+ channels in rabbit myogenic cerebral arteries. *Am J Physiol* 269: H348-355, 1995.

87. Knot HJ, Standen NB, and Nelson MT. Ryanodine receptors regulate arterial diameter and wall [Ca^{2+}] in cerebral arteries of rat via Ca^{2+}-dependent K^+ channels. *J Physiol* 508 (Pt 1): 211-221, 1998.

88. Komalavilas P and Lincoln TM. Phosphorylation of the inositol 1,4,5-trisphosphate receptor. Cyclic GMP-dependent protein kinase mediates cAMP and cGMP dependent phosphorylation in the intact rat aorta. *J Biol Chem* 271: 21933-21938, 1996.

89. Kotecha N and Hill MA. Myogenic contraction in rat skeletal muscle arterioles: smooth muscle membrane potential and Ca^{2+} signaling. *Am J Physiol Heart Circ Physiol* 289: H1326-1334, 2005.

90. Kruse M, Schulze-Bahr E, Corfield V, Beckmann A, Stallmeyer B, Kurtbay G, Ohmert I, Brink P, and Pongs O. Impaired endocytosis of the ion channel TRPM4 is associated with human progressive familial heart block type I. *J Clin Invest* 119: 2737-2744, 2009.

91. Kume H, Graziano MP, and Kotlikoff MI. Stimulatory and inhibitory regulation of calcium-activated potassium channels by guanine nucleotide-binding proteins. *Proc Natl Acad Sci U S A* 89: 11051-11055, 1992.

92. Kume H, Takai A, Tokuno H, and Tomita T. Regulation of Ca^{2+}-dependent K^{+}-channel activity in tracheal myocytes by phosphorylation. *Nature* 341: 152-154, 1989.

93. Large WA and Wang Q. Characteristics and physiological role of the Ca^{2+}-activated Cl^{-} conductance in smooth muscle. *Am J Physiol* 271: C435-454, 1996.

94. Launay P, Cheng H, Srivatsan S, Penner R, Fleig A, and Kinet J-P. TRPM4 Regulates Calcium Oscillations After T Cell Activation. *Science* 306: 1374-1377, 2004.

95. Launay P, Fleig A, Perraud AL, Scharenberg AM, Penner R, and Kinet JP. TRPM4 Is a Ca^{2+}-Activated Nonselective Cation Channel Mediating Cell Membrane Depolarization. *Cell* 109: 397-407, 2002.

96. Ledoux J, Taylor MS, Bonev AD, Hannah RM, Solodushko V, Shui B, Tallini Y, Kotlikoff MI, and Nelson MT. Functional architecture of inositol 1,4,5-trisphosphate signaling in restricted spaces of myoendothelial projections. *Proc Natl Acad Sci U S A* 105: 9627-9632, 2008.

97. Lee SB and Rhee SG. Significance of PIP_2 hydrolysis and regulation of phospholipase C isozymes. *Curr Opin Cell Biol* 7: 183-189, 1995.

98. Marchant JS and Taylor CW. Cooperative activation of IP_3 receptors by sequential binding of IP_3 and Ca^{2+} safeguards against spontaneous activity. *Curr Biol* 7: 510-518, 1997.

99. Marin J, Encabo A, Briones A, Garcia-Cohen EC, and Alonso MJ. Mechanisms involved in the cellular calcium homeostasis in vascular smooth muscle: calcium pumps. *Life Sci* 64: 279-303, 1999.

100. Maruyama Y and Peterson OH. Single-channel currents in isolated patches of plasma membrane from basal surface of pancreatic acini. *Nature* 299: 159-161, 1982.

101. Mathar I, Vennekens R, Meissner M, Kees F, Van der Mieren G, Camacho Londono JE, Uhl S, Voets T, Hummel B, van den Bergh A, Herijgers P, Nilius B, Flockerzi V, Schweda F, and Freichel M. Increased catecholamine secretion contributes to hypertension in TRPM4-deficient mice. *J Clin Invest* 120: 3267-3279, 2010.

102. Matveev V, Zucker RS, and Sherman A. Facilitation through buffer saturation: constraints on endogenous buffering properties. *Biophys J* 86: 2691-2709, 2004.

103. Meguro K, Iida H, Takano H, Morita T, Sata M, Nagai R, and Nakajima T. Function and role of voltage-gated sodium channel $NaV_{1.7}$ expressed in aortic smooth muscle cells. *Am J Physiol Heart Circ Physiol* 296: H211-219, 2009.

104. Michel AD, Xing M, Thompson KM, Jones CA, and Humphrey PP. Decavanadate, a P_2X receptor antagonist, and its use to study ligand interactions with P_2X_7 receptors. *Eur J Pharmacol* 534: 19-29, 2006.

105. Millanvoye E, Freyss-Beguin M, Baudouin-Legros M, Paquet JL, Marche P, Durant S, and Meyer P. Growth rate and phospholipase C activity in cardiac and aortic spontaneously hypertensive rat cells. *J Hypertens Suppl* 6: S369-371, 1988.

106. Miriel VA, Mauban JR, Blaustein MP, and Wier WG. Local and cellular Ca^{2+} transients in smooth muscle of pressurized rat resistance arteries during myogenic and agonist stimulation. *J Physiol* 518 (Pt 3): 815-824, 1999.

107. Mironneau J, Arnaudeau S, Macrez-Lepretre N, and Boittin FX. Ca^{2+} sparks and Ca^{2+} waves activate different Ca^{2+}-dependent ion channels in single myocytes from rat portal vein. *Cell Calcium* 20: 153-160, 1996.

108. Montell C, Birnbaumer L, and Flockerzi V. The TRP channels, a remarkably functional family. *Cell* 108: 595-598, 2002.

109. Morgan KG and Leinweber BD. PKC-dependent signalling mechanisms in differentiated smooth muscle. *Acta Physiol Scand* 164: 495-505, 1998.

110. Mufti RE, Brett SE, Tran CH, Abd El-Rahman R, Anfinogenova Y, El-Yazbi A, Cole WC, Jones PP, Chen SR, and Welsh DG. Intravascular pressure augments cerebral arterial constriction by inducing voltage-insensitive Ca^{2+} waves. *J Physiol* 588: 3983-4005, 2010.

111. Murthy KS. cAMP inhibits IP_3-dependent Ca^{2+} release by preferential activation of cGMP-primed PKG. *Am J Physiol Gastrointest Liver Physiol* 281: G1238-1245, 2001.

112. Naraghi M and Neher E. Linearized buffered Ca2+ diffusion in microdomains and its implications for calculation of [Ca2+] at the mouth of a calcium channel. *J Neurosci* 17: 6961-6973, 1997.

113. Narayanan D, Adebiyi A, and Jaggar JH. Inositol trisphosphate receptors in smooth muscle cells. *Am J Physiol Heart Circ Physiol* 302: H2190-2210, 2012.

114. Narayanan J, Imig M, Roman RJ, and Harder DR. Pressurization of isolated renal arteries increases inositol trisphosphate and diacylglycerol. *Am J Physiol* 266: H1840-1845, 1994.

115. Navedo MF, Amberg GC, Votaw VS, and Santana LF. Constitutively active L-type Ca^{2+} channels. *Proc Natl Acad Sci U S A* 102: 11112-11117, 2005.

116. Neher E. Vesicle pools and Ca^{2+} microdomains: new tools for understanding their roles in neurotransmitter release. *Neuron* 20: 389-399, 1998.

117. Nelson MT. Ca^{2+}-activated potassium channels and ATP-sensitive potassium channels as modulators of vascular tone. *Trends Cardiovasc Med* 3: 54-60, 1993.

118. Nelson MT, Cheng H, Rubart M, Santana LF, Bonev AD, Knot HJ, and Lederer WJ. Relaxation of arterial smooth muscle by calcium sparks. *Science* 270: 633-637, 1995.

119. Nelson MT, Conway MA, Knot HJ, and Brayden JE. Chloride channel blockers inhibit myogenic tone in rat cerebral arteries. *J Physiol* 502 (Pt 2): 259-264, 1997.

120. Nelson MT and Quayle JM. Physiological roles and properties of potassium channels in arterial smooth muscle. *Am J Physiol Cell Physiol* 268: C799-822, 1995.

121. Nelson MT and Quayle JM. Physiological roles and properties of potassium channels in arterial smooth muscle. *Am J Physiol* 268: C799-822, 1995.

122. Nelson MT and Worley JF. Dihydropyridine inhibition of single calcium channels and contraction in rabbit mesenteric artery depends on voltage. *J Physiol* 412: 65-91, 1989.

123. Nichols CG and Lederer WJ. Adenosine triphosphate-sensitive potassium channels in the cardiovascular system. *Am J Physiol* 261: H1675-1686, 1991.

124. Nilius B, Droogmans G, and Wondergem R. Transient receptor potential channels in endothelium: solving the calcium entry puzzle? *Endothelium* 10: 5-15, 2003.

125. Nilius B, Mahieu F, Prenen J, Janssens A, Owsianik G, Vennekens R, and Voets T. The Ca2+-activated cation channel TRPM4 is regulated by phosphatidylinositol 4,5-biphosphate. *EMBO J* 25: 467-478, 2006.

126. Nilius B, Mahieu F, Prenen J, Janssens A, Owsianik G, Vennekens R, and Voets T. The Ca^{2+}-activated cation channel TRPM4 is regulated by phosphatidylinositol 4,5-biphosphate. *EMBO J* 25: 467-478, 2006.

127. Nilius B, Prenen J, Droogmans G, Voets T, Vennekens R, Freichel M, Wissenbach U, and Flockerzi V. Voltage Dependence of the Ca2+-activated Cation Channel TRPM4. *Journal of Biological Chemistry* 278: 30813-30820, 2003.

128. Nilius B, Prenen J, Droogmans G, Voets T, Vennekens R, Freichel M, Wissenbach U, and Flockerzi V. Voltage dependence of the Ca2+-activated cation channel TRPM4. *J Biol Chem* 278: 30813-30820, 2003.

129. Nilius B, Prenen J, Janssens A, Owsianik G, Wang C, Zhu MX, and Voets T. The selectivity filter of the cation channel TRPM4. *Journal of Biological Chemistry* 280: 22899-22906, 2005.

130. Nilius B, Prenen J, Janssens A, Voets T, and Droogmans G. Decavanadate modulates gating of TRPM4 cation channels. *J Physiol* 560: 753-765, 2004.

131. Nilius B, Prenen J, Tang J, Wang C, Owsianik G, Janssens A, Voets T, and Zhu MX. Regulation of the Ca2+ sensitivity of the nonselective cation channel TRPM4. *J Biol Chem* 280: 6423-6433, 2005.

132. Nilius B, Prenen J, Tang J, Wang C, Owsianik G, Janssens A, Voets T, and Zhu MX. Regulation of the Ca^{2+} sensitivity of the nonselective cation channel TRPM4. *Journal of Biological Chemistry* 280: 6423-6433, 2005.

133. Nilius B, Prenen J, Voets T, and Droogmans G. Intracellular nucleotides and polyamines inhibit the Ca2+-activated cation channel TRPM4b. *Pflugers Arch* 448: 70-75, 2004.

134. Ohya Y, Adachi N, Nakamura Y, Setoguchi M, Abe I, and Fujishima M. Stretch-activated channels in arterial smooth muscle of genetic hypertensive rats. *Hypertension* 31: 254-258, 1998.

135. Oliver D, Baukrowitz T, and Fakler B. Polyamines as gating molecules of inward-rectifier K^+ channels. *Eur J Biochem* 267: 5824-5829, 2000.

136. Osol G, Laher I, and Kelley M. Myogenic tone is coupled to phospholipase C and G protein activation in small cerebral arteries. *Am J Physiol* 265: H415-420, 1993.

137. Pacaud P, Loirand G, Baron A, Mironneau C, and Mironneau J. Ca^{2+} channel activation and membrane depolarization mediated by Cl^- channels in response to noradrenaline in vascular myocytes. *Br J Pharmacol* 104: 1000-1006, 1991.

138. Park KS, Kim YA, Lee YC, Earm YE, and Ho W-K. Mechanosensitive cation channels in arterial smooth muscle cells are activated by diacylglycerol and inhibited by phospholipase C inhibitor. *Circ Res* 93: 557-564, 2003.

139. Partridge LD and Swandulla D. Single Ca^{2+}-activated cation channels in bursting neurons of Helix. *Pflugers Arch* 410: 627-631, 1987.

140. Peng H, Matchkov V, Ivarsen A, Aalkjaer C, and Nilsson H. Hypothesis for the initiation of vasomotion. *Circ Res* 88: 810-815, 2001.

141. Peppiatt-Wildman CM, Albert AP, Saleh SN, and Large WA. Endothelin-1 activates a Ca^{2+}-permeable cation channel with TRPC3 and TRPC7 properties in rabbit coronary artery myocytes. *J Physiol* 580: 755-764, 2007.

142. Pfaffl MW. A new mathematical model for relative quantification in real-time RT-PCR. *Nucleic Acids Res* 29: e45, 2001.

143. Platoshyn O, Remillard CV, Fantozzi I, Sison T, and Yuan JX. Identification of functional voltage-gated Na^+ channels in cultured human pulmonary artery smooth muscle cells. *Pflugers Arch* 451: 380-387, 2005.

144. Popescu LM, Gherghiceanu M, Mandache E, and Cretoiu D. Caveolae in smooth muscles: nanocontacts. *Journal of Cellular and Molecular Medicine* 10: 960-990, 2006.

145. Popescu LM, Gherghiceanu M, Mandache E, and Cretoiu D. Caveolae in smooth muscles: nanocontacts. *J Cell Mol Med* 10: 960-990, 2006.

146. Putney JW. The physiological function of store-operated calcium entry. *Neurochem Res* 36: 1157-1165, 2011.

147. Quayle JM, McCarron JG, Asbury JR, and Nelson MT. Single calcium channels in resistance-sized cerebral arteries from rats. *Am J Physiol* 264: H470-478, 1993.

148. Quayle JM, McCarron JG, Brayden JE, and Nelson MT. Inward rectifier K^+ currents in smooth muscle cells from rat resistance-sized cerebral arteries. *Am J Physiol* 265: C1363-1370, 1993.

149. Quignard JF, Ryckwaert F, Albat B, Nargeot J, and Richard S. A novel tetrodotoxin-sensitive Na^+ current in cultured human coronary myocytes. *Circ Res* 80: 377-382, 1997.

150. Rahman T and Taylor CW. Dynamic regulation of IP_3 receptor clustering and activity by IP_3. *Channels (Austin)* 3: 226-232, 2009.

151. Reading SA and Brayden JE. Central role of TRPM4 channels in cerebral blood flow regulation. *Stroke* 38: 2322-2328, 2007.

152. Reading SA, Earley S, Waldron BJ, Welsh DG, and Brayden JE. TRPC3 mediates pyrimidine receptor-induced depolarization of cerebral arteries. *Am J Physiol Heart Circ Physiol* 288: H2055-2061, 2005.

153. Rebecchi MJ and Pentyala SN. Structure, function, and control of phosphoinositide-specific phospholipase C. *Physiol Rev* 80: 1291-1335, 2000.

154. Resink TJ, Scott-Burden T, Baur U, Burgin M, and Buhler FR. Enhanced responsiveness to angiotensin II in vascular smooth muscle cells from spontaneously hypertensive rats is not associated with alterations in protein kinase C. *Hypertension* 14: 293-303, 1989.

155. Robertson BE and Nelson MT. Aminopyridine inhibition and voltage dependence of K^+ currents in smooth muscle cells from cerebral arteries. *Am J Physiol* 267: C1589-1597, 1994.

156. Robertson BE, Schubert R, Hescheler J, and Nelson MT. cGMP-dependent protein kinase activates Ca^{2+}-activated K^+ channels in cerebral artery smooth muscle cells. *Am J Physiol* 265: C299-303, 1993.

157. Robertson BE, Schubert R, Hescheler J, and Nelson MT. cGMP-dependent protein kinase activates Ca-activated K channels in cerebral artery smooth muscle cells. *Am J Physiol* 265: C299-303, 1993.

158. Rubart M, Patlak JB, and Nelson MT. Ca^{2+} currents in cerebral artery smooth muscle cells of rat at physiological Ca^{2+} concentrations. *J Gen Physiol* 107: 459-472, 1996.

159. Ruegg JC, Meisheri K, Pfitzer G, and Zeugner C. Skinned coronary smooth muscle: calmodulin, calcium antagonists, and cAMP influence contractility. *Basic Res Cardiol* 78: 462-471, 1983.

160. Rusch NJ, De Lucena RG, Wooldridge TA, England SK, and Cowley AW, Jr. A Ca^{2+}-dependent K^+ current is enhanced in arterial membranes of hypertensive rats. *Hypertension* 19: 301-307, 1992.

161. Rusch NJ and Hermsmeyer K. Calcium currents are altered in the vascular muscle cell membrane of spontaneously hypertensive rats. *Circ Res* 63: 997-1002, 1988.

162. Saleh S, Yeung SY, Prestwich S, Pucovsky V, and Greenwood I. Electrophysiological and molecular identification of voltage-gated sodium channels in murine vascular myocytes. *J Physiol* 568: 155-169, 2005.

163. Saleh SN, Albert AP, Peppiatt CM, and Large WA. Angiotensin II activates two cation conductances with distinct TRPC1 and TRPC6 channel properties in rabbit mesenteric artery myocytes. *J Physiol* 577: 479-495, 2006.

164. Sanabria H, Digman MA, Gratton E, and Waxham MN. Spatial diffusivity and availability of intracellular calmodulin. *Biophys J* 95: 6002-6015, 2008.

165. Santana LF and Navedo MF. Molecular and biophysical mechanisms of Ca^{2+} sparklets in smooth muscle. *J Mol Cell Cardiol* 47: 436-444, 2009.

166. Schlossmann J, Ammendola A, Ashman K, Zong X, Huber A, Neubauer G, Wang GX, Allescher HD, Korth M, Wilm M, Hofmann F, and Ruth P. Regulation of intracellular calcium by a signalling complex of IRAG, IP_3 receptor and cGMP kinase Ibeta. *Nature* 404: 197-201, 2000.

167. Schramm CM, Chuang ST, and Grunstein MM. cAMP generation inhibits inositol 1,4,5-trisphosphate binding in rabbit tracheal smooth muscle. *Am J Physiol* 269: L715-719, 1995.

168. Schwarz EC, Wolfs MJ, Tonner S, Wenning AS, Quintana A, Griesemer D, and Hoth M. TRP channels in lymphocytes. *Handb Exp Pharmacol*: 445-456, 2007.

169. Scornik FS, Codina J, Birnbaumer L, and Toro L. Modulation of coronary smooth muscle K_{Ca} channels by G_s alpha independent of phosphorylation by protein kinase A. *Am J Physiol* 265: H1460-1465, 1993.

170. Sergeant GP, Hollywood MA, McCloskey KD, McHale NG, and Thornbury KD. Role of IP_3 in modulation of spontaneous activity in pacemaker cells of rabbit urethra. *Am J Physiol Cell Physiol* 280: C1349-1356, 2001.

171. Smith IF and Parker I. Imaging the quantal substructure of single IP_3R channel activity during Ca^{2+} puffs in intact mammalian cells. *Proc Natl Acad Sci U S A* 106: 6404-6409, 2009.

172. Smith PD, Brett SE, Luykenaar KD, Sandow SL, Marrelli SP, Vigmond EJ, and Welsh DG. KIR channels function as electrical amplifiers in rat vascular smooth muscle. *J Physiol* 586: 1147-1160, 2008.

173. Spassova MA, Hewavitharana T, Xu W, Soboloff J, and Gill DL. A common mechanism underlies stretch activation and receptor activation of TRPC6 channels. *Proc Natl Acad Sci U S A* 103: 16586-16591, 2006.

174. Standen NB, Quayle JM, Davies NW, Brayden JE, Huang Y, and Nelson MT. Hyperpolarizing vasodilators activate ATP-sensitive K+ channels in arterial smooth muscle. *Science* 245: 177-180, 1989.

175. Stanfield PR and Sutcliffe MJ. Spermine is fit to block inward rectifier (K_{ir}) channels. *J Gen Physiol* 122: 481-484, 2003.

176. Sturek M and Hermsmeyer K. Calcium and sodium channels in spontaneously contracting vascular muscle cells. *Science* 233: 475-478, 1986.

177. Sturgess NC, Hales CN, and Ashford ML. Inhibition of a calcium-activated, non-selective cation channel, in a rat insulinoma cell line, by adenine derivatives. *FEBS Lett* 208: 397-400, 1986.

178. Sun XP, Callamaras N, Marchant JS, and Parker I. A continuum of InsP3-mediated elementary Ca^{2+} signalling events in Xenopus oocytes. *J Physiol* 509 (Pt 1): 67-80, 1998.

179. Suzuki H, Kito Y, Fukuta H, and Yamamoto Y. Dual effects of cyclopiazonic acid on excitation of circular smooth muscle isolated from the guinea-pig gastric antrum. *J Smooth Muscle Res* 38: 23-37, 2002.

180. Takezawa R, Cheng H, Beck A, Ishikawa J, Launay P, Kubota H, Kinet JP, Fleig A, Yamada T, and Penner R. A pyrazole derivative potently inhibits lymphocyte Ca^{2+} influx and cytokine production by facilitating transient receptor potential melastatin 4 channel activity. *Mol Pharmacol* 69: 1413-1420, 2006.

181. Talavera K, Yasumatsu K, Voets T, Droogmans G, Shigemura N, Ninomiya Y, Margolskee RF, and Nilius B. Heat activation of TRPM5 underlies thermal sensitivity of sweet taste. *Nature* 438: 1022-1025, 2005.

182. Taufiq Ur R, Skupin A, Falcke M, and Taylor CW. Clustering of InsP3 receptors by InsP3 retunes their regulation by InsP3 and Ca^{2+}. *Nature* 458: 655-659, 2009.

183. Teulon J. Ca^{2+}-activated non-selective cation channels. In: *Pharmacology of Ionic Channel Function: Activators and Inhibitors*, edited by Makato Endo YK, and Masayoshi Mishina: Springer Berlin Heidelberg, 2000.

184. Toescu EC. Temporal and spatial heterogeneities of Ca^{2+} signaling: mechanisms and physiological roles. *Am J Physiol* 269: G173-185, 1995.

185. Uehara Y, Ishii M, Ishimitsu T, and Sugimoto T. Enhanced phospholipase C activity in the vascular wall of spontaneously hypertensive rats. *Hypertension* 11: 28-33, 1988.

186. Ullrich ND, Voets T, Prenen J, Vennekens R, Talavera K, Droogmans G, and Nilius B. Comparison of functional properties of the Ca^{2+}-activated cation channels TRPM4 and TRPM5 from mice. *Cell Calcium* 37: 267-278, 2005.

187. Vila E, Macrae IM, and Reid JL. Differences in inositol phosphate production in blood vessels of normotensive and spontaneously hypertensive rats. *Br J Pharmacol* 104: 296-300, 1991.

188. Volk KA, Matsuda JJ, and Shibata EF. A voltage-dependent potassium current in rabbit coronary artery smooth muscle cells. *J Physiol* 439: 751-768, 1991.

189. Wallenstein S, Zucker CL, and Fleiss JL. Some statistical methods useful in circulation research. *Circ Res* 47: 1-9, 1980.

190. Wellman GC, Cartin L, Eckman DM, Stevenson AS, Saundry CM, Lederer WJ, and Nelson MT. Membrane depolarization, elevated Ca^{2+} entry, and gene expression in cerebral arteries of hypertensive rats. *Am J Physiol Heart Circ Physiol* 281: H2559-2567, 2001.

191. Wellman GC, Cartin L, Eckman DM, Stevenson AS, Saundry CM, Lederer WJ, and Nelson MT. Membrane depolarization, elevated Ca(2+) entry, and gene expression in cerebral arteries of hypertensive rats. *Am J Physiol Heart Circ Physiol* 281: H2559-2567, 2001.

192. Wellman GC and Nelson MT. Signaling between SR and plasmalemma in smooth muscle: sparks and the activation of Ca^{2+}-sensitive ion channels. *Cell Calcium* 34: 211-229, 2003.

193. Welsh CF and Assoian RK. A growing role for Rho family GTPases as intermediaries in growth factor- and adhesion-dependent cell cycle progression. *Biochim Biophys Acta* 1471: M21-29, 2000.

194. Welsh DG, Morielli AD, Nelson MT, and Brayden JE. Transient receptor potential channels regulate myogenic tone of resistance arteries. *Circ Res* 90: 248-250, 2002.

195. Welsh DG, Nelson MT, Eckman DM, and Brayden JE. Swelling-activated cation channels mediate depolarization of rat cerebrovascular smooth muscle by hyposmolarity and intravascular pressure. *J Physiol* 527 Pt 1: 139-148, 2000.

196. Williams DL, Jr., Katz GM, Roy-Contancin L, and Reuben JP. Guanosine 5'-monophosphate modulates gating of high-conductance Ca^{2+}-activated K^+ channels in vascular smooth muscle cells. *Proc Natl Acad Sci U S A* 85: 9360-9364, 1988.

197. Worley JF, Quayle JM, Standen NB, and Nelson MT. Regulation of single calcium channels in cerebral arteries by voltage, serotonin, and dihydropyridines. *Am J Physiol* 261: H1951-1960, 1991.

198. Wu L and de Champlain J. Inhibition by cyclic AMP of basal and induced inositol phosphate production in cultured aortic smooth muscle cells from Wistar-Kyoto and spontaneously hypertensive rats. *J Hypertens* 14: 593-599, 1996.

199. Wu S, Lin P, Hsieh K, Liu Y, and Chiang H. Behavior of nonselective cation channels and large-conductance Ca^{2+}-activated K^+ channels induced by dynamic changes in membrane stretch in cultured smooth muscle cells of human coronary artery. *Journal of Cardiovascular Electrophysiology* 14: 44-51, 2003.

200. Xi Q, Adebiyi A, Zhao G, Chapman KE, Waters CM, Hassid A, and Jaggar JH. IP3 constricts cerebral arteries via IP3 receptor-mediated TRPC3 channel activation and independently of sarcoplasmic reticulum Ca2+ release. *Circ Res* 102: 1118-1126, 2008.

201. Yao Y, Choi J, and Parker I. Quantal puffs of intracellular Ca^{2+} evoked by inositol trisphosphate in Xenopus oocytes. *J Physiol* 482 (Pt 3): 533-553, 1995.

202. Zhang Z, Okawa H, Wang Y, and Liman ER. Phosphatidylinositol 4,5-bisphosphate rescues TRPM4 channels from desensitization. *J Biol Chem* 280: 39185-39192, 2005.

203. Zimmermann B, Somlyo AV, Ellis-Davies GC, Kaplan JH, and Somlyo AP. Kinetics of prephosphorylation reactions and myosin light chain phosphorylation in smooth muscle. Flash photolysis studies with caged calcium and caged ATP. *J Biol Chem* 270: 23966-23974, 1995.

204. Zitt C, Obukhov AG, Strubing C, Zobel A, Kalkbrenner F, Luckhoff A, and Schultz G. Expression of TRPC3 in Chinese hamster ovary cells results in calcium-activated cation currents not related to store depletion. *J Cell Biol* 138: 1333-1341, 1997.